KU LEUVEN

ARENBERG DOCTORAL SCHOOL
Faculty of Science

Holographic Wave Functions of the Universe

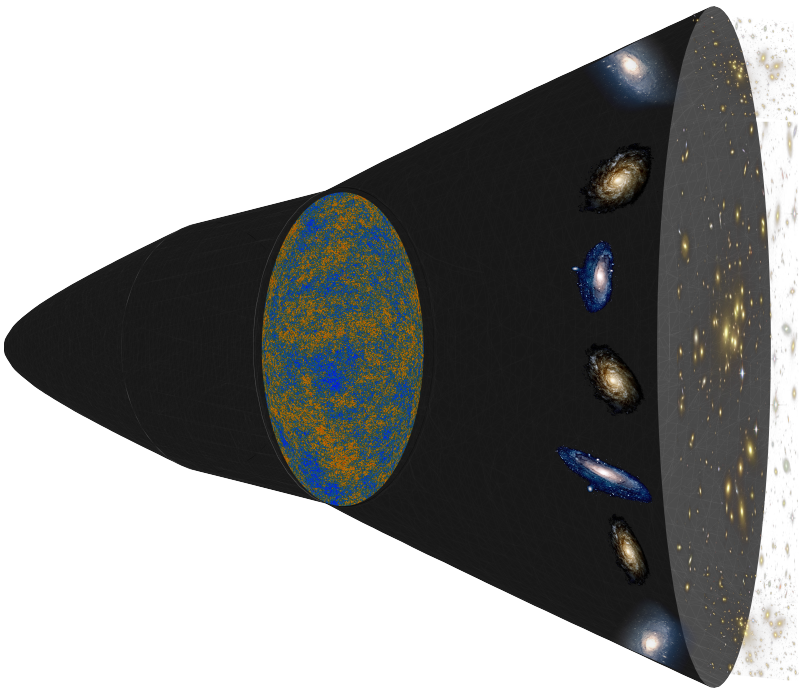

Gabriele Conti

Supervisor:
Prof. dr. T. Hertog

Dissertation presented in partial fulfillment of the requirements for the degree of Doctor of Science (PhD): Physics

November, 2017

Holographic Wave Functions of the Universe

Gabriele CONTI

Examination committee:
Prof. dr. T. Van Riet, chair
Prof. dr. T. Hertog, supervisor
Prof. dr. A. Van Proeyen
Prof. dr. E. Carlon
Prof. dr. A. Castro
(UVA - Universiteit van Amsterdam)
Prof. dr. S. Detournay
(ULB - Universitè Libre de Bruxelles)

Dissertation presented in partial fulfillment of the requirements for the degree of Doctor of Science (PhD): Physics

November, 2017

Aknowledgements

Working at KU Leuven has been a great honor. I would like to thank every single person who made these five years unforgettable. Everyone who supported me on a professional and personal level. Without all of you, this thesis would have been impossible.

First of all I want to thank Thomas Hertog, for being my supervisor and for giving me the opportunity to do this PHD. I want to thank you for all the interesting, nice and advanced projects you gave me. It was a great opportunity for me to work with you on these topics, and I am really grateful for that. You also gave me the opportunity to travel a lot during my PHD, in order to attend conferences, schools, workshops, etc. This gave me the opportunity to grow up a lot both on a professional and personal level, as well as the opportunity to know many new colleagues. I am really grateful to you for all of this.

Secondly, I would like to thank my PHD committee: Enrico Carlon, Antoine (Toine) Van Proeyen, Alejandra Castro, Stephan Detournay and Thomas Van Riet. Thanks for the time you dedicated to the reading of my manuscript and for the valuable comments.

A special thanks to Thomas Van Riet. I really appreciated the useful discussions we had about dS/CFT. Those discussions stimulated me a lot. I have also enjoyed when we were going to some missions together, in particular the one in Madrid. Further, your door is always open when PHD students need to talk about professional or personal issues. This is very important for all us, and it mean a lot to me!

A special thanks to Alejandra Castro. Even if we met only during conferences and schools, I have really appreciated talking with you about my and your work. It has been an honour knowing you. Thank you for giving me the opportunity to give a talk in Amsterdam and to have agreed on being in my PHD committee.

A special thanks to Frederick Denef. It was a pleasure to know you and to have

been your teaching assistant during my first year as a PHD student. It was also very nice to meet with you during conferences or workshop. I really appreciated all the time we talk and we updated each other with our recent works.

I also want to thank all the ITF members. Nikolay Bobev for the stimulating discussions. Christian Maes for all his skepticism. I know it sounds weird, but those discussions help us (phd students) a lot. They push us to give our best all the time, and I really appreciate that.

A very special thanks to Ellen Van der Woerd for sharing this experience with me. I am really happy to have started my PHD with you. We had so many discussions both from a professional and a personal level. I am deeply grateful to have met not only a colleague but also a friend like you during these years.

Thanks to all the ones who shared the office with me during these years: Frederick Coomans, Alessio Marrani, and Yannick Vreys. We spent a lot of time in the same room, and without you it would have been different.

I am also really grateful to all the persons I met at ITF during these years. Thanks to Federico, Alice and Marius for driving me to the office or back home. Thanks to Anneleen for being so professional and nice with everybody. Without you the work at ITF would be way more complicated. Thanks to Filip for being so helpful everytime we needed to fix issues on our computers. Thanks to Matt Williams, it was nice to meet you and to have so many fruitful discussions with you. Thanks to Marjoree, I really enjoyed conversations with you and with your husband. I wish the best luck to both of you. A special thanks to Jesse. I met you only during my final year, but it was really nice, and I wish we would have spent more time together. Thanks for the Dutch translation of the abstract. Thanks also to Edoardo. It was always very nice and pleasant to talk with you. I wish you good luck for your work and your life. Finally, Pablo, Juan, Gabriele, Brecht, Bert, Marco, Fridrik, Vincent, Bert, Ruben, and all the people who shared time with me at ITF, thanks a lot. It was a pleasure to meet with all of you.

Thanks to all the people I met during these years. Blagoje, Jules, Laura, Marco F., Marco S., Teresa, it was really nice to know all of you and I really liked to meet with you during schools or conferences. A special thank also to all the people who shared time with me in Brussels: Marco, Jo, Adolfo, Marianna. I really had a lot of fun with all of you and I will always bring very good memory for the time we spent together.

Thanks to my parents, my sister and my niece. You are always there when I need. You are supporting me every day, and you are a motivation for me to give my best. You are always a light even when everything is dark. You are always a landmark for me.

A special thanks to all my friends in Italy. I am so lucky to have you there always. My life would be boring without you. It is really great to know I can count on all of you everytime I need. You always give me valuable suggestions for my life and you always support me when I need. I really appreciate that.

Thanks to Carole for reading my manuscript and for spotting English mistakes.

Last but not least, the best thanks to my beloved Juliette. My life in Brussels had a turn around when I met you. There are no words I can use to describe how much I am grateful for the chance I had to know you and for the privilege to share my life with you. You give a meaning to every single day. You give a meaning to my life. You were always there to comfort me, to support me, to stimulate me day after day. You were there when I was happy. You were there when I was sad. You were there when I was angry. You were there when I was sick. You have always found the right words and gave me the right motivations to go on, to move on, to follow my dreams. Thank you for your never ending believe in me. Without you, this work and my PHD would have not been possible. Thanks!

Abstract

It is a central goal of theoretical high-energy physics to develop a unified theoretical framework that describes Nature on all scales. A common approach to this involves merging quantum theory and General Relativity into a unified theory of quantum gravity. A theory of this kind has the potential to put cosmology on firm theoretical footing.

String theory is a promising candidate for a unified theory. The second string theory revolution in the '90s has consolidated the role of holography in quantum gravity in the form of a duality between quantum gravity with anti-de Sitter (AdS) boundary conditions and Conformal Field Theories (CFTs) defined on the conformal boundary of AdS. However observations indicate that our universe is asymptotically de Sitter (dS). Together these developments mean it is important to understand whether holographic ideas can be developed and used in a dS context to construct a quantum gravitational model of cosmology.

A central role in quantum cosmology is played by the wave function of the universe. There are several indications indeed that the application of holography to cosmology enables a new formulation of the wave function of the universe in terms of the partition function of Euclidean deformed CFTs defined on the future conformal boundary. However many fundamental questions about the technical and conceptual nature of holographic cosmology or dS/CFT remain open. In this thesis we study and explore a number of features of dS/CFT duality. In one particular example, AdS/CFT implies an explicit realization of dS/CFT, which relates Vasiliev's higher spin theory of gravity to the $O(N)$ vector model of interacting scalars. This example will serve throughout this thesis as a useful toy model with which we will explore and test various developments of the duality more generally.

In the first part of this thesis we develop dS/CFT for Vilenkin's tunneling wave function and contrast its behaviour with that of the Hartle-Hawking wave function. We evaluate the holographic tunneling wave function in the $O(N)$

vector toy model in the presence of a mass deformation and compare this with its behaviour predicted in the usual bulk saddle pont approximation.

In the second part of this thesis we explore the dS/CFT correspondence with $S^1 \times S^2$ future boundary conditions. In this context it has been argued that the probability measure is badly defined, both in the $O(N)$ vector toy model and in Einstein gravity, in the limit where the radius of the S^1 goes to zero. We analyze this using quantum cosmology techniques to elucidate the interpretation of the wave function in this domain. We show that the divergent behaviour of the (bulk and boundary) measures occurs in a regime where the wave function does not describe asymptotically classical, Lorentzian histories and hence admits no clean probabilistic interpretation. We also exhibit the strikingly different behaviour of the tunneling and no-boundary wave function in this regime. The former appears to select this quantum realm whereas the latter predicts the universe is everywhere in the semiclassical domain.

The third part of this thesis consists of a digression into AdS/CFT. In the bulk we consider a consistent truncation of M-Theory compactified on $AdS_4 \times S^7$ consisting of Einstein gravity minimally coupled to a single scalar field with a negative exponential potential. We numerically find a three parameter family of new Euclidean solutions of this theory that asymptote to a locally AdS space with a (double) squashed sphere as conformal boundary configuration. Our solutions are generalization of the AdS Taub-NUT/Bolt solutions to include a second squashing and scalar matter. We study their thermodynamic behaviour as a function of the three boundary parameters and show this qualitatively reproduces that of the free $O(N)$ vector model defined on a double squashed sphere and deformed by a mass term.

This sets the scene for the final part of this thesis where we consider complex generalizations of the above solutions, starting from the same theory, with asymptotically dS boundary conditions. These specify the saddle point wave function in a minisuperspace model of anisotropic deformations of dS with scalar matter driving a regime of eternal inflation. We initiate a holographic exploration of eternal inflation by computing the partition function of the interacting $O(N)$ vector model as a function of the three asymptotic parameters. We find that the amplitude is low for conformal boundary surfaces far from the round conformal structure. This is in line with general field theory expectations and lends support to the conjecture that the exit from eternal inflation is reasonably smooth, producing universes that are relatively regular on the largest scales with globally finite surfaces of constant density.

Beknopte samenvatting

Het is een centrale doelstelling van de theoretische hoge energie fysica om een verenigd theoretisch kader te ontwikkelen dat de natuur op alle schalen beschrijft. Een belangrijk onderdeel hiervan is het unificeren van de kwantummechanica met de algemene relativiteitstheorie van Einstein, tot een zogenaamde kwantumzwaartekracht. Een dergelijke theorie heeft ondermeer de potentie om kosmologie op stevige theoretische basis te zetten. in de jaren '90, heeft door middel van holografie kwantummechanica zwaartekracht in de vorm van een dualiteit tussen kwantumzwaartekracht met anti-de Sitter (AdS) randvoorwaarden en Conforme veldentheorieën (CFT's) gedefinieerd op de conforme grens van AdS. Observaties wijzen er echter op dat ons universum asymptotisch de Sitter (dS) is en niet AdS. Het is een interessant vraagstuk of de holografische ideeen van AdS ook toegepast kunnen worden op dS ruimtes. Dit zou dan leiden tot een kwantum-gravitatiemodel van de kosmologie. Een centrale rol in de kwantumkosmologie wordt gespeeld door de golffunctie van het universum en zal ook in deze thesis een belangrijke rol hebben.

Er zijn inderdaad verschillende aanwijzingen dat de toepassing van holografie in kosmologie een nieuwe formulering van de golffunctie van het universum kan opleveren door middel van andere voorwaarden van de verdelingsfunctie van Euclidsch-vervormde CFT's gedefinieerd voor de toekomstige conforme grens. Veel fundamentele vragen over de technische en conceptuele aard van holografische kosmologie en dS/CFT blijven echter nog altijd open. In dit proefschrift bestuderen en onderzoeken we een aantal kenmerken van de dS/CFT dualiteit. In een specifiek voorbeeld impliceert AdS/CFT een expliciete realisatie van dS/CFT, welke Vasiliev's hogere spintheorie van zwaartekracht relateert aan een O(N) vectormodel interagerende waarmee we verschillende aspecten van de dualiteit zullen verkennen en testen.

In het eerste deel van dit proefschrift ontwikkelen we dS/CFT voor de Vilenkin tunneling-en contrasteren het gedrag met dat van de Hartle-Hawking-golffunctie. We evalueren de holografische tunneling-golffunctie in het O(N)

vectormodel, in aanwezigheid van een massavervorming, en vergelijken dit met het gedrag voorspeld in de gebruikelijke benadering van bulkzadel-punten. In het tweede deel van dit proefschrift onderzoeken we de dS/CFT-correspondentie met S1 × S2 als toekomstige randvoorwaarden. In dit verband is betoogd dat de waarschijnlijkheidsmaat slecht is gedefinieerd, zowel in het O (N) -vectormodel als in de zwaartekrachttheorie, in de limiet waar de straal van de S 1 naar nul gaat. Wij analyseer dit fenomeen met behulp van technieken uit de kwantumkosmologie om de interpretatie van de golffunctie te verduidelijken. We laten zien dat het afwijkende gedrag van de (bulk en grens) maten plaats vindt in een regime waar de golffunctie asymptotische geen klassieke, Lorentziaanse, geschiedenissen beschrijft en daarom geen fatsoenlijke probabilistische interpretatie toelaat. We tonen ook een opvallend anders gedrag aan van de tunneling en "no-boundary"golffuncties in dit regime. De eerstgenoemde lijkt het kwantumrijk te selecteren, terwijl dat laatste het universum voorspelt in een semiklassiek domein.

Het derde deel van dit proefschrift bestaat uit een studie naar AdS/CFT. In de bulk beschouwen we een consistente truncatie van M-Theory gecompactificeerd op AdS 4 × S 7 bestaande uit Einstein-zwaartekracht minimaal gekoppeld aan een scalair veld met een negatieve, exponentiële, potentiaal. Door gebruik te maken van numerieke technieken vinden we een familie aan Euclidische oplossingen met drie parameters, die asymptotisch naar een lokale AdS-ruimte gaan met een (dubbele) geplette bol als conforme grens. Onze oplossingen zijn generalisaties van de AdS Taub-NUT / Bolt-oplossingen die een tweede vervorming van de sfeer toelaten, met scalaire materie. We bestuderen hun thermodynamisch gedrag in functie van de drie familie-parameters en laten zien dat dit kwalitatief het vrije O (N) -vectomodel reproduceert, gedefinieerd op een dubbel geplette bol met een massaterm vervorming.

Dit schetst de setting voor het laatste deel van dit proefschrift, waarin we het een complexe veralgemening beschouwen van de bovengenoemde oplossingen, uitgaande van dezelfde theorie, met asymptotisch dS randvoorwaarden. Deze specificeren de zadelpunt-golffunctie in een minisuperspace-model met anisotrope vervormingen van dS en met scalaire materie dat een regime van eeuwige inflatie aandrijft. We initiëren een holografische verkenning van eeuwige inflatie door de verdelingsfunctie van het interagerende O (N) vectormodel te berekenen als een functie van de drie asymptotische parameters die de familie aan oplossingen definiëren. We vinden dat de de amplitude laag is voor conforme grensvlakken ver van de ronde, conforme, structuur. Dit is in lijn met verwachtingen uit de veldentheorie en geeft steun aan het vermoeden dat de uitweg uit eeuwige inflatie relatief glad is, en dat er universa geproduceerd kunnen worden die op grote schaal regulier zijn met globaal eindige oppervlakken van constante dichtheid.

Contents

Chapter 1

Holography For Cosmology

1.1 Introduction

Our knowledge of the underlying physical mechanisms of Nature underwent a revolutionary advance in the first part of the last century. Einstein's theory of general relativity perfectly describes the behaviour of a weak gravitational field at large scales. Quantum mechanics describes with an incredible accuracy the effects of non-gravitational forces on small scales. However one would expect gravity to behave fundamentally quantum mechanically, with the classical Einsteinian theory emerging as a limiting case under appropriate circumstances.

There is much evidence that a quantum theory of gravity is needed to describe our own universe. In 1929 Hubble discovered that the universe is not static, but is expanding, [1]. Back in time the universe must have been very small, a point source containing all the matter, a point with an infinite density. From a theoretical point of view, classical general relativity cannot describe such scenario. Classical general relativity admits solutions with singularities, but the Penrose – Hawking singularity theorems state that our universe is geodesically incomplete in the past if treated classically. General relativity must break down at least at the Planck time and perhaps more broadly. Hence general relativity cannot be used to describe the region close to a singularity, and a quantum model of gravity is needed.

In 1965 Penzias and Wilson accidentally discovered that the entire universe is filled with a background radiation, [2], a sort of echo of a primordial event. This radiation is called cosmic microwave background (CMB) and it is an electromagnetic type of radiation. It is the leftover of an event which occurred

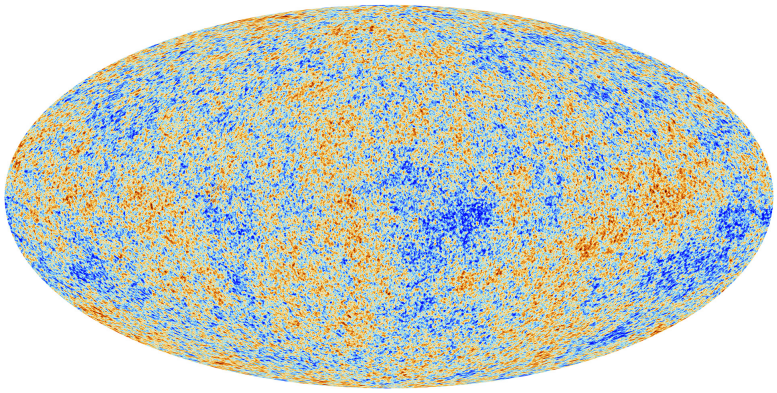

Figure 1.1: The most detailed image of the CMB radiation, released by Planck, [12, 13, 14, 15]. Different color represent different temperatures. These fluctuation are the seeds of galaxy and star formations.

at an early phase of the universe. At the very beginning, the universe was extremely dense and even photons were scattering. In this period the universe was completely opaque. With the expansion, the temperature cooled down and the density dropped down. At a certain time, photons were free to propagate. This period is often referred as surface of last scattering, and the CMB radiation is the visual image of that event. The CMB is in a certain sense a "relic radiation", the earliest image of the universe we can have through electromagnetic radiation. The CMB is almost isotropic everywhere, but there are some tiny, crucial fluctuations (at the part per million level) seed for the galaxy and star formations, [3, 4, 5]. Understanding the CMB radiation is therefore of crucial importance. In the past years, an enormous amount of observations have been done, improving the definition and the details of this primordial image. Among these observations, we have to cite the results of: COBE [6], WMAP [7, 8, 9], ALMA [10, 11], Planck [12, 13, 14, 15], and others [16, 17]. In figure 1.1 we show the picture of the CMB radiation with the highest definition we have today, released by the Planck mission in 2013.

The discovery of the CMB posed further questions. In classical cosmology the hot big bang model successfully describes many, but not all the futures we observe in the universe. For example, it does not explain flatness, absence of horizons and the origin of the density fluctuations we observe in the CMB. Theorists suggested that the universe expanded at an exponential rate at the very beginning. This model is called inflation and provides a solution to the flatness and the horizon problem, and one can obtain the spectrum of density perturbation by requiring that the matter fields started in a particular quantum state [18, 19]. Inflation

is driven by a quantized scalar field that (slowly) rolls down a potential hill and stops at a positive minima of the potential which is the cosmological constant we measure today. Many different types of inflationary models have been proposed in the past years [20, 21, 22, 23, 24, 25, 26, 27, 28]. We refer to [29, 30, 31, 32] for a review. Inflation suggests that the universe cannot be originated from any initial state (i.e. one could choose initial conditions such that inflation does not occur at all). Understanding the observed state of the universe is therefore related to the problem of initial conditions. As often occurs, a new discovery lead to new mysteries. If inflation is eternal, the inflationary phase of the universe's expansion lasts forever in different fractal regions of the universe. Eternal inflation, therefore, produces a hypothetically infinite multiverse, and only in a small volume of the universe inflation come to an end. Eternal inflation appears to be generic, [20], and appears to be the likely outcome of inflation, [18]. If inflation is eternal, whatever can happen, will happen, and it will happen not only once but an infinite numbers of time, with the only requirement that the fundamental law of physics are not violated. Classical gravity itself is not able to describe this scenario, and a quantum gravity theory is needed.

Once we have a model of quantum gravity at our disposal, we need a way to test it. Quantum gravity effects are expected to be relevant at very high energy, and we expect to be able to observe these effects directly as we approach the Planck length ($1.62 \times 10^{-35} m$ or equivalently 1.22×10^{16}TeV). The most powerful high energy particle accelerator (LHC) can probe events at around 14TeV, a scale far smaller to the one needed to directly test a quantum theory of gravity. A lab on earth is not the only way we might have to test such a theory. If quantum gravity effects took place during the early phase of our universe, they might have left a fingerprint on present observations. The early universe might be the best laboratory (and maybe the only one) where to test a model of quantum gravity. Understanding the effects of a quantum theory of gravity in cosmology is therefore of crucial importance. In 2016 the observation of gravitational waves, [33], opened a new window in this scenario. We cannot use electromagnetic waves to observe the universe before CMB time, but we might use gravitational waves to directly observe quantum gravity effects at an earlier phase of the universe. A quantum gravity theory for cosmology is therefore fundamental in these days of important observations.

Recently, astrophysicists realized that the universe is expanding at an accelerating rate. The acceleration is driven by a tiny but crucially positive cosmological constant $\Lambda \sim 10^{-52} m^{-2}$, [34, 35, 36, 37, 38]. The positivity of the cosmological constant rises many issues.

These issues do not represent a motivation for a quantum gravity theory, rather they are problems one needs to face up when dealing with a quantum gravity model in a universe dominated by a positive cosmological constant.

The $d+1$ dimensional pure de Sitter (dS) geometry is a maximally symmetric solution of the Einstein's field equation with a positive cosmological constant Λ

$$\mathcal{G}_{\mu\nu} = R_{\mu\nu} - \frac{1}{2} g_{\mu\nu} R + \Lambda g_{\mu\nu} = 0\,. \tag{1.1}$$

The geometry of dS_{d+1} space can be viewed as the induced metric on the hyperboloid

$$-X_0^2 + \sum_{i,1}^{d+1} X_i^2 = \frac{3}{\Lambda} \equiv \frac{1}{H^2}\,, \tag{1.2}$$

embedded in $d+2$ dimensional Minkowski space. We can describe dS space with different coordinate patches, which cover the whole hyperboloid or part of it.

The so called *global patch*, is described by the line element

$$ds^2 = -d\hat{t}^2 + \frac{1}{H^2}\cosh^2(H\hat{t}) d\Omega_d^2\,. \tag{1.3}$$

A surface of constant $\hat{t}$ is a three-sphere. The sphere shrinks from a maximum size at $\hat{t} = -\infty$, a surface called $\mathcal{I}^-$, to a minimum size at $\hat{t} = 0$. Then it bounces to a maximum size at $\hat{t} = \infty$, a surface called $\mathcal{I}^+$. A single observer cannot access the whole global space. Rather, s/he can only access the region described by the so called *static patch*, with metric

$$ds^2 = -(1 - r^2H^2) d\hat{t}^2 + (1 - r^2H^2)^{-1} dr^2 + r^2 d\Omega_{d-1}^2\,. \tag{1.4}$$

The surface $r = 1/H \equiv l_{dS}$ is a null surface that surrounds an observer at all times (the cosmological horizon). The coordinate ranges are: $r \in [0, l_{dS}]$ and $\hat{t} \in \mathcal{R}$.

We show the Penrose diagram of dS space in figure 1.2. The whole square is covered by the global patch (1.3) only. A physical observer can only access the quarter of the whole square containing the NP (or the SP). One can use other coordinate patches, but we do not discuss them here. We refer to [39] for an exhaustive discussion.

If this expansion persists the fate of our universe might be a cold and "empty" universe. An observer in the far future would observe a universe governed by thermal and quantum fluctuations at a Hawking temperature of $\sim 10^{-29} K$. The main source of energy will be the cosmological constant, which today already constitutes $\sim 70\%$ of the total energy. Obviously no physical person can observe such scenario, hence what is the meaning of an observer or, more in general, of any observable in the far future? That is not the only problem. A feature of the dS universe is the presence of a cosmological horizon, which is observer

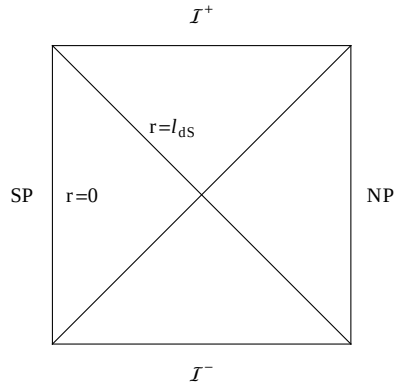

Figure 1.2: Penrose diagram of a dS universe.

dependent. An observer (like us) does not have access to data of the whole universe (in particular, data outside the cosmological horizon). In particular, an observer does not ordinarily have access to the spatial slice at infinite future, $\mathcal{I}^+$. The physical meaning of infinite future itself and, more in general, of data outside the cosmological horizon is a big challenge in theoretical physics (for an overview we refer to [40, 41]). The mystery persists. A cosmological horizon has a gravitational entropy which scales as the area of the horizon, $S = A/4G$, which is a similar behaviour as the gravitational entropy for black holes, [42]. Can we have a micro-canonical description of this gravitational entropy? How can we take into account for the vast number of microstates, $10^{10^{120}}$, coming from the Gibbons-Hawking entropy [43] of the cosmological horizon? A quantum gravity description of dS space needs to face up with all these issues. For a complete review we refer to [39, 44, 45].

Eventually, inflation came to an end, followed by the CMB and the formation of large scale structures we observe today. A quantum theory of gravity should admit cosmological solutions that predict a universe originated from a quantum event and evolved to a classical four-dimensional inflationary Lorentzian universe which is asymptotic de Sitter space. In short, a quantum gravity theory seems to be needed, and it must predict the cosmological observations we see in the classical limit (when the universe expands).

The quantum cosmology program tries to address these questions. In quantum cosmology one assigns a measure to the likelihood of a boundary configuration at a given time, which can be related to the outcome of cosmological observations.

The key object of interest in quantum cosmology is the wave function of the universe,

$$\Psi[h_{ij}(\mathbf{x}), \chi(\mathbf{x}), B]\,, \tag{1.5}$$

where $h_{ij}(\mathbf{x})$ is the space-like section of the universe on a closed surface B, and $\chi(\mathbf{x})$ is the scalar field [1] configuration on this surface.

The square of the wave function gives a measure, in terms of probabilistic weight for that particular configuration,

$$\mathcal{P}[h_{ij}(\mathbf{x}), \chi(\mathbf{x}), B] = |\Psi[h_{ij}(\mathbf{x}), \chi(\mathbf{x}), B]|^2\,. \tag{1.6}$$

The value of the boundary fields generically depends on their location on the entire manifold, whose coordinates are denoted by $\mathbf{x}$. The space of all the possible values of the boundary geometry and matter field configurations $(h_{ij}(\mathbf{x}), \chi(\mathbf{x}))$ is called **superspace**. The superspace can be thought of the space where the classical dynamics take place, it is infinite dimensional but with a finite number of coordinates $(h_{ij}(\mathbf{x}), \chi(\mathbf{x}))$ at every point $\mathbf{x}$ on the boundary-surface.

Superspace is an infinite dimensional configuration space, so the full formalism is extremely challenging. A more practical way to proceed is to reduce the superspace to a finite-dimensional space, i.e. if we consider only those fields that are homogeneous. This reduced version of superspace is called **minisuperspace**. This restriction is achieved by setting most of the field modes and their momenta to zero. In this way we exclude many geometries that might give a non-trivial contribution. We should not think to a minisuperspace model as an approximation of the full theory, but rather as a toy model that shares some aspects of the full theory. We study certain features of the full theory in isolation with the rest.

To determine (1.5), we need three elements: initial conditions, dynamics and interpretations. The equations the wave function must satisfy admit more solutions, and we need to impose initial conditions by hand to specify only one. To evaluate the wave function we need to consider a dynamic theory of gravity which describes the dynamic of the universe. Finally, we need a scheme to interpret our results and find what type of universe is predicted by the wave function.

The outline of this chapter is as follows. In section 1.2 we introduce the equations the wave function must satisfy, we discuss semiclassical solutions and the different proposals of boundary conditions which lead to different measures and different predictions. In section 1.3 we review the wave function approach to the dS/CFT correspondence. We provide an alternative way to compute the

[1] One can also consider vector fields configurations, [46].

full cosmological measure (1.6). In section 1.4 we discuss what is the outcome of the wave function. We will describe how classical solutions emerge from the quantum theory and what we interpret as a prediction. In section 1.5 we give a list of results that were already known and provided a motivation for this thesis work. Finally, in section 1.6 we give an outline of the remainder of the thesis.

1.2 A Semiclassical Cosmological Measure

In this section we will describe the equations that the wave function must satisfy, and we will discuss semiclassical solutions. In short, we review the formalism of quantum cosmology. We refer to [47, 48, 49, 50, 51, 52, 53] for an exhaustive discussion.

In minisuperspace model[2] the wave function is a solution of the quantum version of the Hamiltonian constraint of general relativity, which can be obtained by generalizing the Dirac quantization procedure to minisuperspace models,

$$\hat{H}\Psi(q^A) = \left(-\frac{1}{2}G_{AB}\hat{\pi}^A\hat{\pi}^B + U(q^A)\right)\Psi(q^A) \equiv \left(-\nabla^2 + U(q^A)\right)\Psi(q^A) = 0\,, \tag{1.7}$$

where we have collected the coordinates $q^A \equiv \{h_{ij}(\mathbf{x}), \chi(\mathbf{x})\}$, with $A = 1, 2$. The superpotential is

$$U(q) = \sqrt{h}\left(-{}^3R + 2\Lambda + V(\chi)\right)\,, \tag{1.8}$$

and the momenta are defined as

$$\hat{\pi}_A = -i\frac{\delta}{\delta q^A}\,. \tag{1.9}$$

while $G_{AB} = G_{(ij)(kl)}$, with

$$G_{ijkl} = h^{-\frac{1}{2}}\left(h_{ik}h_{jl} + h_{il}h_{jk} - h_{ij}h_{kl}\right)\,. \tag{1.10}$$

The boundary Ricci scalar ${}^3R$ is evaluated on the surface h_{ij}, and $V(\chi)$ is the potential of the asymptotic scalar field profile χ. Equation (1.10) provides a metric on superspace and G_{ijkl} is called the deWitt metric, [52]. G_{AB} provides a metric on minisuperspace.

Some important properties of this metric are

[2] In superspace models there is also a second constraint, called momentum constraint. In minisuperspace this constraint is automatically satisfied by the minisuperspace ansatz.

- the signature of the deWitt metric is independent of the signature of spacetime;

- the signature of the deWitt metric is hyperbolic at every point $\mathbf{x}$.

The latter property arises from the fact that the coefficient of the momenta in the Hamiltonian constraint (1.7) is regarded as a metric of a 6-dimensional hyperbolic Riemannian manifold $\mathcal{M}$. When h_{ij} is positive definite (as it is for a spacelike hypersurface) $\mathcal{M}$ has the hyperbolic signature $-+++++$. This property was pointed out by deWitt himself in [52].

Equation (1.7) is called Wheeler-deWitt (WdW) equation, and it is the quantum version of the classical constraint of general relativity. It reminds the zero-energy Schröedinger equation of ordinary quantum mechanics. The WdW equation (1.7) describes the dynamic of the wave function in minisuperspace. The volume of the three-metric $\sqrt{h}$ is the label of *time* in the superspace coordinates [3].

The minisuperspace metric G^{AB} depends on q^A. This leads to an operator ordering issue in the kinetic term and in (1.7) a particular choice was made. The superspace metric has indefinite signature and the potential term in (1.7) is not positive definite. We have to consider generically complex functional $\Psi(q^A)$ to solve (1.7).

In quantum mechanics one can find approximate solutions to the Schröedinger equation, [54, 55]. One needs to expand the wave function as a power series in $\hbar$ and to solve the Schröedinger equation order by order. The procedure is called WKB approximation, and can be generalized to minisuperspace models [56, 57].

We expand the wave function as a power series in $\hbar$, and we keep track of its real and imaginary components. To simplify the notation we collect the minisuperpsace coordinates, $q \equiv q^A$. We look for WKB solutions in the form

$$\Psi(q) = e^{-I_R(q)/\hbar + iS(q)/\hbar} + \mathcal{O}(\hbar^{-2})\,, \tag{1.11}$$

where I_R and S are real. We use the wave function (1.11) in equation (1.7). The result is a set of two equations,

$$\begin{gathered} -\frac{1}{2}(\nabla I_R)^2 + \frac{1}{2}(\nabla S)^2 + U(q) = 0\,, \\ \nabla I_R \cdot \nabla S = 0\,. \end{gathered} \tag{1.12}$$

[3] It corresponds to the minus sign in the hyperbolic signature of the superspace metric.

Solutions to the first equation clearly depends on the sign of $U(q)$. In the region of minisuperspace where $U(q) > 0$ we have WKB solutions in the form

$$\Psi_{\pm}^{(1)}(q) = exp\left(\pm\frac{1}{\hbar}\int^{q}\sqrt{U(q')}dq'\right). \tag{1.13}$$

When $U(q) < 0$ we have WKB solutions in the form

$$\Psi_{\pm}^{(2)}(q) = exp\left(\pm\frac{i}{\hbar}\int^{q}\sqrt{-U(q')}dq' \mp \frac{i\pi}{4}\right), \tag{1.14}$$

where the last term arises from the Airy function and it is needed to match the two approximate results in the proximity of $U(q) = 0$.

In the first regime the wave function (1.13) shows an exponentially decaying (or growing) behaviour. In ordinary quantum mechanics this regime is related to a quantum behaviour of the wave function (i.e. the tunneling through a potential barrier). The region of minisuperspace where the wave function shows this behaviour is called **classically forbidden region**. In analogy with quantum mechanics the wave function of the universe is also *tunneling* through a potential barrier, $U(q)$, and in this regime quantum effects are considered non-negligible.

When $U(q) < 0$ the wave function (1.14) shows an oscillatory behaviour. In quantum mechanics an oscillatory wave function is related to a classical regime. Further, if

$$|\nabla S| \gg |\nabla I_R|\,, \tag{1.15}$$

is satisfied, the wave function oscillates with an almost conserved amplitude. The condition (1.15) is called classicality condition, and it is of central role in quantum cosmology. The wave function (1.11) shows a classical behaviour when is in the form $e^{\pm iS(q)}$.

Mathematical consistency alone does not lead to a unique solution of the Wheeler-deWitt equation, as deWitt himself pointed out already in 1967, [52]. Unfortunately, though many progress have been done, this is still an open question. One needs to specify boundary conditions that selects only one of the possible solutions. That is, we choose only one wave function from the many that the dynamic allows. Many proposals have been advanced in the past years, mainly guided by analogies with ordinary quantum mechanics, simplicity, naturalness and predictions in line with experimental data. With the advancement of our knowledge and mathematical techniques, we hope that one day the theory alone will select only one solution as the only wave function that better describes our own universe. In this thesis work we will explore this question from an holographic prospective, but now we first review the two main proposals of initial conditions.

1.2.1 Tunneling Wave Function

A proposal for the wave function of the universe was postulated by Vilenkin [56, 57]. In his point of view the quantum origin of the universe is similar to a tunneling event in ordinary quantum mechanics.

In ordinary quantum mechanics one can expand solutions to the Klein-Gordon equation in terms of mode functions $e^{ip\cdot x}$. These modes can be classified as positive or negative frequency mode in respect to the timelike Killing vector $-i\partial/\partial t$. The solutions are eigenfunctions of this Killing vector and we can classify the solutions by looking at the sign of the eigenvalues. Negative and positive frequency modes are related to the sign of the timelike component, J_0, of the conserved current,

$$J = \frac{i}{2}\left(\Psi^* \bigtriangledown \Psi - \Psi \bigtriangledown \Psi^*\right) , \qquad \bigtriangledown \cdot J = 0 . \tag{1.16}$$

In an analogous manner, Vilenkin tried to classify the solutions of the WdW equation. A similar definition is immediately problematic. A mathematical property of superspace is that it has no Killing vectors at all, so that positive and negative frequency mode cannot be defined in this way. Nevertheless, we can make progress if we restrict ourselves to certain regions of superspace such as when we are close to its boundary. The boundary of superspace consists of configurations that are in some sense singular. This includes regions where $h^{1/2}$ is zero or infinite, or where χ or $(\partial_i \chi)$ are infinite. The boundary consists of regions where the four-geometry is also singular and regions where it is regular. For example, at the north or south pole of a four sphere $h^{1/2}$ vanishes while the four geometry is perfectly regular but, when $h^{1/2}$ is infinite also the four geometry is infinite. We can divide the boundary in two regions. The part of the boundary where the four-geometry is regular is called the non-singular boundary of superspace. The part of the boundary where the four-geometry is singular (i.e. when $h^{1/2}$ is infinite) is called the singular boundary.

If the wave function is oscillatory close to the singular boundary one expects solutions to the WdW equation to be well approximated by the WKB modes (1.14). For each mode we can define a current

$$J = -|C|^2 \nabla S , \tag{1.17}$$

where $|C|$ is related to the amplitude of the wave function. This mode is defined to be outgoing at the boundary if $-\nabla S$ points outwards there, while it is defined to be ingoing if $-\nabla S$ points inward.

Vilenkin's proposal for the Tunneling wave function Ψ_T can be summarized as :

Ψ_T is the solution to the WdW equation that is bounded everywhere and consists solely of outgoing modes at singular boundaries of superspace.

In this way we select only one WKB solution in (1.14). We take a linear combination of the two WKB modes in (1.13) and we define the Tunneling wave function as, [56, 57],

$$\Psi_T|_{U(q)>0}(q) = \Psi_+^{(1)}(q) - \frac{i}{2}\Psi_-^{(1)}(q)\,, \tag{1.18}$$

and

$$\Psi_T|_{U(q)<0}(q) = \Psi_-^{(2)}(q)\,. \tag{1.19}$$

The second term in (1.18) is negligible except in the proximity of the region where $U(q) \sim 0$, [57].

A mode that is outgoing to the boundary of superspace describes an expanding universe. Hence, the Tunneling wave function cannot describe data located $\mathcal{I}^-$.

Vilenkin definition can be viewed as the analogue of the propagator in ordinary quantum mechanics. The propagator of the wave function can be regarded as a Lorentzian functional integral, with weight e^{iS_L}, where S_L is the Lorentzian action. Schematically the Tunneling wave function can be defined as a Lorentzian path integral

$$\Psi_T\left(h_{ij}(\mathbf{x}), \chi(\mathbf{x}), B\right) = \sum_M \int \mathcal{D}g_{\mu\nu}\mathcal{D}\Phi e^{iS_L(g_{\mu\nu},\Phi)/\hbar}\,. \tag{1.20}$$

In this case one needs to consider a class of Lorentzian four metrics $g_{\mu\nu}$. The Lorentzian action for this model is

$$S_L = \frac{1}{2\kappa}\int_{\mathcal{M}} d^4x\sqrt{-g}\left((R-2\Lambda) - (\nabla\Phi)^2 - 2V(\Phi)\right) + \frac{1}{\kappa}\int_{\partial\mathcal{M}} d^3x\sqrt{h}K\,, \tag{1.21}$$

where $\kappa = 8\pi G$ and where h and K are respectively the induced metric on the asymptotic boundary and its extrinsic curvature, and where we have rescaled the scalar field. The wave function defined in this way is not a solution to the whole WdW equation, rather it should be regarded as the Green function of the WdW operator [56, 57]. The Tunneling wave function in the semiclassical approximation can be written as

$$\Psi_T[q] \approx 2\cosh[I_R[q]/\hbar] exp(iS[q]/\hbar)\,, \tag{1.22}$$

where I_R and S are respectively the real and the imaginary parts of iS_L, with S_L given in (1.21).

1.2.2 No-Boundary Wave Function

Hartle and Hawking, in their original paper [58], provided a definition for the no-boundary measures in terms of a path integral. In quantum field theory the ground state can be defined in terms of a Euclidean path integral. In a similar way they defined the wave function of the universe as a Euclidean path integral, over four-geometries and field configurations, with weight e^{-I_E}, where I_E is the Euclidean action. Schematically, the no-boundary wave function is defined as

$$\Psi_{HH}\left(h_{ij}(\mathbf{x}), \chi(\mathbf{x}), B\right) = \sum_{\mathcal{M}} \int \mathcal{D}g_{\mu\nu}\mathcal{D}\Phi e^{-I_E(g_{\mu\nu},\Phi)/\hbar}\,. \tag{1.23}$$

The sum is over a class of four-manifolds $\mathcal{M}$ for which $\partial\mathcal{M}$ is part of their boundary, and over some class of euclidean four-metrics $g_{\mu\nu}$ and matter field configurations Φ which induce the three-metric h_{ij} and matter field configuration χ on the boundary. In this thesis work we consider four-dimensional Einstein gravity minimally coupled to a scalar field in a given potential. The Euclidean action for this model is

$$I_E = -\frac{1}{2\kappa}\int_{\mathcal{M}} d^4x\sqrt{g}\left((R-2\Lambda) - (\nabla\Phi)^2 - 2V(\Phi)\right) - \frac{1}{\kappa}\int_{\partial\mathcal{M}} d^3x\sqrt{h}K\,. \tag{1.24}$$

We write the line element of a closed three-geometry as

$$h_{ij}dx^i dx^j = b^2\tilde{h}_{ij}dx^i dx^j\,, \tag{1.25}$$

where the volume of $\tilde{h}_{ij}$ is fixed to be one and b plays the role of a scale factor and is real. Superspace is therefore spanned by b and $\tilde{h}_{ij}(\mathbf{x})$, and the boundary configuration $\chi(\mathbf{x})$ of the scalar field Φ. Thus $\Psi = \Psi(b, \tilde{h}_{ij}, \chi)$.

The Hartle-Hawking prescription is to set the initial three-surface volume h_{ij} to zero, ensuring the closure of the four-geometry, and the regularity of the fields. The no-boundary proposal naturally selects only one mode in (1.13). Hartle and Hawking required that the wave function is at a minima when the three-surface volume is zero and it grows exponentially in the classically forbidden region. In terms of WKB modes the no-boundary wave function can be defined as,

$$\Psi_{HH}|_{U(q)>0}(q) = \Psi^{(1)}_{-}(q)\,, \tag{1.26}$$

and

$$\Psi_{HH}|_{U(q)<0}(q) = \Psi^{(2)}_{+}(q) + \Psi^{(2)}_{-}(q)\,. \tag{1.27}$$

In the classically allowed region the no-boundary wave function consists of a linear combination of two complex conjugated WKB modes. Hence, the Hartle-Hawking wave function is real.

In the path integral quantization one can construct semiclassical solutions by following the path that extremize the actions (1.24). These have to be complex in order to have a convergent path integral and to have an oscillatory wave function and a classical behaviour. The prescription is to consider complex saddle point of the action, described by the line element

$$ds^2 = \sigma^2 \left(N^2(\lambda) d\lambda^2 + a^2(\lambda) d\Omega_3^2 \right) , \tag{1.28}$$

where $\sigma^2 = 2G/(3\pi) = \kappa/(12\pi^2)$ is a normalization factor, chosen for later convenience. In this thesis work we will work in units where $\kappa = 1$. We locate the South pole at $\lambda = 0$ and the boundary of the manifold $\mathcal{M}$ at $\lambda = 1$, where the scale factor matches a real boundary value $b = a(1)$, and the scalar field matches the real boundary value $\chi = \Phi(1)$. The coordinates λ and x^i are real, while N, a and Φ are complex functions. Variation of the action with respect of $N(\lambda)$ leads to the Hamiltonian constraint, while variations of it with respect of the fields lead the equation of motion for $a(\lambda)$ and $\Phi(\lambda)$. Different choices of $N(\lambda)$ give different representations of the same saddle point. It is convenient to introduce the function $\tau(\lambda)$ defined as

$$\tau(\lambda) \equiv \int_0^\lambda d\lambda' N(\lambda') . \tag{1.29}$$

In this way different choices of $N(\lambda)$ are equivalent to different contours in the complex τ plane. A contour starts from the SP at $\lambda = \tau = 0$ and ends at the boundary $\lambda = 1$ with $\tau(1) \equiv \upsilon$. Each contour that connects $\tau = 0$ to $\tau = \upsilon$ is therefore a different representation of the same complex saddle point. In terms of τ the geometry is

$$ds^2 = \sigma^2 \left(d\tau^2 + a^2(\tau) d\Omega_3^2 \right) . \tag{1.30}$$

The scale factor $a(\tau)$ and the scalar field $\Phi(\tau)$ are solutions of the equations of motion

$$\begin{aligned} \dot{a}^2 + 1 - H^2 a^2 - a^2 \dot{\Phi}^2 - 2a^2 V = 0 , \\ \ddot{\Phi} + 3 \frac{\dot{a}}{a} \dot{\Phi} + \frac{dV}{d\Phi} = 0 . \end{aligned} \tag{1.31}$$

Solutions are the functions $a(\tau)$ and $\Phi(\tau)$ in the complex τ-plane. We consider the contour $C(0, \upsilon)$ which connects the SP at $\tau = 0$ to a point υ where $a(\upsilon)$ and $\Phi(\upsilon)$ take the real values b and χ respectively. For any such contour the on-shell action is given by

$$I_E = \frac{3\pi}{2} \int_{C(0,\upsilon)} d\tau a \left[a^2 \left(H^2 + 2V(\Phi) \right) - 1 \right] . \tag{1.32}$$

The asymptotic behaviour of the fields is better understood if we introduce the variable $u \equiv e^{-H\tau} \equiv e^{-H(y+iz)}$. In term of this variable, the large volume regime corresponds to the large y limit. The asymptotic behaviour of the fields can be written in powers of u,

$$a(u) = \frac{c}{u}\left[1 + \frac{u^2}{4c^2H^2} - \frac{3}{4}\tilde{\alpha}^2 u^{2\delta_-} + \cdots - \frac{2m^2\tilde{\alpha}\tilde{\beta}}{3H^2}u^3 + \cdots\right], \tag{1.33}$$

$$\Phi(u) = u^{\delta_-}(\tilde{\alpha} + \tilde{\alpha}_1 u + \cdots) + u^{\delta_+}(\tilde{\beta} + \tilde{\beta}_1 u + \cdots), \tag{1.34}$$

where $\delta_\pm \equiv \frac{3}{2} \pm \sqrt{\frac{9}{4} - \frac{m^2}{H^2}}$. This factor is real if $0 \leq m^2 \leq 9H^2/4$. This is called the Strominger bound and is a generalizations to dS space of the Breitenlohner-Freedman bound in Anti-de Sitter space, [59, 60].

The complex asymptotic solutions are locally determined in terms of the argument of the wave function, i.e. the 'boundary values' $c^2\gamma_{ij}$ and $\tilde{\alpha}$, up to the u^3 term in (1.33) and to order u^{δ_+} in (1.34). The further coefficients in the expansions encode information about the detailed physics of the matter (the shape of the potential), the interior of the saddle point geometry and the boundary condition of regularity at the SP. We now use this complex asymptotic structure to identify and relate two different geometric representations of the saddle points.

dS Representation

A classical real configuration corresponds to a curve in the complex τ plane where both the scale factor and the scalar field are real. The location of these curves can be seen from the asymptotic expansions (1.33) and (1.34), which to leading order in u can be written as

$$a(u) = \frac{c}{u} = |c|e^{i\theta_c + iHx_T + Hy}, \qquad \Phi(u) = \tilde{\alpha}u^{\delta_-} = |\tilde{\alpha}|e^{i\theta_\alpha - i\delta_- Hx_T - \delta_- Hy}, \tag{1.35}$$

where $c, \tilde{\alpha}$ are constants not determined by the asymptotic equations. The asymptotic form of the solution (1.35), is called Starobinski expansion [61], and is the dS analogue of the Fefferman-Graham expansion in a AdS background, [62, 63].

The fields are real along the curve

$$x_T = -\frac{\theta_c}{H} = \frac{\theta_\alpha}{\delta_- H}. \tag{1.36}$$

The existence of such a tuning and its compatibility with the regularity condition does not follow from this analysis, and in general it is not guaranteed that these

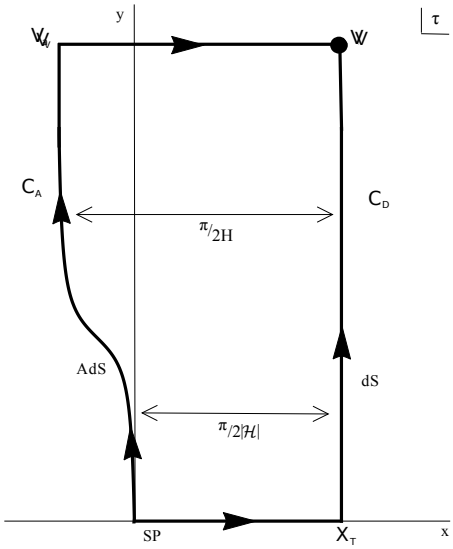

Figure 1.3: Different contours in the complex τ plane leading to different representations of the complex saddle points.

types of saddle points actually exist. It will highly depend on the choice of the scalar field potential and on the initial values of the fields at the SP. In [64] authors describe different sets of initial conditions for the fields that admit the tuning (1.36), and other sets where this does not occur.

An example of this contour is provided by the contour C_D in Fig. 1.3.

Along the $x = x_T$ curve we have

$$ds^2 \approx -dy^2 + |c|^2 e^{2Hy} d\Omega_3^2, \qquad \Phi \approx \tilde{\alpha} e^{-\delta_- Hy}. \tag{1.37}$$

Hence, along this contour, y acts as a time coordinate and the metric represents an asymptotic Lorentzian de Sitter universe with a slowly decaying scalar field profile. The asymptotic contribution to the saddle point action is given by the integral (1.32) along the curve $x = x_T$. It is immediate that there will be no contribution to the amplitude of the wave function from this part of the contour: the integrand in (1.32) is real as $d\tau = idy$. Instead, this part of the contour yields a large negative contribution to the phase of the wave function, required for classicality. Thus Ψ_{HH} oscillates rapidly with an approximately constant amplitude and describes an expanding, inflationary history.

In the neighbourhood of the SP at $\tau = 0$ the saddle point solutions take the form

$$\Phi(0) \approx \phi_0 e^{i\theta}, \qquad a(\tau) \approx \frac{\coth\left[\sqrt{V_\Lambda(\phi_0)}\tau\right]}{\sqrt{V_\Lambda(\phi_0)}}\,, \tag{1.38}$$

where $V_\Lambda = V + \Lambda$. If we consider $x_T \approx i\pi/(2\sqrt{V_\Lambda(\phi_0)})$ and if we define a contour C_D that first runs from $\tau = 0$ to $\tau = x_T$ along the x-axis and then along the y-axis we get a geometric representation of the saddle points in which an approximately Euclidean four sphere is smoothly joined onto a classical, expanding Lorentzian dS universe. This dS representation is illustrated in Fig 1.3.

The action integral over the Euclidean regime determines the amplitude of the corresponding classical history and is approximately given by [57]

$$I_R \approx -\frac{3\pi}{2V_\Lambda(\phi_0)}. \tag{1.39}$$

We can only write this explicitly in terms of the minisuperspace coordinates, when an analytic solution is known along the entire contour. For example when the scalar field is relatively small at the SP and moves in a quadratic potential we have the analytic solution [64],

$$\Phi = \chi \frac{{}_2F_1[\delta_-, \delta_+, 2, (1 + i\sinh H\tau)/2]}{{}_2F_1[\delta_-, \delta_+, 2, (1 + i\sinh[\cosh^{-1}(Hb)])/2]}, \tag{1.40}$$

where ${}_2F_1$ is the hypergeometric function. This specifies a relation $\phi_0 = C\chi b^{\delta_-}$, where C is a constant which depends on H, δ_- and δ_+ . In this case the amplitude of the wave function is given by

$$I_R \simeq \frac{3\pi}{2H^2} - \frac{3\pi m^2 |C|^2 \chi^2 b^{2\delta_-}}{2H^4} + \mathcal{O}(\chi^4). \tag{1.41}$$

To find the measure, we split the extremizing actions (1.24) into a real I_R, and imaginary S, components. On the extremizing path, the Hartle Hawking wave function can be written as, [65],

$$\Psi_{HH}[q] \approx 2exp[-I_R[q]/\hbar]\cos(S[q]/\hbar)\,. \tag{1.42}$$

In the classical regime the wave function consists of two modes, one ingoing and the other outgoing the boundary of superspace, and I_R independent on q and given by (1.41). These modes describe respectively a contracting and expanding phase of the universe. The no-boundary wave function naturally have access to data both at $\mathcal{I}^+$ and $\mathcal{I}^-$.

AdS Representation

The dS representation is not the only useful representation of the saddle points. The saddle point action is given by the integral (1.32) and can be evaluated along any contour $C(0, \upsilon)$ connecting the SP to the endpoint υ. Consider now the contour C_A shown in Fig. 1.3. This contour gradually moves away from the C_D as the scalar field rolls down the hill. For large values of y the two contours are separated asymptotically by $\pi/(2H)$. At the point υ_a it turns and runs horizontally towards the endpoint υ. This contour has the same endpoint υ, the same action, and makes the same predictions as C_D, but the saddle point geometry is different. The fact that the two contours are shifted by $\pi/(2H)$ implies that, along C_A, the asymptotic behaviour of the field can be obtained from (1.35) by replacing u with $-iu$. Since a was real along the x_T curve it will be imaginary along the $x_T - \pi/(2H)$ curve, and therefore the asymptotic behaviour of the scale factor along C_A can be obtained from (1.35) by replacing $a(u)$ with $ia(u)$. Along the C_A the asymptotic form of the metric (2.5) is

$$ds^2 \approx -dy^2 - |c|^2 e^{2Hy} d\Omega_3^2, \tag{1.43}$$

and the asymptotic form of the scalar field is

$$\phi(y) \approx |\tilde{\alpha}| e^{-i\delta_- H\pi/2} e^{-\delta_- Hy} \equiv \alpha e^{-\delta_- Hy}. \tag{1.44}$$

The behaviour of the fields along this part of the contour resembles the form of the asymptotic solutions in an AdS background which is given by the Feffermann-Graham expansion, [62, 63]. The saddle point geometry along this part of the contour is that of an asymptotically AdS, spherically symmetric domain wall with a complex scalar field profile in the radial direction y. The negative signature means that, along this part of C_A, the action (1.32) acts as that of Einstein gravity coupled to a negative cosmological constant $-\Lambda$ and a negative potential $-V$, which explains why the AdS behaviour emerges. Eq. (1.44) shows that the asymptotic phase of the scalar field along C_A of the contour is universal and determined by the boundary condition that it is asymptotically real along the x_T curve.

In figure 1.4 we give a visual image of the two different representations of the complex saddle point.

Along the AdS contour, the action (1.24) is minus the action of Euclidean AdS, and therefore contains the usual diverging term due to the infinite volume of AdS space. In standard AdS/CFT usually one adds specific counterterms to extract the finite regular part, [66]. The counterterms are expressed in terms of the boundary geometry h_{ij}, and the boundary scalar field χ, and are given in

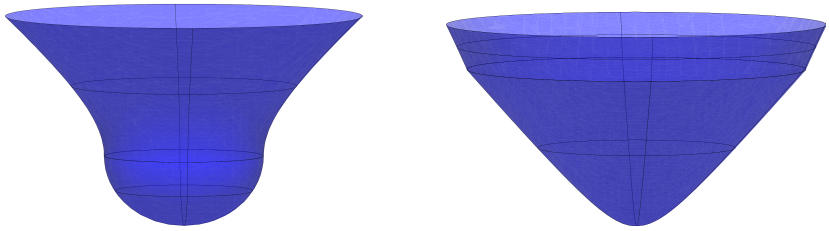

Figure 1.4: deSitter (left) and Anti-deSitter (right) representation of the complex saddle points.

four dimensions by

$$S_{ct} = -\int_{\partial\mathcal{M}} d^3x\sqrt{h}(2 + \frac{{}^3R}{2} + \frac{\chi^2}{2} + \mathcal{O}(\chi^3))\,, \tag{1.45}$$

where ${}^3R$ is the Ricci scalar evaluated on the boundary geometry h_{ij}. We clearly have

$$I_a(0, v_a) = -I_{DW}^{reg} + S_{ct} + \mathcal{O}(e^{-Hy_a})\,, \tag{1.46}$$

where $-I_{DW}^{reg}$ is the constant contribution to the action as the boundary is pushed to infinity, and it is equivalent to the regularized domain wall action typical of AdS/CFT.

The contribution to the saddle point action from the horizontal closing of the contour regulates the divergences. This follows immediately from the fact that the amplitude of Ψ_{HH} along the horizontal part of the dS contour tends to a constant. Therefore, the contribution from the horizontal closing of the contour must cancel the divergences appearing along C_A, and it must provide the phase of the wave function. Therefore, we must have

$$Re[I_h(v_a, v)] = -S_{ct} + \mathcal{O}(e^{-Hy_a})\,, \tag{1.47}$$

and so

$$Re[I(v)] = -I_{DW}^{reg}(v_a)\,, \tag{1.48}$$

hence,

$$I(v) = -I_{DW}^{reg} + iS_{ct}(v) + \mathcal{O}(e^{-Hy_a})\,. \tag{1.49}$$

To summarize, the real part of the action evaluated over complex dS saddle points is equal to the regularized AdS action. Further, the horizontal part of the contour regulates the volume divergences of AdS space and provides the phase needed for classicality.

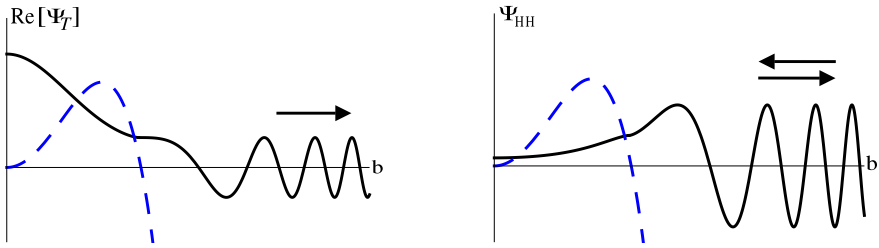

Figure 1.5: Qualitative behaviour of the tunneling wave function Ψ_T (left) and the Hartle-Hawking wave function Ψ_{HH} (right). The blue dashed curve shows a slice of the superpotential U in the presence of a positive cosmological constant.

1.2.3 No-Boundary Vs Tunneling

There are many qualitative and quantitative difference between the two proposals. A representative behaviour of the two wave functions is depicted in figure 1.5, where we considered the no-scalar field case. In this case the superspace is one-dimensional spanned by the coordinate b and the wave function is a function of b only.

When we introduce a scalar field, we can see from equation (1.39) that the no-boundary wave functions predicts higher probability for histories with a smaller potential, so with lower amount of inflation. This is in contrast with observations which suggest around sixty e-folds of inflation. Nevertheless, if we sum only over histories that contain our observational data at least once, we get a shift of the peak of the probability and the wave function predicts a sufficient amount of inflation, [67]. In contrast, the Tunneling wave function appears to be peaked around larger potential, and therefore naturally favours inflationary models.

1.2.4 Issues

As we have discussed above, the equations that specify the dynamic of the wave function in superspace admit more than one solution, and one needs to select only one by imposing initial conditions. The full cosmological measure specified by the Tunneling wave function or the no-boundary wave function are defined respectively in (1.20) and (1.23).

Once we have specified the measure, there are further issues. The sum over four manifolds is already difficult to define, and one usually considers each

admissible four-manifold separately. Further, the gravitational action is not bounded from below. The path integral does not converge if integrated over real Euclidean or Lorentzian metrics. To achieve convergence one needs to integrate over complex four-metrics $g_{\mu\nu}$. In this sense, even the terms "Euclidean" or "Lorentzian" are not properly correct, since they refer to complex geometries. The relation between the two wave functions is more subtle than a simple Wick rotation. We need to refer to (1.23) and (1.20) as two distinct objects, with different properties and therefore different predictions, which provides different probability measures for a given boundary configuration. An other issue is that the outcome of the path integral highly depends on the choice of the end-points in the complex plane.

So far we have specified solutions at the semiclassical level only. To uncover the mysteries of eternal inflation, we need a way to compute the full cosmological measure, in the hope that a theory of quantum gravity provides a smooth exit from eternal inflation, with a finite a reasonably smooth universe as the outcome. We will discuss this at the end of this thesis, while now we provide an alternative way to compute the full cosmological measure.

1.3 Beyond Semiclassicality: A Holographic Cosmological Measure

At the end of the last century, theorists realized that a property of string theory, and a supposed property of quantum gravity, is that the description of a volume of space can be thought of as encoded on a lower-dimensional boundary of the region. This idea is named "holographic principle" and was proposed originally by 't Hooft, [68], and subsequently Susskind gave a precise string theory interpretation, [69]. A first concrete example of this duality was proposed in 1997 by Maldacena [70], who conjectured that a gravity theory in $d+1$-dimensions, defined on AdS space, can be described in terms of a Conformal Field Theory which lives on the d-dimensional boundary. In particular, he showed that $\mathcal{N}=4$ Super Yang Mills, with a SU(N) gauge group, in four dimensions is dual to string theory in Euclidean $AdS_5 \times S^5$. A year later, Witten elaborated this idea and proposed a precise correspondence between field theory observables and those of supergravity, [71].

The AdS/CFT correspondence specifies how the parameters on the two sides of the duality are related to each other. On the string theory side we have two dimensionless parameters, the string coupling g_s and the curvature scale in string units, l_{AdS}/l_s, where $l_{AdS}=\sqrt{-3/\Lambda}$ and l_s is the string length. On the gauge theory side we have the rank of the gauge group, N, and the Yang-Mills

coupling g_{YM}. The relation between these quantities is given by

$$\frac{l_{AdS}}{l_s} = (4\pi g_s N)^{1/4} = \left(g_{YM}^2 N\right)^{1/4} . \tag{1.50}$$

There is an interesting limit, known as 't Hooft limit, when we consider $N \to \infty$ while keeping $g_{YM}^2 N \equiv \lambda$ fixed. The solutions describe classical gravity when l_{AdS} is large in string units, which translates to $\lambda \gg 1$ or, in other words, a strongly coupled field theory. On the other hand, stringy corrections of the geometry become important when l_{AdS} is very small in string units, which translates to $\lambda \ll 1$ (a weakly coupled dual field theory).

Further, a normalizable bulk field in AdS which falls off as shown in Eq. (1.44), corresponds to an operator $\mathcal{O}$ with scaling dimension $\frac{3}{2} - \sqrt{\frac{9}{4} + l_{AdS}^2 m^2}$, and with expectation value $< \mathcal{O} >= \alpha$. When the mass of the bulk scalar field is $m^2 = -2/l_{AdS}^2$, then the scaling dimension of the dual operator and its vacuum expectation value are integers, respectively one and two.

The statement that the gravitational and the field theory are equivalent is better understood in terms of the equivalence between the partition functions of the two theories,

$$Z_{\mathcal{O}}[\tilde{h}_{ij}, \alpha]_{QFT} = Z_{AdS}[\tilde{h}_{ij}, \alpha] . \tag{1.51}$$

The power of this correspondence is that it is a weak/strong duality, as we have discussed above. One can study a weakly coupled field theory (where we do have control of calculations) to get information about a strongly coupled gravity theory and vice versa. For example, if we consider the gravity theory in the semiclassical approximation (i.e. large N limit of the duality), the dictionary reduces to

$$Z_{\mathcal{O}}[\tilde{h}_{ij}, \alpha]_{QFT} \approx e^{-I_{DW}^{reg}[\tilde{h}_{ij}, \alpha]/\hbar} . \tag{1.52}$$

The opposite is also true. A weakly coupled field theory can be regarded as a strongly coupled gravity theory, i.e. which includes quantum gravity effects.

This duality is very well understood in bulk theories whose background is AdS. There are many reasons why this is the case. String theory more directly describes AdS geometries in the holographic limit, and more elaborate techniques need to be employed to uplift the AdS vacuum to dS. An other reason is that AdS has only one spacelike boundary where the dual theory might live.

Observations suggest that we live in a universe with a positive cosmological constant. Therefore it is natural to ask whether the holographic principle can be extended and understood in gravity theory whose background is dS_{d+1}. This is not an easy task, since many problems arise immediately. First of all, dS space has two timelike boundaries. A second issue is that dS space has an event horizon. A physical observer in this space is not able to see the entire universe,

in particular does not have access to the entire boundary. Any known attempt to incorporate de Sitter space in string theory leads to a deSitter space which is metastable [72, 73, 74, 75, 76]. If so, there might not be any future boundary at all. One of the key questions for asymptotically dS universe is whether we can define precise observables encoded on its boundary, [77, 78].

Many argued that there might not exist any dS/CFT correspondence after all and that this might be a fundamental property of string theory. Other theorists tried to derive the dS/CFT correspondence from string theory, employing different types of dualities, [79, 80]. Any attempt to define the dS/CFT correspondence has to do with some sort of derivation from the better known AdS/CFT correspondence.

In this way we can use standard AdS/CFT, deformed by complex operators, to evaluate the probability measure for a classical Lorentzian dS history. The dictionary can be written schematically as

$$\Psi_{HH}[h_{ij},\chi] = \frac{1}{Z_{QFT}[\tilde{h}_{ij},\alpha]} \exp\left(iS_{ct}[h_{ij},\chi]/\hbar\right) , \tag{1.53}$$

where the sources $\tilde{h}_{ij}, \alpha$ are locally related to the asymptotic behaviour of the fields along the AdS part of the contour in Figure 1.3. To make the comparison more explicit one can write the wave function (1.5) in terms of the asymptotic variables α or β. The procedure is similar to the Fourier transformation of ordinary quantum mechanics, and the results can be found in the Appendix A.1. For more details we refer to [81].

The duality (1.53) has been shown to be valid at the semiclassical level only, but it has been conjectured to be valid also beyond the saddle point approximation. If that is the case, and if we have a model where the AdS/CFT dual is known explicitly, we might have a concrete realization of the dS/CFT duality which provides an alternative way to compute the full cosmological measure. A concrete example of this duality is provided by ABJM theory which admits AdS_4 vacuum solutions in the large N limit, [82]. The dictionary (1.53) states that we can evaluate the probability for a dS inflationary universe directly from the partition function of ABJM in the presence of certain relevant complex deformations. Unfortunately, an explicit form of the partition function of ABJM is not feasible at the moment, and we need to proceed in a different way.

In ordinary AdS/CFT, the Vasiliev theory of higher spin is dual to the $O(N)$ vector model of interacting scalars. This duality is suggested by the fact that the $O(N)$ vector model has a singlet sector (in the large N factorization) with conserved currents of the form: $J_{\mu_1....\mu_s} = \Phi_i \partial_{(\mu_1}...\partial_{\mu_s)}\Phi_i$ for integer spins s, which is precisely the spectrum of massless higher spin fields in minimal bosonic higher spin gravity in 4D. In particular, according to the general rules of

AdS/CFT, conserved currents in a CFT are dual to corresponding gauge fields in AdS. Hence, a conserved spin 1 current is dual to a spin gauge field in the bulk. The conserved stress tensor is dual to the graviton. And this generalize to all spins. One can show, [84], that the dual to the free $O(N)$ vector model must have a cubic graviton coupling (which is different from Eintein gravity but can be obtained by adding higher derivative terms to the Einstein action, which is indeed a feature of Vasiliev theory, which therefore suggests the duality).

Recently Anninos et al. [83] have put forward a precise realisation of dS/CFT that is potentially valid beyond the semiclassical approximation. Their proposal relates Vasiliev's theory of higher spin gravity in four-dimensional de Sitter space to a Euclidean, three dimensional conformal field theory with anti-commuting scalars and $Sp(N) \equiv O(-N)$ symmetry. A typical problem with dS/CFT is that one naively has operators with complex weights. It is not the case of the $Sp(N)$ vector model (and thus of Vasiliev theory) because an operator in the free theory of this model has conformal dimension 2, and expectation value $< \mathcal{O} >= 1$. This is very special since, as previously discussed in this section, it corresponds to a bulk scalar field with mass $m^2 = 2/l_{dS}^2$. Any different choice of the bulk scalar field mass would lead to a generically complex weights (and a different field theory dual). In this sense Vasiliev theory and the $Sp(N)$ vector model represent a very special case. Further, the bulk scalar field mass is not arbitrary, but constrained by the holographic dual. We will use this particular value of the scalar field mass in Chapters 4 and 5.

The work of Anninos et al. [83] has made possible the first precise holographic calculations of the wave function of a Vasiliev universe, by evaluating the partition function of the $Sp(N)$ CFT as a function of various deformations. It was found however that the resulting measure exhibits several divergences that are unexpected in well-defined, stable theories [85, 86]. This includes divergences associated with mass deformations in the dual on S^3 and with the topological complexity on more complicated future boundaries.

We will compare our results with these field theories dual to Vasiliev higher spin theory of gravity. A comparison between Einstein gravity with the dual of Vasiliev's gravity, might appear odd for most, but it can be interesting for two reasons. It is crucial to understand if the divergences found in the $Sp(N) \equiv O(-N)$ model are also present in Einstein gravity, and what is their physical implication on classical cosmology. The second reason is that, if the two theories share some similarities, we can have access to a qualitative behaviour of the wave function of the universe beyond the saddle point approximation.

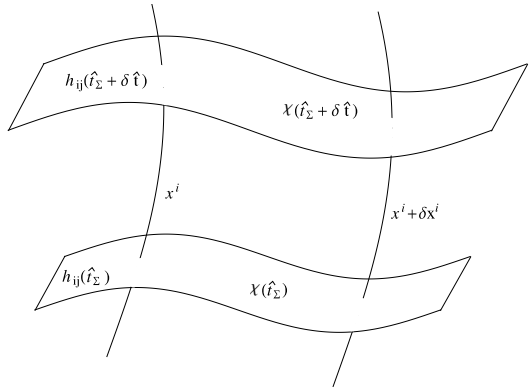

Figure 1.6: Pictorial representation of the classical evolution of boundary data on a surface Σ at $\hat{t} = \hat{t}_\Sigma$, and their evolution at a subsequent instant of time.

1.4 From Quantum to Classical

A quantum system is regarded as classical when the wave function is strongly peaked about one or more classical configurations. In the latter case, a classical behaviour is achieved if the quantum mechanical interference between those states is negligible (those states should decohere), [54, 55].

The way we interpret the wave function in quantum cosmology is to regard a strong peak of the wave function as a prediction, [87, 88, 64]. The wave function is peaked about some correlation between coordinates and momenta when it is in the form e^{iS}. A **classical history** is predicted whenever the evolution of the three-geometry and scalar field configurations in time is governed by the classical Lorentzian Einstein equations, where time is only defined in context of that specific history.

Classical gravity can be described in terms of data living on a space-like surface Σ. The Einstein's equations (1.1) determine their evolution in time. In minisuperspace models, the data (h_{ij}, χ) only depend on the location in time of the surface. Say we measure h_{ij} and χ at a given time $\hat{t} = \hat{t}_\Sigma$. A dynamic theory, such as general relativity, gives their value at a subsequent instant of time $\hat{t} = \hat{t}_\Sigma + \delta\hat{t}$.

In figure 1.6, we give a pictorial representation of this construction. If we evolve the Einstein's field equations (1.1) in time, we find a set of values for the fields $q^A \equiv (h_{ij}, \chi)$, with $A = 1, 2$. In minisuperspace models, this class of paths is subjected to a single constraint. The underlined theory, general relativity, is a

parametrized theory, in the sense that "time" is already contained amongst the dynamical variables h_{ij}, χ and for this reason the wave function (1.5) does not depend on the time coordinate label $\hat{t}$, but only on the boundary fields h_{ij}, χ. Since the three-surfaces are compact, their intrinsic geometry fixes their location on the four-manifold, [89, 90, 91, 92]. This leads to the classical Hamiltonian constraint, [52],

$$H = \frac{1}{2} G_{AB} \pi^A \pi^B + U(q) = 0 \,, \tag{1.54}$$

where the classical momenta are defined as

$$\pi_A = \frac{\delta}{\delta q^A} \,, \tag{1.55}$$

In the region of superspace where the classicality condition (1.15) holds, the WDW equation (1.7) reduces to the classical Lorentzian Hamilton-Jacobi equation of the classical theory, (1.54). A wave function in the form $\Psi \sim e^{iS}$ is a solution of the classical Hamiltonian constraint (1.54). In this region, the wave function rapidly oscillates with a conserved probability measure. A classical history of the universe is not something that is imposed by hand, rather it is predicted.

1.4.1 Lorentzian Histories

How to interpret the classical spacetime and field configuration predicted by the wave function? What is the physics encoded in the phase of the wave function? To answer these questions, we evaluate the classical Hamilton-Jacobi field equation, (1.54), for a wave function in the form e^{iS}. We use the value of the boundary field configurations b, χ as boundary conditions and we evaluate the equations back in time.

To summarize: we evaluate the semiclassical probability measure over complex saddle points of the Einstein-Hilbert action, by looking for those regions of minisuperspace where the wave function shows a classical behaviour. The coordinates of minisuperspace, of this region, provide a set of boundary field configurations b, χ that we use as a set of boundary conditions to solve the classical Lorentzian equation of motion back in time. These are in the form

$$\begin{aligned} &- \dot{b}^2 + 1 - H^2 b^2 + b^2 \dot{\chi}^2 - 2 b^2 V = 0 \,, \\ &- \ddot{\chi} - 3 \frac{\dot{b}}{b} \dot{\chi} + \frac{dV}{d\chi} = 0 \,, \end{aligned} \tag{1.56}$$

where $\dot{f} = df/d\hat{t}$, and $\hat{t}$ is the Lorentzian time defined on that particular history. Classical Lorentzian dS space in the global patch, (1.3), provides a solution to equation (1.56) in the no-scalar field case.

Hence, complex saddle points defining the wave function provide a semiclassical measure for a given history which is encoded in the phase of the wave. The behaviour of that history can be evaluated by evaluating the equations of motion along the vertical part of the dS contour depicted in figure 1.3, which is equivalent to solve (1.56).

There are several key points, [64]:

- A Lorentzian history might be bouncing in the past or have an initial (or final) singularity.

- Singularities in the classical history should not be regarded as a signal of the breaking down of the quantum theory. Rather they should be thought as a breaking down of the approximation.
- The wave function predicts probabilities for Lorentzian histories and not for their initial data. In a certain sense, we can say that the wave function resolves classical singularities.
- The classical histories should not be confused with the saddle points that provide the steepest descents approximation to the integral defining the wave functions. The classical histories are real and Lorentzian, while the saddle points are generally complex. The Lorentzian histories may bounce in the past, for example they can have a period of contraction from an infinity in the past, bounce and re-expand to another one in the future. The saddle points have only one infinity.

We should look at the wave function of the universe as an object that gives probabilistic weight to the possible histories of a quantum universe.

1.5 Open Questions

In the course of this thesis we will use the $O(N)$ vector model of interacting scalar fields in 3-dimensions. This model is conjectured to be dual to Vasiliev's higher spin gravity with asymptotically AdS_4 boundary. We will consider different types of deformations. Here, we review the main ingredients and we will show more details in the next chapters.

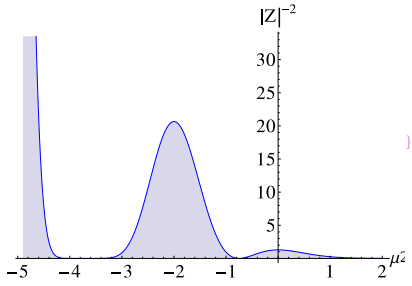

Figure 1.7: $|Z_{free}|^{-2}$ as a function of the mass deformation.

1.5.1 Free O(N) Vector Model Massed

We consider the free $O(N)$ vector model on a Euclidean three sphere of radius r, and a finite constant mass deformation μ^2. The action for this model is, [93],

$$S = \frac{1}{2}\int d^3x\sqrt{g}\left[(\nabla\vec{\Phi})^2 + \frac{R}{8}\vec{\Phi}^2 + \mu^2\vec{\Phi}^2\right], \tag{1.57}$$

where $\vec{\Phi}$ is an N-component field which transforms as a vector under $O(N)$ rotations, R is the Ricci scalar and ∇ is the covariant Laplacian operator of S^3.

The partition function of this model is known explicitly [94],

$$\begin{aligned}\log Z_{free}[\mu^2] = \\ -\frac{N}{48\pi^2}\Big\{6\pi^2(1-4r^2\mu^2)\log\left(1-e^{-i\pi\sqrt{1-4r^2\mu^2}}\right) + 12Li_3\left(e^{-i\pi\sqrt{1-4r^2\mu^2}}\right) \\ + i\pi\sqrt{1-4r^2\mu^2}\left[\pi^2(1-4r^2\mu^2) + 12Li_2\left(e^{-i\pi\sqrt{1-4r^2\mu^2}}\right)\right]\Big\}.\end{aligned} \tag{1.58}$$

In figure 1.7 we show the inverse squared of the partition function of the free model sourced by a mass deformation of conformal dimension two, related to the holographic no-boundary probability. The holographic probability measure diverges for negative mass deformation.

The mass deformation μ^2 has conformal dimension two, and therefore it is related to the wave function expressed in terms of an operator of conformal dimension $\delta_+ = 2$, (i.e. wave function in the $\tilde{\beta}$ basis). The dictionary relates $\mu^2 \propto -\tilde{\beta}$. Even if the dual of this model is Vasiliev's higher spin theory of gravity, [93], the divergence appearing at negative mass deformations rises the question whether or not this divergence can be observed in the context

of Einstein's gravity and, if so, what is its interpretation and implication on the Lorentzian histories. In the final chapters of this work we will address this question.

1.5.2 Critical O(N) Vector Model

One can consider the free theory and deform it with a relevant double trace deformation $\lambda(\vec{\Phi}\cdot\vec{\Phi})^2/(8N)$, where λ is a constant of conformal dimension one, whose action is [95, 96]

$$S=\frac{1}{2}\int d^3x\sqrt{g}\left[(\nabla\vec{\Phi})^2+\left(\frac{1}{8}R+\lambda\sigma\right)\vec{\Phi}^2+\frac{\lambda(\vec{\Phi}\cdot\vec{\Phi})^2}{2N}\right]. \tag{1.59}$$

In the limit $r\lambda\to\infty$ and $N\to\infty$ the partition function of this model is related to the partition function of the free theory by a Fourier type transformation [85]. One introduces an auxiliary field $N\tilde{\mu}=\vec{\Phi}\cdot\vec{\Phi}$, and the action can be rewritten in terms of single trace operators

$$S=\frac{1}{2}\int d^3x\sqrt{g}\left[(\nabla\vec{\Phi})^2+\left(\frac{1}{8}R+\lambda\sigma+\lambda\tilde{\mu}\right)\vec{\Phi}^2-\frac{N\lambda\tilde{\mu}^2}{2}\right]. \tag{1.60}$$

Integrating out the $\vec{\Phi}$ field one obtains

$$Z_{crit}[\sigma]=e^{\frac{N\lambda}{2}\int d\Omega_3\sigma^2}\int\mathcal{D}\mu^2\exp\left[N\int d\Omega_3\left(\frac{\mu^4}{2\lambda}-\sigma\mu^2\right)\right]Z_{free}[\mu^2], \tag{1.61}$$

where $\mu^2\equiv\lambda\sigma+\lambda\tilde{\mu}$. The first factor on the r.h.s. in (1.61) is local. At large N one can evaluate the integral (1.61) in the saddle point approximation. Using (1.58) the saddle point equation reduces to

$$\frac{16\pi r^2\mu^2}{r\lambda}+16\pi r\sigma=\sqrt{1-4r^2\mu^2}\cot\left(\frac{\pi}{2}\sqrt{1-4r^2\mu^2}\right). \tag{1.62}$$

In the large $r\lambda$ regime the first term vanishes and the saddle point equation can be solved analytically for small deformations σ. The result can be found in [85, 94], and we will provide a more detailed discussion in the next chapter. The partition function of this model does not show any divergence. The deformation is of conformal dimension one and therefore is dual to a gravity theory with a source of dimension $\delta_-=1$, i.e. wave function in the $\tilde{\alpha}$ basis. The dictionary relate $\sigma\propto-i\tilde{\alpha}$. This model is dual to Vasiliev's gravity, [95, 96], nevertheless a comparison with Einstein gravity might give some insights on the non-perturbative description of the wave function. We will explore this later.

1.5.3 Free O(N) Vector Model Squashed

The free O(N) vector model can be defined on a (double) squashed background. The squashing introduce a geometrical deformation. The squashed geometry is described by the line element

$$ds^2 = \frac{r_0^2}{4}\left((\sigma_1)^2 + \frac{1}{1+A}(\sigma_2)^2 + \frac{1}{1+B}(\sigma_3)^2\right), \tag{1.63}$$

where

$$\begin{aligned}\sigma_1 &= -\sin\psi d\theta + \cos\psi\sin\theta d\phi\ ,\\ \sigma_2 &= \cos\psi d\theta + \sin\psi\sin\theta d\phi\ ,\\ \sigma_3 &= d\psi + \cos\theta d\phi\ ,\end{aligned} \tag{1.64}$$

are group invariant differential forms of the round sphere. If we consider the square of the same σ_i, as in equation (1.63), we have $SU(2)\times SU(2) = SO(4)$ isometry, i.e. a round sphere. Cross products between the σ_i, i.e. $\sigma_1\sigma_2$ would break this symmetry to $SU(2)\times U(1)$. Further, off-diagonal terms might give a metric that might not even be continuously deformed to a round sphere. These were the reasons why the authors of [98] considered only the ansatz (1.63), and for the same reasons we will consider only this ansatz in chapters 4 and 5. The range of the coordinates in equation (1.64) are, $0 \le \theta \le \pi$, $0 \le \phi \le 2\pi$ and $0 \le \psi \le 4\pi$. The factors A and B parametrize the squashing.

The free energy of this model was shown to be peaked around the round sphere case when a single squashing is applied [85, 97, 98, 99, 100]. At negative squashing, there is an interesting regime where the boundary Ricci scalar changes sign and becomes negative. This will be the subject of chapter 4 and 5.

1.5.4 U(N) Vector Model

The O(N) theory can be modified to a U(N), if we consider the background geometry to be $S^1\times S^2$, with metric

$$ds^2 = \Theta^2 d\lambda^2 + d\Omega_2^2\,, \tag{1.65}$$

where Θ is the relative size of the two sphere, and λ has periodicity one. The partition function is dependent on Θ. There are interesting regimes. When $1/\Theta \ll \sqrt{N}$, the partition function is, [101],

$$\log Z_{free}[\Theta] = -N^2\log 2\,, \tag{1.66}$$

and when $1/\Theta \gg \sqrt{N}$ the partition function reduces to, [101],

$$\log Z_{free}[\Theta] = \frac{4\zeta(3)N}{\Theta^2} \,. \tag{1.67}$$

This field theory partition function suggested that dS and AdS are not in general related by analytic continuation at the nonperturbative level, though they might be in many cases in perturbation theory, [85].

1.6 Outline of the Thesis

In the remainder of this thesis, we will address some of the problems we have discussed so far. We will explore in more details several properties of the wave functions of the universe and its holographic interpretation. We now give an outline of this thesis work with a brief revision of the main topics and results discussed through the thesis. Every chapter is based on a personal research work of the author.

In chapter 2 we provide a holographic formulation for the Tunneling wave function. In analogy with the Hartle-Hertog proposal for the no-boundary wave function, we write the Tunneling amplitude in terms of the partition function of field theories usually employed in the context of AdS/CFT. We compare the Tunneling measure in different field basis with the partition functions (1.58) and (1.61). We perform a perturbative calculation and we explore whether a diverging behaviour similar to (1.58) can be found in Einstein gravity. We discuss the holographic interpretation of the two wave functions in the hope that holography might give some insights on which wave function better describes our own universe.

In chapter 3, we analyze a divergence appearing in Einstein gravity similar to the one observed in (1.67). In Einstein gravity a similar divergence was found in the case of saddle points predicting Lorentzian histories that are Schwarzschild de Sitter black holes [85]. We will analyze this diverging behaviour in the context of the Hartle-Hawking state, and of the Tunneling state. We study the Lorentzian histories predicted by these saddle points, and the physical interpretation of these divergences, and we resolve it.

In chapter 4 and 5, we explore in further details the comparison of the divergence found in (1.58) and Einstein gravity. The relation between the source and the vacuum expectation value of the dual theory defines the potential for the scalar field in the gravity model, [102]. We find this potential and we study the solutions. We also introduce two squashing parameters and we generalize what we have discussed in section 1.5.3. The analysis in chapter 4 is standard AdS/CFT and

with this analysis we can study a generalization of the Taub-NUT/Bolt phase transition in the presence of scalar hairs and a further squashing. We combine the squashing and the massive deformation and we study the behaviour of the partition function and of the $O(N)$ vector model in this three-dimensional portrait. The presence of the squashing introduces a region in configuration space where the boundary Ricci scalar changes sign and becomes negative. In chapter 5 we focus on the cosmological solutions that we can construct from this model. We study the Lorentzian histories of these solutions which are of a mixmaster universe in the presence of a scalar field in a non-trivial potential, and we evaluate their semiclassical probability in the no-boundary state. Finally, we evaluate the full cosmological probability by looking at the holographic dual. This provides a toy model to support the Hartle-Hawking conjecture about a smooth exit from eternal inflation [103].

Chapter 2

Holographic Tunneling Wave Function

2.1 Introduction

The dS/CFT proposal [104, 105, 106, 107] conjectures that 'the' wave function of the universe with asymptotic de Sitter (dS) boundary conditions is given in terms of the partition function of a Euclidean CFT deformed by various operators. But which wave function of the universe does the CFT select? Alternatively dS/CFT may be able to accommodate different wave functions. Some evidence for this comes from the explicit higher spin version of dS/CFT [83] where the partition functions appear to exhibit certain features reminiscent of the Hartle-Hawking wave function in Einstein gravity [85], whereas other properties have a natural interpretation in the tunneling state [65].

The potential in the Wheeler-DeWitt (WDW) equation in an asymptotically AdS context is everywhere positive. Generic solutions Ψ thus have a growing and a decaying branch in the large volume regime. A closer look at the behavior of the Hartle-Hawking wave function in its AdS domain shows it corresponds to a very special, decaying wave function in AdS [108, 109]. This is closely connected to the fact that the holographic Hartle-Hawking measure involves the inverse of the AdS/CFT dual partition function [110].

In this chapter we investigate whether there are reasonable quantum states in cosmology corresponding to the growing branch of AdS wave functions. In a sense one might argue such states have a cleaner holographic interpretation,

because the dual theory in AdS/CFT most directly computes the growing branch of bulk wave functions only. Indeed, the local surface terms one usually adds to the bulk action to extract information essentially eliminate the decaying branch.

We find that Vilenkin's tunneling wave function [57, 56], in the semiclassical approximation and up to local surface terms, is equivalent to the growing branch of the most natural wave function in AdS, in which the amplitudes of boundary configurations are specified by the partition function of a dual CFT with certain finite deformations. To show this we again exploit the complex structure of the bulk saddle points. This allows us to establish a relation between the tunneling wave function with asymptotic dS boundary conditions and an AdS wave function which we interpret in the context of AdS/CFT. As a first test of our proposal for a holographic tunneling state we compute the partition function of the $O(N)$ vector model on the round three sphere as a function of a homogeneous, finite mass deformation. We do this both for the critical and for the minimal model. We find the partition functions in both cases qualitatively agree with the behaviour of the minisuperspace tunneling wave function in Einstein gravity coupled to a positive cosmological constant and a massive scalar field, and we interpret this as evidence in favour of our proposal.

As solutions to the WDW equation the tunneling and Hartle-Hawking wave functions obey different boundary conditions. As a consequence they specify a different cosmological measure, which translates into different predictions for what we should expect to observe[1]. A controversial feature of the tunneling wave function has been whether it actually predicts that the amplitude of inhomogeneous fluctuations is suppressed, as required by observation. In order for this to be the case the fluctuation action must enter in the wave function with a different sign than the action for the background histories. This sign change has been motivated on the basis of regularity of the wave function [57, 112, 113]. We revisit this point in the Discussion below and conclude there is no evidence for this from a holographic viewpoint.

2.2 The Tunneling Wave Function

We consider Einstein gravity coupled to a positive cosmological constant Λ and a scalar field moving in a positive potential V. A quantum state of the universe in this model is given by a wave function Ψ on the superspace of all three-metrics $h_{ij}(\vec{x})$ and field configurations $\chi(\vec{x})$ on a closed spacelike surface Σ. It is described by the wave functional (1.5).

[1] See e.g. [111] for a sharp illustration of this.

All wave functions must satisfy an operator implementation of the classical constraints. These include the Wheeler-DeWitt (WDW) equation $\mathcal{H}\Psi = 0$. To solve the WDW equation one must specify boundary conditions on Ψ. A choice of boundary conditions specifies a quantum state of the universe, which together with the dynamics provides a predictive framework of cosmology.

In the tunneling approach to quantum cosmology [56, 57], the boundary condition on the wave function is that Ψ_T in the large three-volume regime of superspace should include only outgoing waves, describing expanding universes. Physically this boundary condition implements the idea that our expanding classical universe originated in a quantum tunneling event. The motivation for this comes from an analysis in homogeneous isotropic minisuperspace where the WDW equation has a potential $U(b)$ of the form (cf. Fig. 1.5)

$$U(b) = b^2 - b^4 V_\Lambda(\chi), \tag{2.1}$$

with b the scale factor and $V_\Lambda(\chi) \equiv \Lambda/3 + V(\chi)$. The WDW equation therefore has growing and decaying solutions in a classically forbidden region $0 < b < b_c$ under the barrier, where $b_c = 1/\sqrt{V_\Lambda(\chi)}$, but it has outgoing and ingoing wave solutions - corresponding to expanding and contracting universes - for $b \geq b_c$. One can thus envision a tunneling process from $b = 0$, or 'nothing', to a closed universe of radius b_c which then subsequently expands. This selects the outgoing solution at large scale factor. In the semiclassical approximation and at large volume the resulting wave function will then oscillate rapidly and be of the form (1.22). The tunneling probabilities are approximately given by [57]

$$\mathcal{P} \sim \exp\left(-2\int_0^{b_c} db\sqrt{U(b)}\right) \approx \exp\left(\frac{-3\pi}{V_\Lambda(\phi_0)}\right), \tag{2.2}$$

where ϕ_0 is the absolute value of the scalar at the $b = 0$ boundary (cf. Section 2.4). Once a universe nucleates it evolves classically and expands in an inflationary manner. The boundary condition that the wave function should include only outgoing waves in the large volume limit implies it is a linear combination of the growing and decaying solutions in the classically forbidden region[2]. However the nucleation probabilities (2.2) are specified by the decaying solution under the barrier [57].

This is in sharp contrast with the Hartle-Hawking boundary conditions which select the growing solution under the barrier. This yields a real linear combination of ingoing and outgoing waves in the large volume region, describing a time-symmetric ensemble of contracting and expanding universes. Relative

[2]A more formal definition of the tunneling wave function in terms of a Lorentzian path integral was put forward in [114]. However this can only be evaluated in the semiclassical limit we discuss here.

probabilities in the Hartle-Hawking state are specified by the amplitude of the growing solution when it emerges from the classically forbidden region. As a result both wave functions differ in their predictions: the tunneling wave function (2.2) favours universes in which the scalar field starts high up its potential, leading to a long period of inflation, whereas the Hartle-Hawking wave function favours histories with a low amount of inflation [58].

In the semiclassical approximation both wave functions can be evaluated using saddle points. These are complex solutions of the Einstein equation, discussed in more detail below, which interpolate between 'nothing' at the South Pole of an approximate four-sphere of radius $\sim 1/\sqrt{V(\phi_0)}$ to a Lorentzian, classical, inflationary universe. The saddle points specifying Ψ_T are the same as those defining the semiclassical Hartle-Hawking wave function. However they are weighted differently in both wave functions, because they behave very differently under the barrier. The Hartle-Hawking probabilities are of the form $|\Psi_{HH}|^2 \sim \exp(-2I_E)$, where $I_E \approx -3\pi/|V_\Lambda(\phi_0)|$ is the real part of the Euclidean saddle point action.

It is subtle, however, to implement the tunneling boundary condition in the full superspace. A naive extension of the above framework to include perturbations around homogeneous isotropic configurations does not yield a normalizable probability distribution for perturbations. For this reason it has been argued [57, 112, 113] that the probabilities for perturbations in the tunneling state are given by the growing branch of the wave function under the barrier, as in the Hartle-Hawking state. One motivation for our work is to revisit this point from a holographic perspective. We return to this in the Discussion.

2.3 Representations of Complex Saddle Points

We briefly review the saddle point geometries defining the semiclassical tunneling wave function. This construction is equivalent to the one discussed in Sec. 1.2.2 in the case of the no-boundary wave function, and here we highlight the main differences.

The Lorentzian action S_L of our model is given in (1.21).

We consider the line element of a closed three-geometry as the one given in equation (1.25). Hence, $\Psi_T = \Psi_T(b, \tilde{h}_{ij}, \chi)$.

The compact saddle point geometries that specify the semiclassical approximation to the wave function are of the form

$$ds^2 = -N^2(\lambda)d\lambda^2 + g_{ij}(\lambda, \vec{x})dx^i dx^j, \tag{2.3}$$

where $\{\lambda, x^i\}$ are four real coordinates on the real manifold $\mathcal{M}$. We take $\lambda = 0$ to locate the South Pole (SP) of the saddle point, where the geometry caps-off, and $\lambda = 1$ to locate the boundary Σ of $\mathcal{M}$. Regularity at the SP together with the boundary condition that the geometry and field matches the real boundary configuration $(b, \tilde{h}_{ij}, \chi)$ on Σ mean that the saddle points are generally complex solutions of the Einstein equation.

The Einstein equation can be solved for $\{g_{ij}(\lambda, \vec{x}), \phi(\lambda, \vec{x})\}$ for any complex $N(\lambda)$ that is specified. As for the no-boundary wave function, different choices of $N(\lambda)$ yield different geometric representations of the same saddle point. If we define the complex variable

$$\tau(\lambda) \equiv \int_0^\lambda d\lambda' N(\lambda') + \tau_0, \tag{2.4}$$

then different choices of $N(\lambda)$ correspond to different contours in the complex τ-plane. Contours begin at the SP at $\lambda = 0$, with $\tau(0) \equiv \tau_0$, and end at the boundary $\lambda = 1$, with $\tau(1) \equiv \upsilon$. Each contour that connects τ_0 to υ yields a different representation of the same complex saddle point. This freedom in the choice of contour gives physical meaning to a process of analytic continuation — not of the Lorentzian histories themselves — but of the saddle points that define their probabilities.

In the next section we recall that this can be used to identify two different useful representations of all saddle points corresponding to asymptotically locally de Sitter, classical, Lorentzian histories. In one representation (dS) the interior saddle point geometry behaves as if the cosmological constant and the scalar potential were positive. In the other (AdS) the Euclidean part of the interior geometry behaves as if these quantities were negative, and specifies an asymptotically locally AdS space. Asymptotically Lorentzian de Sitter universes and Euclidean anti-de Sitter spaces are thereby connected in the semiclassical wave function.

The action of a saddle point is an integral of its complex geometry and fields, which includes an integral over complex time τ. Different contours for this time integral each yield the same amplitude of the boundary configuration the saddle point corresponds to. This provides the basis for the holographic form of Ψ_T as we now discuss.

2.4 Homogeneous Minisuperspace

We are interested in the tunneling wave function at large volume. In this regime the semiclassical approximation to the WDW equation holds and implies an

asymptotic expansion of the wave function which is essentially equivalent to the asymptotic expansion of solutions to the Einstein equation with asymptotic dS boundary conditions [108, 109]. We can therefore work directly with the asymptotic saddle point equations to study the asymptotic structure of Ψ_T.

We begin by considering $O(4)$ invariant saddle points for which $\tilde{h}_{ij}(\vec{x})$ is fixed to be the metric of a round unit three sphere γ_{ij}. Homogeneous and isotropic minisuperspace is thus spanned by the scale factor b and the homogeneous value of the scalar field χ, and $\Psi = \Psi(b, \chi)$.

The line element of the four-geometries that contribute to the minisuperspace wave function can be written as

$$ds^2 = -d\tau^2 + a^2(\tau)\gamma_{ij}dx^i dx^j \tag{2.5}$$

and the saddle point equations implied by the action (1.21) become (1.31).

Solutions specify functions $a(\tau)$ and $\phi(\tau)$ in the complex τ-plane. A contour $C(\tau_0, \upsilon)$ representing a saddle point connects the SP at τ_0 to a point υ where $a(\upsilon)$ and $\phi(\upsilon)$ take the real values b and χ respectively. For any such contour the on-shell action is given by

$$S_L = -\frac{3\pi}{2}\int_{C(\tau_0,\upsilon)} d\tau a\left[a^2\left(H^2 + 2V(\phi)\right) - 1\right]. \tag{2.6}$$

In terms of the variable $u \equiv e^{-H\tau} \equiv e^{-H(y+iz)}$ the large volume regime corresponds to the large y limit. The asymptotic expansions in powers of u of the scale factor and field are the same as for the no-boundary wave function and are given by (1.33), and (1.34).

2.4.1 dS representation of saddle points

At large volume the wave function predicts an ensemble of classical, Lorentzian histories. Classical histories correspond to curves in the complex τ-plane along which both the scale factor and field are real. It was found in [64] that in the above parameterisation all curves corresponding to classical histories asymptote to a constant value z_f[3].

[3]In [64] these curves were found by starting at the SP with a complex value of the scalar field $\phi(\tau_0)$. By tuning the phase of $\phi(\tau_0)$ together with the value of z_f they found all asymptotically vertical curves $z = z_f$ along which a and ϕ are both real and the classicality conditions satisfied. There is one such curve, defining one classical Lorentzian history, for each value $|\phi(\tau_0)| \equiv \phi_0$. In a single field potential this yields a one-parameter family of homogeneous and isotropic, asymptotically de Sitter, classical Lorentzian histories.

This can also be seen from the asymptotic expansions (1.33) and (1.34), which to leading order in u can be written as (1.35).

The condition that a and ϕ are both real in the large volume limit along a constant value z_f requires that

$$\theta_c = -Hz_f, \qquad \theta_\alpha = \delta_- Hz_f. \tag{2.7}$$

Then along the $z = z_f$ curve we have

$$ds^2 \approx -dy^2 + |c|^2 e^{2Hy}\gamma_{ij}dx^i dx^j, \qquad \phi \approx \tilde{\alpha}e^{-\delta_- Hy}. \tag{2.8}$$

Hence along this contour y acts as a time coordinate and the metric represents an asymptotic Lorentzian de Sitter universe with a slowly decaying scalar field. The asymptotic contribution to the saddle point action is given by the integral (2.6) along the curve $z = z_f$. It is immediate that there will be no contribution to the amplitude A of the wave function from this part of the contour: The integrand in (2.6) is real as is $d\tau = dy$. Instead this part of the contour yields a large negative contribution to the phase of the wave function, as required by the outgoing tunneling boundary conditions. Thus Ψ_T oscillates rapidly with an approximately constant amplitude and describes an expanding, inflationary history.

It does not follow from the above analysis that the tuning (2.7) is possible with regularity conditions at the origin and therefore that the saddle points actually exist. However [64] have shown they do. In the neighbourhood of the SP at $\tau = \tau_0$ the $O(4)$ invariant saddle point solutions take the form (1.38).

Taking $\tau_0 \approx i\pi/(2\sqrt{V_\Lambda(\phi_0)})$ and defining a contour C_D that first runs from τ_0 to $z_f = 0$ along the z-axis and then along the y-axis yields a geometric representation of the saddle points in which an approximately Euclidean four sphere is smoothly joined onto a classical, expanding Lorentzian dS universe. This dS representation is illustrated in Fig 2.1(a).

The action integral over the Euclidean regime determines the amplitude A of the corresponding classical history and is approximately given by [57]

$$\log A \approx -\frac{3\pi}{2V_\Lambda(\phi_0)}. \tag{2.9}$$

We can only write this explicitly, when an analytic solution is known along the entire contour. For example when the scalar field is relatively small at the SP and moving in a quadratic potential we have the analytic solution discussed in equation (1.40). In the present case the amplitude of the Tunneling wave function is given by

$$\log A \simeq -\frac{3\pi}{2H^2} + \frac{3\pi m^2|C|^2\chi^2 b^{2\delta_-}}{2H^4} + \mathcal{O}(\chi^4). \tag{2.10}$$

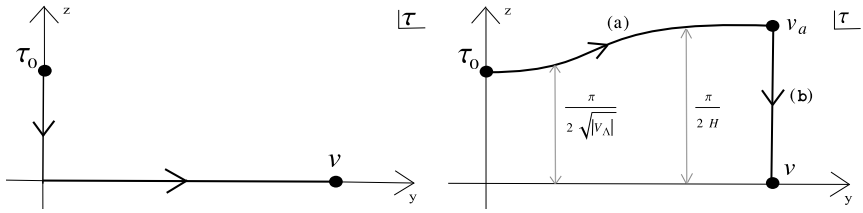

Figure 2.1: The dS contour C_D (left) and the AdS contour C_A (right) in the complex τ-plane yield two distinct geometric representations of the same complex saddle point.

2.4.2 AdS representation of saddle points

The contour C_D is not the only useful representation of the saddle points. The saddle point action is given by the integral (2.6) and can be evaluated along any contour $C(\tau_0, \upsilon)$ connecting the SP to the endpoint υ. Consider now the contour C_A shown in Fig. 2.1(b). In the neighbourhood of the SP the contour lies along

$$z_a(y) \simeq \frac{\pi}{2\sqrt{|V_\Lambda(\phi(y))|}}. \tag{2.11}$$

Hence the first branch (a) gradually moves away from the dS contour as the scalar field rolls down the hill. For large values of y the contour asymptotes to $z_a = \pi/(2H)$. At the point $\upsilon_a \equiv i\pi/(2H) + y_\upsilon$ it turns and runs vertically down along (b) towards the endpoint υ. This contour has the same endpoint υ, the same action, and makes the same predictions as C_D, but the saddle point geometry is different. Eq.(1.44) shows that the displacement from the real axis to z_a replaces u by $-iu$ and therefore $a(u)$ by $ia(u)$, to leading order. Since a was real along the real axis it will be imaginary along $z = z_a$. The asymptotic form of the metric (2.5) along $z = z_a$ is (1.43) and the asymptotic form of the scalar field along the $z = z_a$ curve is given by (1.44).

Hence the saddle point geometry along this part of the contour is that of an asymptotically AdS, spherically symmetric domain wall with a complex scalar field profile in the radial direction y. This construction is analogue as the one discussed in Sec. (1.2.2) in the case of the no-boundary wave function.

The contribution $iS_{L(a)}$ to the saddle point action iS_L coming from the integral along (a) is equal to minus the Euclidean AdS action of the domain wall solution and therefore exhibits the usual volume divergences associated with AdS. In this AdS domain the tunneling wave function thus behaves as the growing wave function familiar from AdS/CFT. This is in sharp contrast with the Hartle-

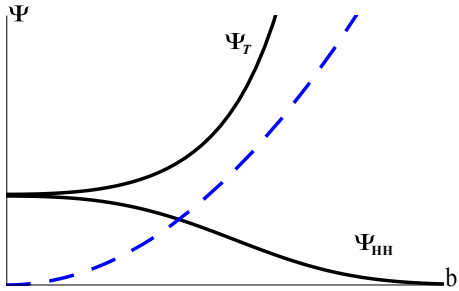

Figure 2.2: Qualitative behavior of Ψ_T and Ψ_{HH} in the AdS regime of the saddle points along branch (a) of the contour C_A. The tunneling state corresponds to the usual growing wave function in AdS familiar from AdS/CFT whereas Ψ_{HH} is a decaying wave function in its AdS regime. The blue dashed line shows the superpotential U.

Hawking wave function which behaves as a decaying wave function in its AdS domain [110]. We illustrate this difference in Fig.2.2.

The contribution to the saddle point action from the vertical closing of the contour (b) regulates the divergences. This follows immediately from the fact that the amplitude of Ψ_T along the horizontal part of the dS contour tends to a constant. The contribution from (b) therefore must cancel the divergences from (a), and also provide much of the phase of the wave function.

There remains the relation between the finite 'regulated' action $iS^{reg}_{L(a)} = -I^{reg}_{DW}$ on (a), where I^{reg}_{DW} is the usual regulated Euclidean AdS action of the domain wall, and the amplitude A of the wave function evaluated at the endpoint υ. This connection is supplied by the action integral (2.6) along (b). In the next section we show that for all asymptotically locally de Sitter saddle points, i.e. including those corresponding to inhomogeneous final configurations, the vertical branch (b) does not contribute to the amplitude.

2.5 General Saddle points

The above discussion is not restricted to minisuperspace. It extends to saddle points corresponding to general boundary configurations specified by complex metrics of the form (2.3). In terms of the variable u the large volume expansion

of the general complex solution of the Einstein equation is given by [110]

$$g_{ij}(u,\vec{x}) = \frac{c^2}{u^2}\left[\tilde{h}_{ij}^{(0)}(\vec{x}) + \tilde{h}_{ij}^{(2)}(\vec{x})u^2 + \tilde{h}_{ij}^{(-)}(\vec{x})u^{2\delta_-} + \cdots + \tilde{h}_{ij}^{(3)}(\vec{x})u^3 + \cdots\right], \tag{2.12}$$

$$\phi(u,\vec{x}) = u^{\lambda_-}(\tilde{\alpha}(\vec{x}) + \tilde{\alpha}_1(\vec{x})u + \cdots) + u^{\lambda_+}(\tilde{\beta}(\vec{x}) + \tilde{\beta}_1(\vec{x})u + \cdots), \tag{2.13}$$

where $\tilde{h}_{ij}^{(0)}(\vec{x})$ has unit volume. As in the homogeneous case, the asymptotic solutions are specified by the asymptotic equations in terms of the boundary functions $c^2\tilde{h}_{ij}$ and $\tilde{\alpha}$, up to the u^3 term in (2.12) and to order u^{δ_+} in (2.13). Beyond this the interior dynamics and the boundary condition of regularity on $\mathcal{M}$ become important.

In saddle points associated with asymptotically classical histories the phases at the origin are tuned so that g_{ij} and ϕ become real for small u along the horizontal part of a contour C_D at $z = z_f$. Since the expansions are analytic functions of u that means there is again an alternative contour C_A that asymptotically runs at $z_a = z_f + \pi/(2\sqrt{|V_\Lambda|})$ along which the metric g_{ij} is also real, but with the opposite signature. Thus we recover more generally the same story as in the homogeneous and isotropic example.

Furthermore, it was shown in [110] that the asymptotically finite contribution to iS_L coming from the first branch of C_A is the same as the logarithm of the saddle point amplitude at the endpoint υ. To see this one can evaluate the action integral along the vertical branch (b) of the contour connecting (a) to υ, order by order in u. The on-shell action integral along the vertical part is given by

$$S_{L(b)}(\upsilon_a,\upsilon) = -\frac{1}{8\pi}\int_{z_a}^{z_f} dz \int d^3x\sqrt{-g}\left[6H^2 - {}^3R + 12V(\phi) + 6(\vec{\nabla}\phi)^2\right], \tag{2.14}$$

where ${}^3R$ is the scalar three curvature of g_{ij}. As shown in [110] the asymptotic Einstein equation implies this does not contribute to the amplitude of the wave function in the large y_υ limit. This means $iS_{L(b)}$ only regulates the divergences of the action from (a) and supplies the phase necessary for classicality at υ. In particular one has

$$iS_{L(b)}(\upsilon_a,\upsilon) = (i-1)(I_1 + I_2 + I_\phi)(\upsilon_a) + \mathcal{O}(e^{-Hy_\upsilon}), \tag{2.15}$$

where I_1 and I_2 are the familiar (real) gravitational counterterms and I_ϕ are additional (complex) scalar field counterterms which cancel the divergences arising from the slow fall-off of ϕ for large y_υ [110]. Hence for sufficiently large

y_v the combination

$$iS_{L(a)}(v_a) - (I_1 + I_2 + I_\phi)(v_a) \to -I^{\rm reg}_{DW}. \tag{2.16}$$

Summing the contributions from (a) and (b) yields

$$iS_L[b, \tilde{h}_{ij}(\vec{x}), \chi(\vec{x})] = -I^{\rm reg}_{DW}[\tilde{h}_{ij}(\vec{x}), \alpha(\vec{x})] + iS_{ct}[b, \tilde{h}_{ij}(\vec{x}), \tilde{\alpha}(\vec{x})] + \mathcal{O}(e^{-Hy_v}), \tag{2.17}$$

where $iS_{ct} \equiv (I_1 + I_2 + I_\phi)(v)$.

In this expression α is determined by the argument of the wave function as described in Eq.(1.44). Thus we find that in the limit of large scale factor the tunneling probabilities for all Lorentzian, asymptotically locally de Sitter histories with scalar matter are specified by the action of an ensemble of Euclidean AdS domain wall saddle points with a complex scalar field profile. This result leads directly to a holographic form of Ψ_T as we discuss next.

2.6 Holographic tunneling wave function

The AdS representation of the saddle points provides a natural connection between Ψ_T in the large volume limit and Euclidean AdS/CFT. In the supergravity approximation the Euclidean AdS/CFT dictionary states that

$$\exp(-I^{reg}_{DW}[\tilde{h}_{ij}(\vec{x}), \alpha(\vec{x})]) = Z_{QFT}[\tilde{h}_{ij}, \alpha(\vec{x})] \equiv \langle \exp \int d^3x \sqrt{\tilde{h}} \alpha(\vec{x}) \mathcal{O} \rangle_{QFT}, \tag{2.18}$$

where the dual QFT lives on the conformal boundary represented here by the three-metric $\tilde{h}_{ij}$. For radial domain walls this is the round three-sphere, but in general α and $\tilde{h}_{ij}$ are arbitrary functions of all boundary coordinates $\vec{x}$.

Applying (2.18) to (2.17) yields the following holographic formulation of the asymptotic tunneling wave function,

$$\Psi_T[h, \chi] = Z_{QFT}[\tilde{h}, \alpha] e^{iS_{ct}[h,\chi]}, \tag{2.19}$$

in which the probabilities of boundary configurations in the large volume limit are given by the partition function of CFTs defined on the AdS boundary and deformed by certain operators[4].

As discussed above the sources $(\tilde{h}, \alpha)$ of Z_{QFT} in (2.19) are locally related to the argument (h, χ) of the wave function. The dependence of the field theory

[4]It has been suggested that the wave function at finite scale factor can be obtained from an RG flow in the dual [115].

partition function on the sources gives a measure on different asymptotically locally de Sitter configurations. For sufficiently small values of the matter sources and sufficiently mild deformation of the round three sphere geometry one expects the integral defining the partition function to converge.

Eq. (2.19) is an example of a dS/CFT duality, albeit at the semiclassical level only. By this we mean that the derivation leading to (2.19) is based on the saddle point approximation of the bulk wave function, and hence concerns the large N limit of any dual field theory. It is an important open question whether a dS/CFT duality like (2.19) holds when loop corrections in the bulk are taken into account.

A concrete dynamical model to which the duality (2.19) applies is provided by $\mathcal{N} = 8$ gauge supergravity in four dimensions, which admits an AdS_4 vacuum solution and is dual to ABJM theory in the large N limit. The bulk theory contains negative mass scalars and admits several consistent truncations to AdS gravity coupled to one or more $m^2/H^2 = -2$ scalars. These scalars act as light, positive mass scalars in the dS regime of the bulk saddle points and thus can drive inflation in the corresponding Lorentzian history. The (complex) sources in the boundary theory that correspond to those scalars turn on finite, relevant deformations of the CFT. The duality (2.19) states that the large N ABJM partition function as a function of those particular sources yields a dual way to compute the tunnelling measure in this model.

We should note, however, that the space of field theory deformations that are allowed is rather restricted. This is because one can only turn on those sources that preserve the asymptotic dS structure. This excludes in particular all irrelevant deformations corresponding to positive mass scalars in the AdS theory since these act as tachyonic scalars on the dS branch of the contour which, when turned on, destroy the asymptotic dS structure. Even scalars in dS with positive masses larger than $+9H^2/4$ are difficult to incorporate. This is because if they don't decay they can form stable bound halos, slowing or even reversing the expansion in local regions of the universe thereby again altering the asymptotic structure. In the AdS regime such fields behave as tachyonic scalars with masses below the Breitenlohner-Freedman bound. Any AdS theory with such scalars would admit bubble solutions that describe the decay of the AdS vacuum, consistent with the absence of a well-defined asymptotic dS structure.

In summary, the asymptotic dS structure which is a prerequisite in any dS/CFT proposal acts as a final condition that strongly constrains the possible deformations and therefore the dynamics.

2.7 Testing the duality

It is not feasible at present to compute the partition function for deformed CFTs on S^3 that are dual to Einstein gravity. To gain intuition and support for the duality (2.19) we therefore consider the simpler Klebanov-Polyakov version of the correspondence wherein the large N field theory is tractable [95]. This conjectures a duality between a higher spin gravity in AdS_4 and the singlet sector of the critical $O(N)$ vector model at large N in three dimensions. In the spirit of [96, 85] we will compare exact results on the field theory side with properties of the bulk wave function in Einstein gravity, and interpret a qualitatively similar behavior as a positive test of the above conjectured duality.

Specifically we consider the partition function of small but finite, constant mass deformation of the critical $O(N)$ vector model on S^3. Since the operator that is sourced has dimension two we take the bulk to be four dimensional Einstein gravity theory coupled to a positive cosmological constant and a scalar field of mass $m^2 = 2H^2$. Along the AdS branch of the saddle points the asymptotic expansion of the scalar field is then

$$\phi = \alpha e^{-Hy} + \beta e^{-2Hy}, \tag{2.20}$$

where $\alpha = i\tilde{\alpha}$ and $\beta = -\tilde{\beta}$. We will compare the partition function as a function of a mass deformation of the critical $O(N)$ model sourced by α with the asymptotic bulk wave function in the field basis as a function of the scalar boundary value $\tilde{\alpha}/(2Hb)$.

Before doing so, however, we first consider a mass deformation of the simpler, minimal $O(N)$ vector model. The partition function of this is related to that of the critical model by a double trace RG flow [93, 83]. In the minimal model a mass deformation is sourced by β multiplying an operator of conformal dimension one. In the bulk this means one adopts the alternative quantisation in which β is the source, corresponding to calculating the bulk wave function in a different basis. Given the subtleties with the signs of the coefficients in the complex saddle points it is instructive to illustrate how the duality works in both bases, and thus to consider both the critical and the minimal model.

2.7.1 Minimal O(N) vector model

First we consider the action of the minimal $O(N)$ vector model on a three sphere of radius r and a finite constant mass deformation μ^2, given by [93], and written in (1.57).

The free energy of this model is

$$-F = \log Z_{min}[\mu^2] = -\frac{N}{2}\log\det\left[\frac{-\Box + \frac{R}{8} + \mu^2}{\epsilon^2}\right] \tag{2.21}$$

where ϵ is an arbitrary dimensionful constant, interpreted as a sliding renormalization scale. The functional determinant can be calculated using a zeta function regularization scheme. This yields to (1.58).

For small $r^2\mu^2$ the partition function becomes

$$\log Z_{min}[\mu^2] \sim -\frac{N}{8}\left[\log 4 - \frac{3\zeta(3)}{\pi^2}\right] + \frac{N}{16}r^4\pi^2\mu^4 + \mathcal{O}(r^6\mu^6). \tag{2.22}$$

The first term is the partition function of the massless $O(N)$ vector model on S^3. The second term is the change in the partition function induced by a small but finite mass term that deforms the theory away from its $r^2\mu^2 = 0$ fixed point.

To show that Z_{min} exhibits the same behaviour as Ψ_T we first perform a canonical transformation to write Ψ_T as a function of $\tilde{\beta}$. It suffices for our purposes here to consider the small scalar field regime described at the end of Section 2.4.1. We write the asymptotic scalar profile as

$$\phi = \frac{\tilde{\alpha}}{2H}a^{-1} + \frac{\beta}{4H^2}a^{-2} \equiv \tilde{\alpha}a^{-1} + \tilde{\beta}a^{-2}. \tag{2.23}$$

The general form of a canonical transformation at the level of the action is

$$\Pi d\phi - \mathcal{H}(\phi, \Pi, \lambda) = Bd\tilde{\beta} - \mathcal{K}(\tilde{\beta}, B, \lambda) + \frac{dG(\phi, \tilde{\beta})}{dt}, \tag{2.24}$$

where $\Pi = \dot{\phi}a^3$ is the conjugate momentum of ϕ, and $B = \tilde{\alpha}H$ is the conjugate momentum of $\tilde{\beta}$. Also, $\mathcal{H}$ and $\mathcal{K}$ are the respective Hamiltonians and G is the generating function. This formulation is derived by requiring that the transformed action gives the same equations of motion. That is, the variation of both actions is the same up to a total derivative.

We are interested in a canonical transformation of the form

$$\begin{pmatrix}\phi\\ \Pi\end{pmatrix} = \begin{pmatrix}a^{-2} & H^{-1}a^{-1}\\ -2Ha & -a^2\end{pmatrix}\begin{pmatrix}\tilde{\beta}\\ B\end{pmatrix}. \tag{2.25}$$

To find the generating function we evaluate

$$\begin{aligned}\int \Pi d\phi = \int &\left[\left(3H^2a^{-1}\tilde{\beta}^2 + 4H\tilde{\beta}B + \frac{3}{2}aB^2\right)d\lambda + Bd\tilde{\beta}\right]\\ &+ \left[-Ha^{-1}\tilde{\beta}^2 - 2\tilde{\beta}B - \frac{1}{2}H^{-1}aB^2\right]_{BD}.\end{aligned} \tag{2.26}$$

The boundary term is the generating function G, when expressed as a function of $\tilde{\beta}$ and χ only. The wave functions in different bases are thus related by

$$\Psi_T(\tilde{\beta}, b) = \int d\chi \exp\left[\frac{3\pi i H}{4}(\chi^2 b^3 + 2\tilde{\beta}\chi b - \tilde{\beta}^2 b^{-1})\right] \Psi_T(\chi, b). \tag{2.27}$$

We showed in section 2.4.1 that the scalar part of $\Psi_T(\chi, b)$ is given by[5]

$$\Psi_T(\chi, b) = \exp\left[\frac{3\pi}{4}\left(-iH\chi^2 b^3 + \chi^2 b^2\right)\right]. \tag{2.28}$$

Hence we find

$$\Psi_T(\tilde{\beta}, b) = \int d\chi \exp\left[\frac{3\pi}{4}(\chi^2 b^2 + 2iH\tilde{\beta}\chi b + \mathcal{O}(b^{-1}))\right]. \tag{2.29}$$

A steepest descent approximation of the integral yields the relation $\chi = -iH\tilde{\beta}b^{-1}$. The amplitude of Ψ_T in terms of $\tilde{\beta}$ is thus given by

$$\log A[\tilde{\beta}] = -\frac{3\pi}{2H^2} + \frac{3\pi\tilde{\beta}^2}{64H^2} + \mathcal{O}(\tilde{\beta}^4). \tag{2.30}$$

Remarkably this is qualitatively similar to the behavior of Z_{min} in (2.22), since the holographic dictionary relates $N \sim H^{-2}$ and $\mu^2 \sim \beta = -\tilde{\beta}$. We conclude that $\log Z_{min}[\mu^2] \simeq \log A[\tilde{\beta}]$, in agreement with our general result (2.19).

2.7.2 Critical O(N) vector model

We now proceed to compute the partition function of the critical $O(N)$ vector model. This model can be obtained from the free theory by deforming it with a relevant double trace deformation $\lambda(\vec{\Phi}\cdot\vec{\Phi})^2/(8N)$, where λ is a constant of conformal dimension one, and taking the dimensionless coupling $r\lambda \to \infty$. We include an additional single-trace deformation $\vec{\Phi}\cdot\vec{\Phi}$ with coefficient $\lambda\sigma$, where σ corresponds to the asymptotic bulk coefficient $\tilde{\alpha}$. The action is [95, 96]

$$S = \frac{1}{2}\int d^3x\sqrt{g}\left[(\nabla\vec{\Phi})^2 + \left(\frac{1}{8}R + \lambda\sigma\right)\vec{\Phi}^2 + \frac{\lambda(\vec{\Phi}\cdot\vec{\Phi})^2}{2N}\right]. \tag{2.31}$$

In the limit $r\lambda \to \infty$ the partition function of this model is related to the partition function of the minimal model by a basis transformation [85], similar to the transformation of Ψ_T above. To compute this one introduces an auxiliary

[5] Here we use that $C = 1/(2iH)$ for $m^2 = 2H^2$, with C defined above eq.(2.10).

field $N\tilde{\mu} = \vec{\Phi} \cdot \vec{\Phi}$, such that the action can be rewritten in terms of single trace operators

$$S = \frac{1}{2} \int d^3x \sqrt{g} \left[(\nabla \vec{\Phi})^2 + \left(\frac{1}{8} R + \lambda\sigma + \lambda\tilde{\mu} \right) \vec{\Phi}^2 - \frac{N\lambda\tilde{\mu}^2}{2} \right]. \tag{2.32}$$

Integrating out the $\vec{\Phi}$ field one obtains

$$Z_{crit}[\sigma] = e^{\frac{N\lambda}{2} \int d\Omega_3 \sigma^2} \int \mathcal{D}\mu^2 \exp \left[N \int d\Omega_3 \left(\frac{\mu^4}{2\lambda} - \sigma\mu^2 \right) \right] Z_{min}[\mu^2], \tag{2.33}$$

where $\mu^2 \equiv \lambda\sigma + \lambda\tilde{\mu}$. The equivalence with Eq.(2.27) shows that both models are indeed related by a Fourier type transformation. The first factor on the r.h.s. in (2.33) is local. As we discussed this is canceled by the contribution to the action integral along the second, vertical part of the saddle point contour. At large N one can evaluate the integral (2.33) in the saddle point approximation. Using (1.58) the saddle point equation reads

$$\frac{16\pi r^2\mu^2}{r\lambda} + 16\pi r\sigma = \sqrt{1 - 4r^2\mu^2} \cot \left(\frac{\pi}{2} \sqrt{1 - 4r^2\mu^2} \right). \tag{2.34}$$

In the large $r\lambda$ regime the first term vanishes and the saddle point equation can be solved analytically. For small dimensionless deformations $r\sigma \ll 1$ eq.(2.34) implies that $r^2\mu^2 \ll 1$, which then yields

$$\log Z_{crit}[\sigma] \sim -\frac{N}{8} \left[\log 4 - \frac{3\zeta(3)}{\pi^2} \right] - N\pi^2 r^2 \sigma^2 + \mathcal{O}(r^3\sigma^3). \tag{2.35}$$

On the other hand, the amplitude of Ψ_T in the field basis in this regime is given by (cf. (2.10))

$$\log A[\tilde{\alpha}] = -\frac{3\pi}{2H^2} + \frac{3\pi\tilde{\alpha}^2}{16H^2} + \mathcal{O}(\tilde{\alpha}^4), \tag{2.36}$$

where we used that $C = 1/(2iH)$ for $m^2 = 2H^2$ and $\chi = \tilde{\alpha}/(2Hb)$. Since $N \sim H^{-2}$ and $\sigma \sim \alpha = i\tilde{\alpha}$ we again find qualitative agreement between the bulk and boundary calculations.

2.8 Discussion

We have shown that the complex structure of the bulk saddle points specifying the semiclassical tunneling wave function in cosmology allows one to use Euclidean AdS/CFT to derive a dual formulation of Ψ_T. In this, the relative probabilities of asymptotically locally de Sitter configurations in the tunneling

state are given in terms of the partition function of AdS/CFT duals defined on the conformal boundary and deformed by certain relevant operators.

Our derivation applies to general, inhomogeneous boundary configurations. It is therefore legitimate and interesting to ask whether the holographic form of Ψ_T predicts fluctuations away from homogeneity are damped as required by observation. It is immediately clear from (2.19) that this is not the case, because the two point functions of the AdS/CFT dual operators are positive [106]. Hence holography indicates that the tunneling state does not yield a well-defined, normalisable cosmological measure beyond minisuperspace. Independently of any application to cosmology our analysis shows that in the WKB approximation, Ψ_T and Ψ_{HH} can also be viewed as wave functions with asymptotic AdS boundary conditions. This is because their complex saddle points have a geometric representation in which their interior geometry is locally AdS. The tunneling wave function corresponds to the usual growing wave function in its AdS domain that features in AdS/CFT applications. By contrast the Hartle-Hawking wave function is a decaying wave function in its AdS domain. At the semiclassical level the probability distributions they predict are inversely related to each other. Indeed in [110] the Hartle-Hawking measure involves the inverse of the AdS/CFT dual partition function. But this simple symmetry is unlikely to hold beyond tree level; there is no reason why the loop corrections to both wave functions should be inversely related to each other. Instead one would expect that a complete dS/CFT framework for Einstein gravity that is rooted in Euclidean AdS/CFT will require a direct understanding of the decaying branch of the bulk wave function in AdS/CFT. Having said this, a somewhat similar inverse relation shows up in the higher spin realisation of dS/CFT, where the partition function of the $Sp(N)$ model as a function of certain deformations (often) is the inverse of the original $O(N)$ partition function. Yet recent calculations of finite N partition functions in this context do not conclusively settle whether the field theory describes Ψ_{HH}, Ψ_T or yet another state. In fact they hint at the possibility that different choices of boundary conditions on the fermions in the dual may provide the freedom needed to model different bulk wave functions. Our results clarify at least the bulk side of this question.

Chapter 3

Two Wave Functions and dS/CFT on $S^1 \times S^2$

3.1 Introduction

Current models of the wave function of the universe such as Vilenkin's tunneling state [56, 57] or the Hartle-Hawking wave function [58] successfully predict that our classical universe emerged in an early period of inflation. In their present form however they are based on a weighting of four-geometries that is difficult to define beyond the semiclassical leading order in $\hbar$ approximation. It is an important goal of quantum gravity to obtain a precise formulation of the quantum state that can be used to reliably calculate the probability measure beyond the saddle point approximation.

Results of Anninos et al. [85, 97], showed that Vasiliev's theory of higher spin gravity in four-dimensional de Sitter space exhibit several divergences. Evidently it is important to understand what this means and whether these divergences also occur in other theories of gravity in asymptotic de Sitter space[1]. If so this potentially undermines the very notion of a wave function of the universe in quantum gravity. To elucidate these questions we perform a careful analysis of both the tunneling and the Hartle-Hawking wave function on $S^1 \times S^2$ boundaries in Einstein gravity[2]. In [85] a similar divergence was found in the small S^1 limit both in a bulk calculation in Einstein gravity and in a boundary calculation

[1] At least some of the divergences discussed in the context of Vasiliev gravity appear to be present also in Einstein gravity[85, 116, 86].

[2] See e.g. [117] for early work on the Hartle-Hawking wave function on $S^1 \times S^2$.

in the dual to Vasiliev gravity. Here we identify the former divergence in the tunneling state, but we find that the Hartle-Hawking measure converges at small S^1.

However we then analyse in detail the classical predictions of both wave functions and show that the divergence in the tunneling state is connected with the contribution of an unphysical branch of saddle points associated with negative mass black holes in de Sitter space. There are strong arguments that configurations describing negative mass black holes must be excluded from the physical configuration space in quantum gravity in order for the theory to be well-defined and stable. We show that discarding the corresponding saddle points branches renders both the tunneling and the Hartle-Hawking wave function in Einstein gravity on $S^1 \times S^2$ well-behaved. Whether this is the correct approach in Vasiliev gravity, which may or may not be stable, remains to be seen.

The outline of this chapter is as follows: In Section 3.2 we compute the tunneling wave function on $S^1 \times S^2$ in the large overall volume limit, as a function of the relative size of S^1 and S^2. We rediscover the divergence in the small S^1 limit discussed in [85, 86]. In Section 3.3 we compute the Hartle-Hawking wave function on $S^1 \times S^2$ and find it converges at small S^1. In Section 3.4 we evaluate the wave functions at finite volume and, in particular, in the classically forbidden region. We show that classical evolution emerges only at exceedingly large overall volumes in the small S^1 limit. In Section 3.5 we derive the classical predictions of the asymptotic wave functions on $S^1 \times S^2$. We demonstrate that the divergence in the tunneling wave function is associated with a branch of saddle points describing negative mass Schwarzschild-de Sitter black holes. In Section 3.6 we derive a holographic formulation of the semiclassical Hartle-Hawking wave function on $S^1 \times S^2$ and clarify its connection with a Euclidean AdS wave function.

3.2 Asymptotic Tunneling Wave Function

In quantum cosmology in the semiclassical approximation the state of the universe is given by a wave function Ψ defined on the superspace of all possible three-geometries and matter field configurations. All wave functions must satisfy the operator implementation of the classical Hamiltonian constraint known as the Wheeler-DeWitt (WDW) equation $\mathcal{H}\Psi = 0$, where $\mathcal{H}$ is a differential operator on superspace. To solve the WDW equation one has to specify a set of boundary conditions on Ψ. This is the analogue in quantum cosmology of specifying the initial conditions for the universe.

Vilenkin has proposed [56, 57] that Ψ consists of outgoing waves only at singular boundaries of superspace. The physical idea behind this proposal is that the universe originates in a non-singular quantum tunneling event. Vilenkin's tunneling proposal can be implemented as a boundary condition on the WDW equation. In the semiclassical approximation in which the wave function is written as a sum of terms of the form

$$\Psi_T = \sum_n A_n e^{iS_L^n}, \tag{3.1}$$

the tunneling boundary condition amounts to a positivity condition on the conserved current $J_n = \frac{i}{2}\Psi_T^* \overset{\leftrightarrow}{\nabla} \Psi_T = -|A_n|^2 \nabla S_L^n$ associated with WDW evolution.

In a cosmological context, for spherical boundaries and in a minisuperspace approximation, the semiclassical tunneling wave function predicts an ensemble of classical, expanding universes with an early period of inflation [56, 57]. Here we are interested in Ψ_T on $S^2 \times S^1$ boundaries in four dimensional Einstein gravity coupled to a positive cosmological constant Λ. The Lorentzian action of this model is given by[3]

$$S_L = \frac{1}{16\pi}\int_{\mathcal{M}} d^4x\sqrt{-g}\,(R - 2\Lambda) + \frac{1}{8\pi}\int_{\partial\mathcal{M}} d^3x\sqrt{h}K\,. \tag{3.2}$$

To find Ψ_T we evaluate the action on regular solutions with a boundary geometry of the form[4]

$$R_c^2\gamma_{ij}dx^i dx^j = R_c^2\left(\left(\frac{\Theta d\theta}{2\pi}\right)^2 + d\Omega_2^2\right). \tag{3.3}$$

Hence the minisuperspace of this model is the two-dimensional manifold $0 \leq R_c \leq \infty,\ 0 \leq \Theta \leq \infty$. The four-dimensional 'saddle point' solutions that match onto boundaries of this form are complex generalizations of Schwarzschild – de Sitter space. They can be written as

$$ds^2 = -\rho^2(\chi)d\lambda^2 + d\chi^2 + R^2(\chi)d\Omega_2^2\,, \tag{3.4}$$

where χ is a complex variable that runs from χ_0 at the 'South Pole' (SP) of the saddle points, where the geometry closes off, to χ_c at the boundary where $R(\chi_c) = R_c$ and $\rho(\chi_c) = \rho_c$. To match the periodicity of the S^1 at the boundary (3.3) the variable λ must be periodic with a period λ_0 given by

$$\lambda_0 = \frac{\Theta R_c}{\sqrt{-\rho_c^2}}. \tag{3.5}$$

[3] We use Planck units where $\hbar = G = c = 1$.

[4] Our calculations in this Section closely follow [85, 86].

The equations of motion for the scale factors $\rho(\chi)$ and $R(\chi)$ are

$$\frac{\ddot{\rho}}{\rho}R + \ddot{R} + \frac{\dot{\rho}}{\rho}\dot{R} + \Lambda R = 0$$

$$2R\ddot{R} + \dot{R}^2 - 1 + \Lambda R^2 = 0$$

$$\dot{R}^2 + 2\frac{\dot{\rho}}{\rho}\dot{R}R - 1 + \Lambda R^2 = 0$$

where $\dot{R} \equiv \partial_\chi R$.

We concentrate on solutions where the S^1 shrinks to zero size at the South Pole, at a nonzero value of the S^2 radius $R(\chi_0) = R_0$. This class of solutions determines the Θ-dependence of Ψ_T, which is our main focus in this paper[5]. Regularity of the solutions at the SP implies

$$\lambda_0 = \pm\frac{2\pi i}{\dot{\rho}(\chi_0)} = \pm\frac{4\pi i R_0}{1 - \Lambda R_0^2} \ . \tag{3.6}$$

The second equality follows from the equations of motion (3.6) which admit a first integral of the form

$$\rho^2 = \dot{R}^2 = 1 - \frac{\nu}{R} - \frac{\Lambda}{3}R^2 \,, \tag{3.7}$$

where the constant of integration $\nu = R_0 - (\Lambda/3)R_0^3$. Evaluating the action (3.2) on these solutions yields

$$S_L = -\frac{\lambda_0}{12}\left(9R_0 - \Lambda R_0^3 - 12R_c + 4\Lambda R_c^3\right) \ . \tag{3.8}$$

The boundary value R_c is real and positive of course, but R_0 is in general complex. The latter can be used to label the different saddle points. Combining (3.6) with (3.5) and using (3.7) yields the following quintic equation for R_0 in terms of the argument (Θ, R_c),

$$-16\pi^2 R_0^2\left(-\frac{1}{R_c^2} + \frac{R_0 - \frac{\Lambda}{3}R_0^3}{R_c^3} + \frac{\Lambda}{3}\right) = \Theta^2(1 - \Lambda R_0^2)^2 \,. \tag{3.9}$$

We discuss the solution of this equation for general values of the argument (Θ, R_c) in Section 3.4. Here we concentrate on the classical region of superspace

[5]When the S^2 shrinks to zero size regularity at the SP implies that the saddle point is a quotient of de Sitter space with an amplitude that is independent of Θ. Hence this class of solutions merely accounts for an overall normalisation factor.

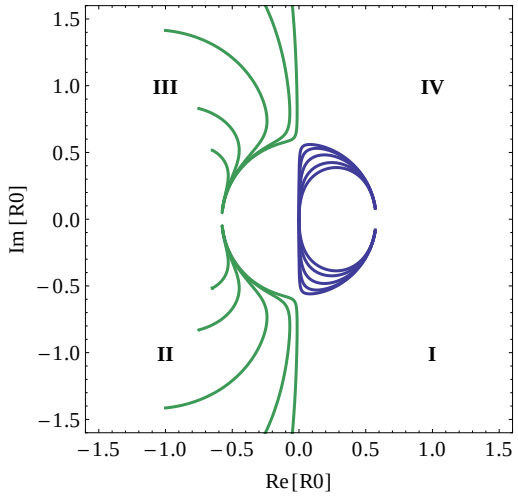

Figure 3.1: The saddle points can be labeled by the complex value R_0 of the overall scale factor R at the South Pole. They are naturally divided in four classes corresponding to values R_0 in different quadrants of the complex R_0-plane. For each boundary configuration (R_c, Θ) in the classical region of superspace there is one saddle point in each quadrant that potentially contributes to the wave function. We show the behavior of R_0 as a function of Θ (along the curves in each quadrant), for a number of values of the overall boundary radius R_c in the classical region of superspace. As $\Theta \to \infty$ we have $R_0 \to \pm 1/\sqrt{\Lambda}$, and $\Lambda = 3$ here. In the $R_c \to \infty$ limit the four curves lie on the imaginary axis for $\Theta \leq 2\pi/\sqrt{3}$ and on the circle at radius $|R_0| = 1/\sqrt{\Lambda}$ for larger Θ.

$R_c \gg 1/\sqrt{\Lambda}$. In this region there are four classes of solutions corresponding to values R_0 in different quadrants of the complex R_0-plane. For each boundary configuration (R_c, Θ) there is one saddle point in each quadrant. Figure 3.1 shows the behavior of R_0 as a function of Θ in each quadrant, for a number of values of the overall boundary radius R_c in the classical region of superspace.

In the $R_c \to \infty$ limit the four curves tend to curves that run along the imaginary axis for $\Theta \leq 2\pi/\sqrt{3}$ and along a circle of radius $|R_0| = 1/\sqrt{\Lambda}$ for larger values of Θ. In this limit (3.9) reduces to a quartic equation which can be solved analytically [85, 86], yielding

$$R_0 = -\frac{2\pi}{\Theta\Lambda}\left(\rho_c/R_c \pm \sqrt{(\rho_c/R_c)^2 + \frac{\Theta^2}{4\pi^2\Lambda}}\right) + \mathcal{O}\left(\frac{1}{R_c}\right) \ . \tag{3.10}$$

The equations of motion together with the boundary conditions (3.6) at the

SP imply that $\rho_c/R_c \to -i\sqrt{\Lambda/3}$ in the large R_c regime if $Im[R_0] > 0$ and $\rho_c/R_c \to +i\sqrt{\Lambda/3}$ for saddles with $Im[R_0] < 0$. Hence (3.10) describes the limiting (large R_c) behaviour of the four classes of solutions shown in Fig. 3.1. In the large R_c regime eq. (3.5) becomes

$$\lambda_0 = \frac{\Theta}{\sqrt{\Lambda/3}}\left(1 + \frac{3}{2\Lambda R_c^2} - \frac{3\nu}{2\Lambda R_c^3}\right) + \mathcal{O}\left(\frac{1}{R_c^4}\right) \ . \tag{3.11}$$

Substituting this in the action (3.8) yields

$$iS_L = -i\frac{\Theta}{\sqrt{\Lambda/3}}\left(\frac{\Lambda}{3}R_c^3 - \frac{1}{2}R_c + \frac{1}{4}R_0(1 + \frac{\Lambda}{3}R_0^2)\right) + \mathcal{O}\left(\frac{1}{R_c}\right) , \tag{3.12}$$

with R_0 given by (3.10). Hence the action obeys the positivity condition on the conserved current[6] in the Lorentzian regime for all four classes of saddle points. It would therefore seem they all contribute to the tunneling wave function Ψ_T.

At large overall volume the semiclassical wave function can be elegantly expressed in terms of a universal phase factor - which accounts for the 'counterterms' in holographic discussions - multiplied by a sum of asymptotically finite 'regularized' saddle point actions. From (3.12) we obtain

$$\Psi_T[\Theta, R_c] \propto \frac{1}{2}e^{iS_{ct}}\left(\cosh(I_R^1)e^{iS_R} + \cosh(I_R^2)e^{-iS_R}\right) \tag{3.13}$$

where

$$iS_{ct}(\Theta, R_c) = -i\frac{\Theta}{\sqrt{\Lambda/3}}\left(\frac{\Lambda}{3}R_c^3 - \frac{1}{2}R_c\right) , \tag{3.14}$$

and

$$iS_R(\Theta) = -i\left(\frac{\left(\Theta^2 - 4\pi^2\right)^{3/2}}{9\Lambda\Theta^2}\right) \tag{3.15}$$

if $\Theta > 2\pi/\sqrt{3}$, and $iS_R = 0$ otherwise. The amplitudes in eq. (3.13) are given by

$$\begin{aligned} I_R^1(\Theta) = -I_R^4(\Theta) &= \frac{4\pi^2}{9\Theta^2\Lambda}\mathrm{Re}\left[\left(-1 + \sqrt{1 - \frac{3\Theta^2}{4\pi^2}}\right)\left(\frac{3\Theta^2}{2\pi} - \pi + \pi\sqrt{1 - \frac{3\Theta^2}{4\pi^2}}\right)\right] \\ I_R^2(\Theta) = -I_R^3(\Theta) &= \frac{4\pi^2}{9\Theta^2\Lambda}\mathrm{Re}\left[\left(1 + \sqrt{1 - \frac{3\Theta^2}{4\pi^2}}\right)\left(-\frac{3\Theta^2}{2\pi} + \pi + \pi\sqrt{1 - \frac{3\Theta^2}{4\pi^2}}\right)\right] \end{aligned} \tag{3.16}$$

[6] See discussion below Eq. (1.17)

where the superscript on I_R in (3.16) corresponds to the label of the quadrant in Fig 3.1.

For $\Theta > 2\pi/\sqrt{3}$ we have $I_R^1 = \bar{I}_R^2$ with imaginary part given by (3.15) and real part given by

$$I_R^1(\Theta) = -\left(\frac{\pi}{\Lambda} - \frac{8\pi^3}{9\Lambda\Theta^2}\right), \tag{3.17}$$

which tends to the well known Nariai amplitude $-\pi/\Lambda$ as $\Theta \to \infty$. Even though the phase of the wave function is dominated by the universal iS_{ct} factor at large overall volume, we will see in Section 3.5 that the imaginary part of the regularized actions (3.17) plays a crucial role on the classical predictions of the wave function.

For $\Theta \leqslant 2\pi/\sqrt{3}$ the solutions R_0 are purely imaginary. The regularized actions (3.16) are all real in this regime, but there is no obvious relation between I_R^1 and I_R^2. Indeed in the $\Theta \to 0$ limit,

$$I_R^1 \to 0\,, \qquad I_R^2 = \frac{16\pi^3}{9\Lambda\Theta^2} \to \infty\,. \tag{3.18}$$

The second class of solutions gives rise to a diverging amplitude as observed in [85, 86]. Here we have found that this divergence emerges as a feature of the tunneling wave function. We return to its interpretation below, but we first evaluate the Hartle–Hawking wave function on $S^1 \times S^2$.

3.3 Asymptotic Hartle–Hawking Wave Function

A different proposal for boundary conditions on the Wheeler-de Witt equation is due to Hartle and Hawking [58] who have suggested, inspired by the Euclidean construction of the ground state wave function in field theory, that the wave function of the universe is given in terms of an appropriately defined Euclidean path integral. In the semiclassical approximation the Hartle–Hawking (HH) wave function is thus given by

$$\Psi_{HH}(\xi) \simeq \sum_n e^{-I_E^n[\xi]} \tag{3.19}$$

where I_E^n is the Euclidean action of a compact, regular - and therefore generally complex - saddle point solution that matches the real boundary data ξ on its only boundary. The sum over saddle points is such that the resulting wave function is real.

The Euclidean action of the model we consider here reads

$$I_E = -\frac{1}{16\pi}\int_{\mathcal{M}} d^4x\sqrt{g}\,(R-2\Lambda) - \frac{1}{8\pi}\int_{\partial\mathcal{M}} d^3x\sqrt{h}K\,. \tag{3.20}$$

To evaluate the HH wave function on $S^1 \times S^2$ boundaries (3.3) we consider Euclidean four-geometries of the form

$$ds^2 = d\chi^2 + \rho^2(\chi)\,d\omega^2 + R^2(\chi)\,d\Omega_2^2\,. \tag{3.21}$$

where, as before, the variable χ goes from χ_0 at the SP where the S^1 smoothly caps off and $R(\chi_0) = R_0$, to χ_c at the boundary where $R(\chi_c) = R_c$. In order for the circle in (3.21) to match the periodicity of the S^1 at the boundary (3.3) we must have

$$\omega_0 = \frac{\Theta R(\chi_c)}{\rho(\chi_c)}\,. \tag{3.22}$$

The Euclidean action evaluated on solutions of the form (3.21) is given by

$$I_E = \frac{\omega_0}{12}\left(9R_0 - \Lambda R_0^3 - 12R_c + 4\Lambda R_c^3\right)\,. \tag{3.23}$$

Smoothness at the SP requires ω to be periodic with periodicity

$$\omega(\chi_0) \equiv \omega_0 = \frac{2\pi}{\dot{\rho}(\chi_0)} = \frac{4\pi R_0}{1-\Lambda R_0^2}\,, \tag{3.24}$$

where the last equality follows from the equations of motion. Combining this with (3.22) yields again the quintic equation (3.9) for R_0 as a function of R_c and Θ. Hence we obtain the same set of saddle points in the large R_c-limit as before, specified by the solutions (3.10). Their relative weighting however will be different as we see below.

It follows from (3.24) that saddle points specified by complex conjugate values of R_0 have complex conjugate ω_0. Using (3.22) this means that complex conjugate R_0 go together with complex conjugate values $\rho(\chi_c)$ (since Θ and R_c are real and positive). Expanding (3.22) for large R_c thus gives

$$\omega_0 = \pm i\frac{\Theta}{\sqrt{\Lambda/3}}\left(1 + \frac{3}{2\Lambda R_c^2} - \frac{3\nu}{2\Lambda R_c^3}\right) + \mathcal{O}\left(\frac{1}{R_c^4}\right)\,, \tag{3.25}$$

where the overall plus sign corresponds to saddles with $Im[R_0] > 0$ and vice versa. Substituting this in the Euclidean action (3.23) yields

$$I_E = \pm i\frac{\Theta}{\sqrt{\Lambda/3}}\left(\frac{\Lambda}{3}R_c^3 - \frac{1}{2}R_c + \frac{1}{4}R_0(1+\frac{\Lambda}{3}R_0^2)\right) + \mathcal{O}\left(\frac{1}{R_c}\right)\,, \tag{3.26}$$

where the overall plus sign again corresponds to saddle points with $Im[R_0] > 0$. Summing the contributions of all four saddle points yields the following result for the semiclassical HH wave function evaluated on $S^1 \times S^2$,

$$\Psi_{HH}[\Theta, R_c] \propto e^{-I_R^1} \cos[S_{ct} + S_R] + e^{-I_R^2} \cos[S_{ct} - S_R] \tag{3.27}$$

where S_{ct} and S_R are given by (3.14) and (3.15), and I_R^1 and I_R^2 are given by (3.16).

The semiclassical HH wave function (3.27) is manifestly real as expected. Its behaviour in the regime $\Theta > 2\pi/\sqrt{3}$ follows directly from (3.17). The usual Nariai limit in which $I_R^1 = I_R^2 = -\pi/\Lambda$ emerges as $\Theta \to \infty$. At the critical value $\Theta \equiv \Theta_c = 2\pi/\sqrt{3}$ the amplitude of both terms in (3.27) is given by $I_R = -\pi/(3\Lambda)$. At low Θ the HH wave function behaves very differently from the tunneling wave function (3.13). Whereas Ψ_T diverges in this limit, the HH wave function is manifestly well-behaved since $I_R^1 \to 0$ and $I_R^2 \to \infty$ as $\Theta \to 0$.

3.4 Wave Functions in the Classically Forbidden Regime

We now proceed to evaluate Ψ_T and Ψ_{HH} for all values of R_c and in particular in the classically forbidden region of superspace $0 \leq R_c \leq 1/\sqrt{\Lambda}$ where the superpotential, (1.8),

$$U(R_c, \Theta) = R_c\Theta(1 - \Lambda R_c^2) \tag{3.28}$$

is positive. This is the regime where the wave functions don't oscillate - and hence cannot be interpreted in terms of (an ensemble of) classical histories - but where they either grow or decay. This is also where the difference between the boundary conditions on Ψ_T and Ψ_{HH} becomes most manifest.

The semiclassical tunneling wave function is specified by the boundary condition that the wave function consists of outgoing modes only in the classical region of superspace $R_c \gg 1/\sqrt{\Lambda}$. Therefore to evaluate Ψ_T at finite values of R_c and in particular in the classically forbidden region we start from its large R_c form (3.13) and solve (3.9) numerically to find the wave function at smaller values of R_c.

For each value of Θ this yields four curves $R_0(R_c)$ in the complex R_0-plane, corresponding to four families of saddle points. As R_c increases the curves tend to two pairs of complex conjugate values R_0 that define Ψ_T in the $R_c \to \infty$ limit as discussed above. Fig. 3.2 shows several examples of saddle point trajectories $R_0(R_c)$ in the complex R_0-plane, for a number of different values of Θ.

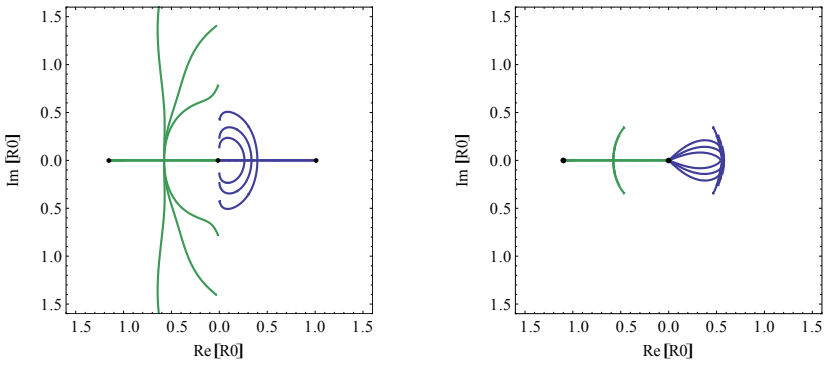

Figure 3.2: The trajectories in the complex R_0-plane that specify the four saddle points contributing to Ψ_T as a function of the boundary value R_c, for a number of different values of Θ. The left panel shows the four solutions $R_0(R_c)$ for three values of Θ, when this is small $\Theta \leq 2\pi/\sqrt{3}$. In this regime R_0 tends to a purely imaginary value as $R_c \to \infty$. The right panel shows $R_0(R_c)$ for three values of Θ when this is large, $\Theta > 2\pi/\sqrt{3}$. In this case the four curves tend to a point on the circle $|R_0| = 1/\sqrt{\Lambda}$ in the $R_c \to \infty$ limit.

As before we can clearly distinguish a low - and a high temperature regime. If $\Theta \leq \frac{2\pi}{\sqrt{3}}$ the trajectories start out somewhere on the imaginary axis in the $R_c \to \infty$ limit. At a critical boundary radius $R_c \sim 1/\sqrt{\Lambda}$ each pair of complex conjugate solutions tends to a real solution[7]. The latter then becomes a pair of real solutions as R_c decreases further, with $R_0 \to \pm\sqrt{3/\Lambda}$ and $R_0 \to 0$ in the $R_c \to 0$ limit.

If $\Theta > \frac{2\pi}{\sqrt{3}}$ the trajectories start out somewhere on the circle in Fig. 3.1. Other than this their behaviour is rather similar to the low Θ regime, except that the branch of solutions with $\mathrm{Re}[R_0] > 0$ is specified by complex R_0 over the entire range of radii R_c.

To find $\Psi_T(R_c, \Theta)$ we evaluate the action (3.8) on the above solutions $R_0(R_c, \Theta)$ and sum over the different saddle points. As eq. (3.13) shows in the large R_c regime this yields a superposition of two outgoing waves. Each wave receives contributions from a set of saddle points with complex conjugate R_0.

At the boundary of the classical region - or more precisely, at the critical value of the boundary radius R_c where the saddle points become real - we use the

[7]The precise value of R_c at which the transition from complex to real saddle points occurs slightly depends on Θ and on the branch.

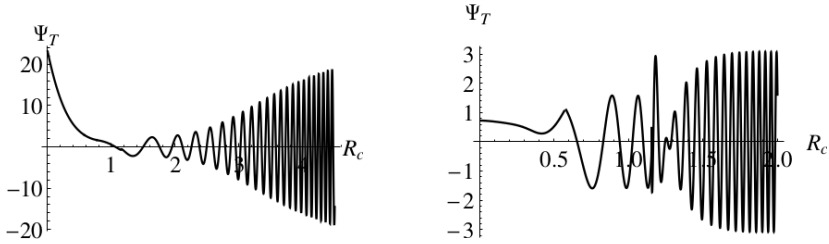

Figure 3.3: The semiclassical tunneling wave function evaluated on $S^1 \times S^2$ as a function of the overall scale factor R_c, for two different (representative) values of the relative size Θ, i.e. $\Theta = 1.6$ (left) and $\Theta = 15$ (right). As Θ decreases the amplitude of the asymptotic classical configuration increases.

WKB connection formulae to find the wave function under the barrier. The latter takes the form [57]

$$\Psi_T(R_c, \Theta) = \sum_{j=1,2} \left(\Psi_+^j(R_c, \Theta) - \frac{i}{2} \Psi_-^j(R_c, \Theta) \right). \tag{3.29}$$

Here the index j labels the individual terms (waves) in (3.13). That is, the linear combinations in (3.29) are matched, for each j, onto an outgoing wave in the classical region. The subscript $+/-$ refers to the leading/subleading saddle point under the barrier. The solutions $\Psi_\pm$ in the classically forbidden region are approximately real.

We illustrate the resulting behaviour of the tunneling wave function in Fig.3.3 for two representative values of Θ, namely $\Theta = 1.6$ as an example in the high temperature regime and $\Theta = 15$ as an example at low temperature. One clearly sees that the oscillatory behaviour characteristic of the classical WKB regime only emerges at sufficiently large boundary values $R_c \gg 1/\sqrt{\Lambda}$ - well inside the classical region of superspace. The amplitude of the outgoing wave increases for decreasing Θ, and diverges for $\Theta \to 0$ as we discussed above. In the classically forbidden region the wave function grows under the barrier in a way reminiscent of the tunneling wave function on S^3 boundaries in a cosmological context [57].

We now turn to the Hartle–Hawking Wave Function in the classically forbidden region. A defining feature of Ψ_{HH} is the boundary condition that the wave function decays in the $R_c \to 0$ limit. In the saddle point approximation this selects the branches of saddle points for which $R_0 \to 0$ as $R_c \to 0$. In terms of the wave function, this selects only the Ψ_-^j WKB components under the barrier.

Therefore to find the Hartle-Hawking wave function at finite nonzero values of R_c we numerically solve (3.9) and select the branches of solutions which

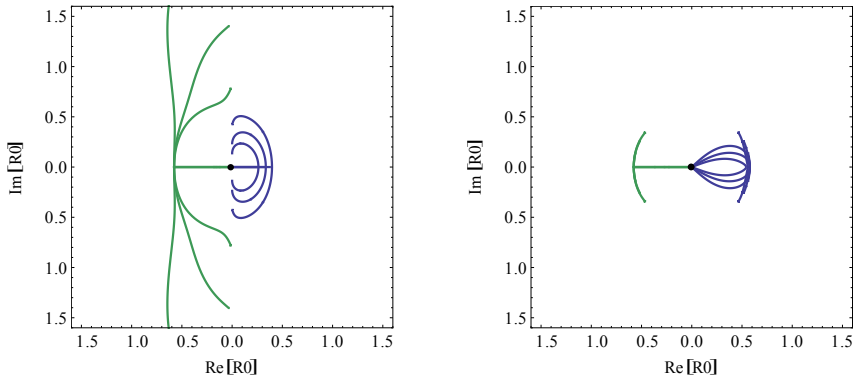

Figure 3.4: The trajectories in the complex R_0-plane that specify the saddle points contributing to Ψ_{HH} as a function of the boundary value R_c, for a number of different values of Θ. The left panel shows the solutions $R_0(R_c)$ for three values of Θ in the regime $\Theta \leq 2\pi/\sqrt{3}$ in which R_0 tends to a purely imaginary value as $R_c \to \infty$. The right panel shows $R_0(R_c)$ for three values of Θ in the regime $\Theta > 2\pi/\sqrt{3}$ in which the curves tend to a point on the circle $|R_0| = 1/\sqrt{\Lambda}$ in the $R_c \to \infty$ limit.

yield a semiclassical wave function that obeys the above boundary condition as $R_c \to 0$. As expected from the form of the superpotential (3.28) we find Ψ_{HH} decays under the barrier and oscillates with an approximately constant amplitude given by (3.27) in the region $R_c \gg 1/\sqrt{\Lambda}$.

The wave function also depends on Θ. As before we can clearly distinguish a low - and a high temperature regime. For $\Theta \leq 2\pi/\sqrt{3}$ the Hartle-Hawking boundary condition selects two saddle point solutions in the small R_c regime which are specified by real values of R_0. At a critical boundary radius R_c around $1/\sqrt{\Lambda}$ each real solution splits[8] in a pair of saddle points specified by complex conjugate values of R_0. We use the WKB matching conditions at that point to obtain the wave function at larger values of R_c where we recover the oscillating wave function (3.27) in the region $R_c \gg 1/\sqrt{\Lambda}$.

We show the saddle point trajectories $R_0(R_c)$ in the complex R_0-plane in Fig. 3.4(a), for four values of $\Theta \leq 2\pi/\sqrt{3}$. The trajectories of course tend to two pairs of complex conjugate points on the imaginary axis as $R_c \to \infty$. In the $\Theta \to 0$ limit the limiting points have $|R_0| \to \infty$ for one pair of solutions and $|R_0| \to 0$ for the second pair.

[8]The exact value of R_c at which this happens depends on Θ and on the branch.

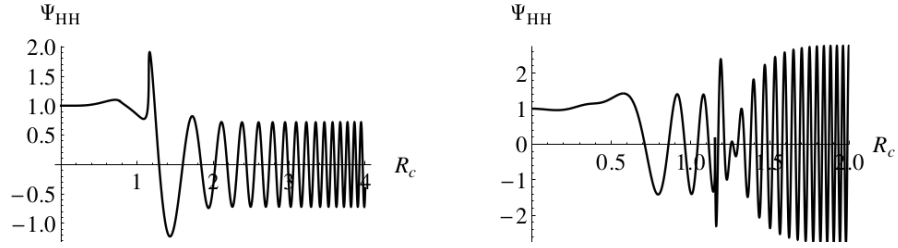

Figure 3.5: The semiclassical Hartle–Hawking wave function evaluated on $S^1 \times S^2$ as a function of the overall scale factor R_c, for two different (representative) values of the 'temperature' Θ, i.e.$\Theta = 1.6$ (left) and $\Theta = 15$ (right). The wave function oscillates when $R_c \gg 1/\sqrt{\Lambda}$ where it predicts an ensemble of Lorentzian, classical Schwarzschild - de Sitter spaces with relative probabilities given by the amplitude of the wave.

The behaviour of $R_0(R_c)$ in the low temperature regime $\Theta > \frac{2\pi}{\sqrt{3}}$ is summarised in Fig. 3.4(b). The trajectories of the branch that starts out at $R_0 < 0$ for small R_c tend to a point on the $|R_0| = 1/\sqrt{\Lambda}$ circle away from the imaginary axis as $R_c \to \infty$. The second pair of solutions has complex R_0 for all values of $R_c > 0$, except at $R_c = 0$ and at $R_c = 1/\sqrt{\Lambda}$ when $R_0 = 1/\sqrt{\Lambda}$.

To find $\Psi_{HH}(R_c, \Theta)$ we evaluate the Euclidean action (3.23) on the above solutions $R_0(R_c, \Theta)$ and sum over the different saddle points. The resulting wave function is shown in Fig. 3.5 for two representative values of Θ, namely $\Theta = 1.6$ as an example in the high temperature regime and $\Theta = 15$ as an example at low temperature. One clearly sees that the oscillatory behaviour characteristic of the classical WKB regime only emerges at sufficiently large boundary values $R_c \gg 1/\sqrt{\Lambda}$ - well inside the classical region of superspace. The asymptotic amplitude of Ψ_{HH} increases with increasing Θ and tends to the Nariai amplitude $e^{\frac{\pi}{\Lambda}}$ in the $\Theta \to \infty$ limit. For boundary values $R_c < 1/\sqrt{\Lambda}$ in the classically forbidden region the wave function is given by a sum of approximately real saddle points. As expected it does not oscillate but generally exhibits a growing behaviour. A transition region around $R_c \sim 1/\sqrt{\Lambda}$ connects both regimes.

3.5 Predictions in the Classical Domain

In the previous sections we saw that Ψ_T and Ψ_{HH} oscillate fast in the large overall volume region. This is the realm of superspace where we expect both

wave functions to predict a set of real classical histories that are solutions of the Lorentzian Einstein equations [64]. In this section we compute this classical ensemble.

Classical evolution emerges at large R_c because both wave functions take a WKB form (more specifically, a sum of such forms)

$$\Psi[\Theta, R_c] \approx A(\Theta, R_c) \exp\{\pm i S(\Theta, R_c)/\hbar\}, \tag{3.30}$$

where S varies rapidly over the region and A varies slowly [64]. That is[9], each term satisfies

$$|\nabla_\Theta A/A| \ll |\nabla_\Theta S|, \qquad |\nabla_{R_c} A/A| \ll |\nabla_{R_c} S| \tag{3.31}$$

with $A = \exp \pm I_R^n$ and $S = S_{ct} \pm S_R$.

Under these circumstances the WDW equation implies that S satisfies to a good approximation the classical Hamilton-Jacobi equation [64]. In a suitable coarse-graining the only histories that have a significant probability are then the classical histories corresponding to the integral curves of S. This is analogous to the prediction of the classical behavior of a particle in a WKB state in non-relativistic quantum mechanics.

Integral curves are found by integrating the classical relations relating momenta to derivatives of the action,

$$p_\Theta = \nabla_\Theta S, \qquad p_{R_c} = \nabla_{R_c} S. \tag{3.32}$$

The solutions $\Theta(t)$ and $R_c(t)$ of (3.32) are curves in superspace that define a set of classical, Lorentzian histories of the form

$$ds^2 = -dt^2 + R_c^2(t) \left(\left(\frac{\Theta(t) d\theta}{2\pi} \right)^2 + d\Omega_2^2 \right). \tag{3.33}$$

The relations between superspace coordinates and momenta (3.32) mean that to leading order in $\hbar$, and at any one time, the classical histories predicted by a wave function of the universe do not fill classical phase space. Rather, they lie on a surface within classical phase space of half its dimension.

The relative probabilities of the individual coarse-grained classical histories in the ensemble are given by A. They are constant along the integral curves as a consequence of the Wheeler-DeWitt equation (cf [64]). Hence they give the tree level measure of different possible universes in the classical ensemble predicted by a particular wave function.

[9] We assume for now that Θ is not too small and return to the $\Theta \to 0$ limit in Section 3.4.

The classical predictions of Ψ_T and Ψ_{HH} evaluated on $S^1 \times S^2$ in the large R_c limit can be obtained from their asymptotic form (3.27) and (3.13). It is immediately clear that both wave functions predict the same ensemble of classical histories, albeit with different relative probabilities[10]. The asymptotic classical ensemble comprises two distinct sets of histories. For $\Theta \leq 2\pi/\sqrt{3}$, where R_0 is purely imaginary at large R_c, the saddle points are associated with classical histories that are simply quotients of de Sitter space. This is because in this region the phase of both wave functions is given entirely by the universal factor S_{ct} given by (3.14).

By contrast, if $\Theta > 2\pi/\sqrt{3}$ then the 'renormalised' actions (3.17) contribute a phase factor $\pm S_R$ to the wave function given by (3.15). In this regime we have

$$\pm \nabla_\Theta S_R = -\frac{1}{2}\sqrt{3/\Lambda}\mathrm{Re}[\nu]\,, \tag{3.34}$$

and the integral curves specified by

$$\begin{aligned} \dot{R}_c &= \frac{1}{\sqrt{\Lambda/3}}\left(\frac{\Lambda}{3}R_c - \frac{1}{2R_c} + \frac{\mathrm{Re}[\nu]}{2R_c^2}\right) \\ \dot{\Theta} &= \frac{\Theta}{\sqrt{\Lambda/3}}\left(\frac{1}{R_c^2} - \frac{3\mathrm{Re}[\nu]}{2R_c^3}\right)\,. \end{aligned} \tag{3.35}$$

Eq. (3.35) is nothing but the Lorentzian version of the large R_c expansion of the first integral (3.7). The asymptotic solutions are

$$\hat{R}(t) \equiv R_c(t) = \exp\left[\sqrt{\frac{\Lambda}{3}}t\right] + \mathcal{O}(1/\hat{R}^2), \qquad \Theta = \Theta_\infty + \mathcal{O}(1/\hat{R}^2) \tag{3.36}$$

where Θ_∞ is a constant of integration that specifies the asymptotic relative size of S^1 and S^2. Using the first integral (3.35) and defining an S^1 scale factor $\hat{\rho} \equiv \dot{\hat{R}}$ the asymptotic Lorentzian solutions (3.33) with $\hat{R}$ and Θ given by (3.36) can be written as

$$ds^2 = -\frac{d\hat{R}^2}{-1 + \frac{2M}{\hat{R}} + \frac{\Lambda}{3}\hat{R}^2} + \left(-1 + \frac{2M}{\hat{R}} + \frac{\Lambda}{3}\hat{R}^2\right)dx^2 + \hat{R}^2 d\Omega_2^2\,, \tag{3.37}$$

where the mass M is given by

$$M = \frac{1}{2}\mathrm{Re}[\nu] = \frac{1}{2}\mathrm{Re}[R_0 - \frac{\Lambda}{3}R_0^3] \tag{3.38}$$

and we have introduced hats to distinguish the real variable $\hat{R}$ that enters in the classical, Lorentzian histories from the complex variable R that describes the

[10]The lack of a divergence as $\Theta \to 0$ in Ψ_{HH} is just one manifestation of this.

saddle point geometries. Therefore at low Θ both wave functions predict (two copies of) an ensemble of Schwarzschild-de Sitter spaces. The black holes have positive mass M in histories associated with saddle points that have $\mathrm{Re}[R_0] > 0$. By contrast $\mathrm{Re}[R_0] < 0$ saddle points correspond to negative mass black holes. For a quantum gravity theory to be well-defined and stable, configurations like negative mass black holes should be excluded from the physical configuration space [118]. In the context we consider here this means the contributions to the wave function of the corresponding branches of saddle points should be discarded. This also eliminates the divergence of Ψ_T in the small Θ limit, which (cf. eq. (3.18)) is associated with the saddle point branch in the second quadrant in Fig. 3.1.

Only part of the Lorentzian geometry is directly (geometrically) connected to the complex saddle points. However one can classically extrapolate the asymptotic solutions using the Lorentzian Einstein equations to obtain other parts of the Lorentzian histories, such as the region inside the horizons where $\hat{R}$ behaves as a radial direction and x becomes the time direction. To what extent a classical extrapolation beyond the horizon is justified will be discussed elsewhere [119].

Finally let us return to the $\Theta \to 0$ regime. In the $\Theta \to 0$ limit the ratio of the gradients (3.31) with respect to Θ is given by

$$|\nabla_\Theta I_R|/|\nabla_\Theta S| \sim 1/\Theta^3 R_c^3. \tag{3.39}$$

This suggests that classical evolution may not be predicted by the wave functions as $\Theta \to 0$, even at large values of R_c. We illustrate this in Figure 3.6 where we show $\Psi_{HH}(R_c)$ for $\Theta = 0.1$. One sees that the classical, oscillatory WKB behaviour emerges at boundary radii R_c that are much larger than the radii at which the quantum/classical transition occurs in the wave function evaluated at the larger values of Θ shown in Fig. 3.5.

It is interesting that neither Ψ_T nor Ψ_{HH} appears to predict classical evolution in this limit. Moreover this is independent of the inclusion of the divergent branch in Ψ_T in this limit. This is because the breakdown of the classicality conditions as $\Theta \to 0$ is not so much due to large variations in the amplitude but rather to slow variations of the phase.

The fact that the classicality conditions fail in the $\Theta \to 0$ limit need not itself be an indication of an instability. However in regions of superspace where the wave function does not predict classical evolution it is difficult to interpret, because probabilities in quantum cosmology are generally assigned to four-dimensional, decoherent classical histories only.

We have seen that the real Lorentzian histories are not the same as the complex saddle points that determine their probabilities. There is however a convenient

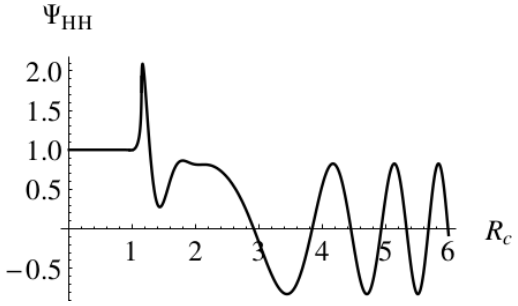

Figure 3.6: Classical evolution only emerges at large boundary radii when Θ is small.

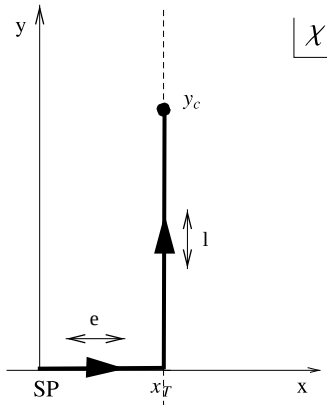

Figure 3.7: Contour in the complex χ-plane along which the geometry of saddle points in the fourth quadrant of Fig. 3.1 consists of a complex, approximately Euclidean geometry smoothly joined onto a Lorentzian, classical, Schwarzschild-de Sitter space.

geometric representation of the saddle points in which their connection with asymptotically classical histories is explicit [64, 110]. This is obtained by representing the complex solutions $\rho(\chi)$ and $R(\chi)$ along an appropriate contour in the complex χ-plane, starting from χ_0 at the SP to χ_c at the boundary. An example of such a contour for a saddle point in the fourth quadrant of Fig. 3.1 is shown in Fig. 3.7, where we have chosen $\chi_0 = 0$ without loss of generality. Writing $\chi = x + iy$ the contour first runs along the real x-axis to a turning point x_T from where it goes vertically. The turning point is chosen so that as

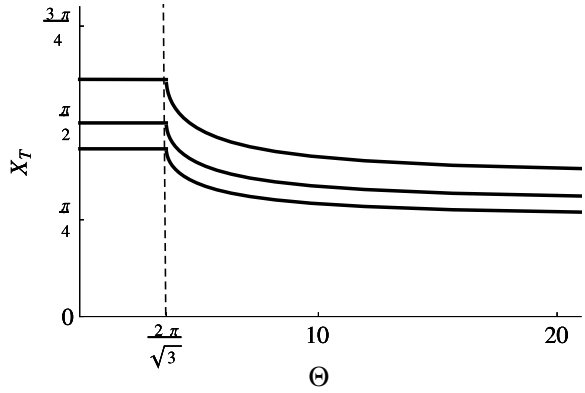

Figure 3.8: The turning point x_T as a function of Θ for saddle points in the 1st and 4th quadrant of fig. 3.1. From top to bottom $\Lambda = 2, 3, 4$. For $\Theta \leq 2\pi/\sqrt{3}$ the turning point is independent of Θ and given by $x_T = \pi/2H$ with $H = \sqrt{\Lambda/3}$ as expected.

$y \to \infty$,

$$\mathrm{Re}[\rho(y)] \to 0\,, \qquad \mathrm{Im}[R(y)] \to 0 \tag{3.40}$$

along the contour. A vertical curve of this kind exists in the complex R_0-plane provided R_0 is a solution of (3.9). The value of the turning point x_T depends on the boundary data Θ and Λ. This is illustrated in Figure 3.8 where we plot $x_T(\Theta)$ for three different values of Λ.

If the conditions (3.40) hold then the complex saddle point geometry (3.21) smoothly tends to a real, Lorentzian four-geometry along the vertical part of the contour, of the form

$$ds^2 = -d\hat{y}^2 + \hat{\rho}^2 d\hat{\omega}^2 + \hat{R}^2 d\Omega_2^2\,, \tag{3.41}$$

where $\hat{\rho}(y) \equiv \mathrm{Im}[\rho]$, $\hat{R}(y) \equiv \mathrm{Re}[R]$ and $\hat{\omega} \equiv \mathrm{Im}[\omega_0]$. This agrees with the classical histories obtained from the integral curves of the phase of the saddle point action. Indeed using the Lorentzian version of the first integral it is straightforward to write the solution (3.41) in the form (3.37).

3.6 Holographic Wave Functions

In this section we derive a holographic form of both wave functions on $S^1 \times S^2$ by generalising the results in [110] for the Hartle-Hawking wave function on

topologically spherical boundaries.

In [110] it was shown that in the large volume limit, the complex saddle points of the Hartle–Hawking wave function on S^3 in cosmological models with a positive cosmological constant and a positive scalar potential have a representation in which the geometry consists of a regular Euclidean AdS domain wall that makes a smooth transition to a Lorentzian, inflationary universe that is asymptotically de Sitter. In this representation, the complex transition region between AdS and dS regulates the volume divergences of the AdS action and accounts for the universal phase factor of the wave function. The approximately Euclidean AdS region in turn encodes the information about the state and provides the tree level measure. Specifically the action of all saddle points in this model can be written as

$$I_E(\phi, a) = -I^{\rm reg}_{AdS}(\tilde{\phi}) + iS_{ct}(\phi, a) + \mathcal{O}(1/a) \tag{3.42}$$

where a and ϕ are the boundary values of the scale factor and field, and $\tilde{\phi}$ is a complex intermediate value in the asymptotic AdS region that is fully determined by ϕ [110].

Eq. (3.42) directly leads to a dual formulation of the *semiclassical* Hartle–Hawking measure in which Ψ_{HH} is given in terms of the partition function on S^3 of (complex) deformations of the same CFTs that occur in AdS/CFT [110].

We now show that this result generalises to the Hartle-Hawking wave function evaluated on $S^1 \times S^2$. Further, since the semiclassical tunnelling wave function involves the same saddle points - albeit weighted differently - a similar derivation also yields a holographic form of the tunnelling wave function.

The action of a saddle point is an integral of its complex geometry that includes an integral over time χ. Different complex contours[11] for this time integral yield different geometric representations of the saddle point, without changing the action. This freedom in the choice of contour gives physical meaning to a process of analytic continuation — not of the Lorentzian histories themselves — but of the saddle points that through their action define the probability measure on the classical ensemble.

The contour we considered in Section 3.4 and shown in Fig. 3.7 was particularly useful to exhibit a geometric connection between the complex saddle points and the real, Lorentzian histories. But it is not the only useful representation of the saddle points. Consider the contour shown in Fig. 3.9, for a solution with $\mathrm{Im}[R_0] > 0$. This has the same endpoints, the same action, and makes the same predictions. But the geometry is different. The contour can be divided in a part

[11] This should not be confused with the choice of contours of path integrals that determines which saddle points to include. We are talking here about different representations of a *given* saddle point.

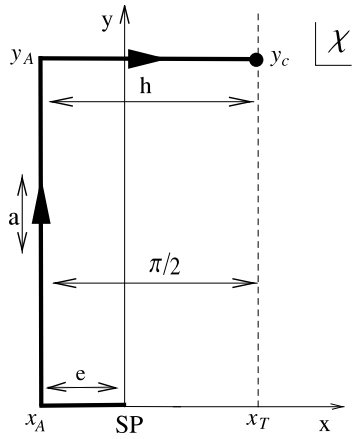

Figure 3.9: The saddle point representation in which the saddle point geometry is Euclidean Schwarzschild-AdS along the vertical part (a) of the contour. This representation serves as a guide in the derivation of a holographic formulation of the Hartle-Hawking wave function in terms of a field theory defined on the conformal boundary geometry.

(e) along the horizontal axis from the SP at $\chi_0 = 0$ to $\chi_e = x_a = x_T - \pi/2$, a part (a) that runs vertically to an intermediate point $\chi_a = x_a + iy_a$ where $R \equiv= iR_c$ and a part (h) along the horizontal branch connecting χ_a to the endpoint $\chi_c = x_T + iy_c$.

The geometry along part (a) is especially interesting. Along this part of the contour

$$\mathrm{Im}[\rho] \to 0\,, \qquad \mathrm{Re}[R] \to 0\,, \qquad \mathrm{Re}[\omega] \to 0. \tag{3.43}$$

Hence for sufficiently large y_a the saddle point can be conveniently written in terms of approximately real variables,

$$ds^2 = -dy^2 - \rho^2 d\tilde{\omega}^2 - \tilde{R}^2 d\Omega_2^2 \tag{3.44}$$

where $\tilde{R} \equiv -iR$ and $\tilde{\omega} = -i\omega$. Using the first integral (3.7) this becomes

$$ds^2 = -\frac{d\tilde{R}^2}{1 - \frac{2\tilde{M}}{\tilde{R}} - \frac{\Lambda_{AdS}}{3}\tilde{R}^2} - \left(1 - \frac{2\tilde{M}}{\tilde{R}} - \frac{\Lambda_{AdS}}{3}\tilde{R}^2\right) d\tilde{\omega}^2 - \tilde{R}^2 d\Omega_2^2\,. \tag{3.45}$$

This is Euclidean Schwarzschild – AdS with $\Lambda_{AdS} = -\Lambda$ and mass

$$\tilde{M} \equiv -\frac{i}{2}\nu = -\frac{i}{2}(R_0 + \frac{\Lambda_{AdS}}{3}R_0^3) = \frac{1}{2}(\tilde{R}_0 - \frac{\Lambda_{AdS}}{3}\tilde{R}_0^3) \tag{3.46}$$

with R_0 given by (3.10).

Fig. 3.1 shows that the AdS black hole mass is real and positive in the large volume limit for $\Theta \leq 2\pi/\sqrt{3}$ whereas it is complex for larger Θ. This is expected since there is a critical temperature $T_c = \sqrt{\Lambda}/(2\pi)$ below which there are no (real!) AdS black holes [120]. Evaluating eq. (3.22) in the large R_c limit shows that $\Theta = 2\pi/\sqrt{3}$ precisely corresponds to T_c. The saddle point branch outside the $|R_0| = 1/\sqrt{\Lambda}$ circle in Fig. 3.1 corresponds to the large black holes that are thermodynamically stable in AdS.

A similar AdS representation can be found for saddle points with $\mathrm{Im}[R_0] < 0$. In this case the vertical part (a) of the contour runs down to negative values of y. The Schwarzschild-AdS geometry (3.45) of these saddle points can be made explicit in terms of the radial variable $\tilde{R} \equiv iR$ which is real and positive along the AdS part of the contour. The black hole mass $\tilde{M} = +\frac{i}{2}\nu$ which is again given by the right hand side of (3.46) and positive.

It remains to compute the action along the AdS contour of Fig. 3.9, in the large volume limit $R_c \gg 1/\sqrt{\Lambda}$. The total action integrated along the first two legs of the contour is given by

$$I_E^{(e)+(a)}(\Theta, \tilde{R}_c) = -\frac{\Theta}{\sqrt{\Lambda/3}} \left(\frac{\Lambda_{AdS}}{3} \tilde{R}_c^3 - \frac{1}{2}\tilde{R}_c - \frac{i}{4} R_0 (1 - \frac{\Lambda_{AdS}}{3} R_0^2) \right) + \mathcal{O}\left(\frac{1}{\tilde{R}_c}\right) \tag{3.47}$$

As expected the action along (a) exhibits the usual volume divergences in the $\tilde{R}_c \to \infty$ limit that are characteristic of the action of asymptotically AdS spaces. The divergent terms are universal and account for what are known as the counterterms (3.14) in holographic discussions [66, 121]. The asymptotically finite contribution to the action along (a) is not universal and encodes information about the state and the dynamics. It is closely related to the regularised AdS action which in terms of the natural radial AdS variable $\tilde{R}$ reads

$$I_{AdS}^{\mathrm{reg}}(\Theta) = \frac{\Theta}{4\sqrt{\Lambda/3}} \tilde{R}_0 (1 + \frac{\Lambda_{AdS}}{3} \tilde{R}_0^2) \ . \tag{3.48}$$

Substituting this in (3.47) yields

$$I_E^{(e)+(a)}(\Theta, \tilde{R}_c) = -I_{AdS}^{\mathrm{reg}}(\Theta) + S_{ct}(\Theta, \tilde{R}_c) + \mathcal{O}\left(1/\tilde{R}_c\right) \ , \tag{3.49}$$

where the counterterms S_{ct} are given by (3.14) evaluated on the boundary $(\Theta, \tilde{R}_c)$. The action along the horizontal leg of the contour is given by

$$I_E^{(h)}(\Theta, \tilde{R}_c, R_c) = -S_{ct}(\Theta, \tilde{R}_c) - iS_{ct}(\Theta, R_c) \, . \tag{3.50}$$

Hence this part of the contour merely regulates the volume divergences and supplies the universal phase factor of the wave function. Taken together this

means the saddle point actions in the large volume limit can be written as

$$I_E(\Theta, R_c) \approx -I^{\rm reg}_{AdS}(\Theta) - iS_{ct}(\Theta, R_c)\,. \tag{3.51}$$

Therefore the requirement that a configuration on the final boundary behaves classically, with constant I_R, automatically regulates the volume divergences associated with the action of the Euclidean AdS regime of the saddle point. This implies that the leading order in $\hbar$ probabilities of the classical Schwarzschild-de Sitter histories can be calculated either from the dS representation of the saddle points or from their representation as Euclidean Schwarzschild-AdS spaces.

Eq. (3.51) provides a natural connection between Ψ_{HH} on $S^1 \times S^2$ boundaries in pure de Sitter gravity and Euclidean AdS/CFT. The Euclidean AdS/CFT correspondence relates $I^{\rm reg}_{AdS}(\Theta)$ in turn to minus the logarithm of the large N limit of the partition function $Z_{CFT}[\Theta]$ of a dual conformal field theory defined on the conformal boundary γ (cf. eq. (3.3)). This yields a dual formulation of the semiclassical NBWF – and hence a concrete realization of a semiclassical dS/CFT duality – in terms of one of the known, unitary dual field theories familiar from AdS/CFT [110]. In this dual description, the semiclassical Hartle-Hawking wave function (3.27) is of the form

$$\frac{1}{Z_{CFT}(\Theta)}\cos[S_{ct}(\Theta, R_c)]\,. \tag{3.52}$$

Hence the argument Θ of the wave function in the large volume limit enters as an external source in the dual partition function. The dependence of the partition function on the value of Θ then gives a dual Hartle-Hawking probability measure on the space of classical asymptotic configurations.

The semiclassical tunnelling wave function (3.13) involves the same complex saddle points as the HH wave function but weighted differently. Therefore (3.51) can also be used to put forward a holographic form of Ψ_T in the large R_c-regime [94]. Substituting (3.51) in (3.13) yields the following holographic representation of the growing branch of Ψ_T,

$$\Psi_T \sim Z_{CFT}(\Theta) e^{iS_{ct}(\Theta, R_c)}. \tag{3.53}$$

In principle one can use the holographic expressions (3.52) and (3.53) to compare semiclassical bulk results for the wave functions with the predictions of a dual boundary theory. At this point explicit boundary calculations with scalar sources are feasible only for the $Sp(N)$ or $O(N)$ conformal field theories which are conjectured to be dual to Vasiliev's higher-spin gravity, respectively in asymptotic de Sitter space [83] and in AdS [95].

Nevertheless the partition functions of those models might qualitatively capture certain aspects of the behaviour of wave functions in Einstein gravity. This was the approach pursued in [85, 86] in the context of the dS/CFT proposal of [83], where it was found that the partition function of the $Sp(N)$ model on $S^1 \times S^2$ exhibits a divergence in the small S^1 limit that is of the same form as the behaviour of Ψ_T in Einstein gravity, *provided the second branch is included*[12].

The holographic form of the wave functions we derived above differs somewhat from the dS/CFT proposal [83] used in [85, 86] in that it (again for Vasiliev gravity) involves the AdS dual $O(N)$ model rather than the $Sp(N)$ model. This is because we have used the complex analytic structure of the saddle points to relate the semiclassical wave functions in asymptotic dS to (Euclidean) AdS rather than taking $N \to -N$ in the dual to 'continue' from AdS to dS. However the net result at this level of comparison is the same. Indeed the partition function of the bosonic $O(N)$ vector model at large temperature is [101]

$$\log Z_{CFT} = 4\zeta(3)N/\Theta^2 \,. \tag{3.54}$$

Substituting this in (3.53) one sees this qualitatively reproduces the behaviour (3.18) of Ψ_T along the divergent branch in the small S^1 limit.

It follows from (3.52) that the dual partition function (3.54) also qualitatively reproduces the behaviour of Ψ_{HH} along the same branch. In the Hartle-Hawking state however this is a subleading branch of the wave function. It is an important open problem in holographic cosmology and in holography in general to access the second branch of bulk wave functions from a dual boundary theory.

3.7 Discussion

We have evaluated the semiclassical tunneling and Hartle-Hawking wave functions on $S^1 \times S^2$ in Einstein gravity coupled to a positive cosmological constant. Over most of superspace there are four branches of complex saddle points that can contribute to the wave functions. In the classical region of superspace – at large overall volume – the wave functions predict an ensemble of real Lorentzian histories. Asymptotically the wave functions are functions of the relative size of S^1 and S^2. When the S^1 is sufficiently large (relative to the S^2) the real, asymptotic classical histories that correspond to the complex saddle points are Schwarzschild-de Sitter black holes. Two branches describe black holes with positive mass whereas the remaining two are associated with

[12] In [85, 86] the divergence in the $Sp(N)$ model was associated with a divergence of the Hartle-Hawking wave function in Einstein gravity. However Section 2 of this paper illustrates that the calculations in [85, 86] actually compute the tunnelling wave function.

negative mass black holes. The latter branches give rise to a divergence in the tunneling state at small S^1. By contrast the Hartle-Hawking wave function appears to be well-behaved in this regime. Singularities associated with negative mass black holes are not expected to be 'resolved' in quantum gravity. This is because the resolution of such singularities would yield regular solutions with negative energy and thus lead to a theory without a stable ground state [118]. Configurations like negative mass black holes with naked, timelike singularities should therefore be excluded from the physical configuration space. This is possible if they lie in a separate 'superselection' sector of the theory. In the quantum cosmological context considered here the most natural way to do this is to discard the contribution [13] to the wave function of the branches of saddle points associated with negative mass black holes at large S^1. We have shown this also resolves the problem of the divergence of the tunneling state in Einstein gravity in the small S^1 limit.

Whether this is the correct procedure in Vasiliev gravity remains an open question, because Vasiliev gravity may not be a stable theory. At present most of what we know about Vasiliev gravity is based on calculations in the boundary theory. One might argue that our results in the context of an Einstein gravity bulk support the interpretation [85, 86] that the divergences indicate Vasiliev gravity is unstable, because we have shown they are associated with negative mass black holes in de Sitter space.

[13] In a holographic calculation of the wave function the analogous restriction amounts to a choice of (periodic) boundary conditions on the fermions in the dual. This would be the correct procedure to evaluate the wave function if Vasiliev gravity in de Sitter space were stable.

Chapter 4

A digression into AdS/CFT

4.1 Introduction

The analysis of the behaviour of field theories on a curved background is very fruitful and leads to many interesting insights into the structure of quantum field theory. Deformations away from the flat metric can reveal universal properties in CFTs itself, but also on the gravity side of the duality. The boundary of AdS is usually taken to be flat Euclidean space or the round sphere since the two are related by a conformal transformation. Any geometrical deformation away from this conformally flat class is related to a new bulk geometry which is a deformation of AdS.

Another type of deformation of the field theory is provided by the addition of operators with a given conformal dimension. These are related to scalar field profiles in the bulk theory. In this chapter we will focus on deformations of conformal dimension one and on deformations of conformal dimension two. The standard AdS/CFT dictionary [122, 123] states that a dual field theory in the presence of one or the other type of deformation are both interpreted as bulk gravity solution with a non-trivial scalar field profile with mass $m^2 = -2$. This yields to a bulk partition function that can be written in different basis [94, 81]. The two flavours of the partition function can be viewed as the generalization in quantum cosmology of the position and momentum space in ordinary quantum mechanics, and are related by a basis change transformation, [81]. This is seen in the dual theory as well where, in certain limits the partition function of the field theory with deformations of conformal dimension one can be related through a basis change transformation to a field theory deformed by an operator

of conformal dimension two, [97].

In this chapter we investigate the effects of these type of deformations on both sides of the duality. We consider CFTs and their holographic duals on a two-parameter family of squashed three spheres whose metric can be written as (1.63). In particular we evaluate the partition function of the free $O(N)$ vector model as a function of the two squashing parameters A and B in (1.63). In the limit when one of the squashing parameters vanishes we recover the results of [85].

We analyze the $O(N)$ vector model, which is well-known to be dual to Vasiliev higher-spin gravity in AdS_4 [124, 95, 125]. Here we will not consider higher-spin gravitational theories directly. Instead we will aim for a qualitative comparison between the physics of the $O(N)$ model on the squashed sphere in (1.63) and Einstein gravity with AdS boundary conditions. We first construct new solutions of general relativity with a negative cosmological constant that are everywhere regular and have a double squashed sphere of the form (1.63) as their boundary. Our solutions are generalisations of the well known AdS Taub-NUT and Taub-Bolt solutions [126, 127], and fall into the type IX Bianchi classification. We study the thermodynamic properties of these new solutions with the partition function of the free $O(N)$ model as a function of the two squashing parameters A and B and as a function of different type of deformations. We find that both systems exhibit a qualitatively similar behaviour over the entire configuration space of boundary geometries. On the other hand they differ in specific features such as the NUT to Bolt transition at large positive values of the squashing parameters, which is evidently absent in the free dual theory, and a shift of the local peak of the field theory partition function as sources are turned on.

One of the main interest of this chapter is provided by the background geometry (1.64). In general the Ricci scalar of a double squashed three sphere of the form (1.63) is given by

$$R = \frac{6 + 8A + 8B + 2AB(6 - AB)}{(1 + A)(1 + B)}, \tag{4.1}$$

which is symmetric in A and B. For $B = 0$ there is a single region $A < -3/4$ where R is negative. Adding a second squashing, however, leads to an additional $R < 0$ region associated with large positive values of both A and B. This is illustrated in Figure 4.1.

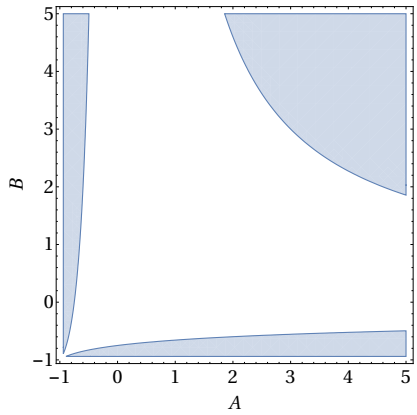

Figure 4.1: The shaded blue region is where the Ricci scalar, R, becomes negative. For one squashing there is only one place where R changes sign, but away from these points there are for given A or B two regions where R is negative.

4.2 Scalar Excitations of Squashed AdS Taub-NUT/Bolt

We consider the real 'AdS domain' of the wave function evaluated on squashed spheres of the form (1.63). In the semiclassical approximation in the bulk this is specified by four-dimensional solutions of general relativity with a negative cosmological constant with action

$$I_E = -\frac{1}{16\pi G}\int_{\mathcal{M}} d^4x\sqrt{g}(R-(\nabla\Phi)^2-2V(\Phi)) - \frac{1}{8\pi G}\int_{\partial\mathcal{M}} d^3x\sqrt{h}K\,, \quad (4.2)$$

where h and K are respectively the induced metric on the asymptotic boundary (1.63) and its extrinsic curvature. For reasons that will become clear below we consider the consistent truncation of M-theory on $AdS_4\times S^7$ consisting of gravity coupled to a single scalar Φ with potential

$$V(\Phi) = -2-\cosh(\sqrt{2}\Phi) \quad (4.3)$$

in units where $\Lambda=-3$ and hence $l^2_{AdS}=1$. For $\Phi=0$ and a single squashing, i.e. $B=0$ in (1.63), the solutions that asymptotically tend to (1.63) are well-known and can be thought of as generalizations of the asymptotically flat Taub-NUT and Taub-Bolt solutions [126, 127, 66]. These are two sets of topological distinct solutions that are asymptotically AdS. The NUT solutions have a zero-dimensional fixed point set, the NUT, around which the solutions

are topologically $\mathbb{R}^4$. The second set, the Bolt solutions, have a two-dimensional fixed point set, the Bolt. These solutions are locally $\mathbb{R}^2 \times S^2$ in the neighbourhood of the Bolt.

The metric of solutions that have the same NUT/Bolt topology in the interior and that asymptote to the squashed sphere (1.63) with two non-vanishing squashing parameters A and B can be written in the following form,

$$ds^2 = l_0(r)^2 dr^2 + l_1(r)^2 \sigma_1^2 + l_2(r)^2 \sigma_2^2 + l_3(r)^2 \sigma_3^2 \,, \tag{4.4}$$

together with a radial scalar profile $\Phi(r)$.

Plugging this Ansatz into the equations of motion derived from the action (4.2) one finds a system of non-linear second order differential equations for the metric functions $l_a(r)$ and the scalar $\Phi(r)$ which are given in Appendix A.2. Numerical solutions to this system with the scalar set to zero were found in [98]. Here we generalize these by including a scalar excitation and its backreaction on the geometry.

We start by considering an expansion at large values of r which, employing holographic terminology, we call UV expansion. The UV expansion is of the Fefferman-Graham type and the same for both the NUT and Bolt solutions since in both cases the non-trivial information is encoded in the interior of the solutions, i.e. in the IR. The leading order terms in the metric for large r are given by

$$ds^2 = dr^2 + e^{2r} \left(A_0 \sigma_1^2 + B_0 \sigma_2^2 + C_0 \sigma_3^2 \right) \,. \tag{4.5}$$

Notice that we have implemented the gauge $l_0(r) = 1$. The next terms in the UV expansion of the solutions read

$$\begin{aligned} l_1(r) &= A_0 e^r + A_k e^{(1-k)r} \,, \\ l_2(r) &= B_0 e^r + B_k e^{(1-k)r} \,, \\ l_3(r) &= C_0 e^r + C_k e^{(1-k)r} \end{aligned} \tag{4.6}$$

$$\Phi(r) = \frac{\alpha}{2(A_0 B_0 C_0)^{1/3}} e^{-r} + \frac{\beta}{4(A_0 B_0 C_0)^{2/3}} e^{-2r} + D_k e^{-(2+k)r} \tag{4.7}$$

where the sum over k goes over all positive integers.

We plug the series expansions (4.6)-(4.7) into the Einstein equations and solve them order by order in powers of e^r. The results of this procedure are summarized in Appendix A.2. The important upshot is that the UV expansion is controlled by seven independent parameters $\{A_0, B_0, C_0, A_3, B_3, \alpha, \beta\}$. It turns out that the Einstein equations are invariant under constant shifts of r

which we use to eliminate one of the parameters, setting $A_0 = \frac{1}{4}$. Comparing the asymptotic form of the metric with the metric (1.63) on the double squashed sphere one can find the following relation between the squashing parameters A and B and the leading order coefficients B_0 and C_0

$$A = \frac{1}{4C_0} - 1 \,, \qquad B = \frac{1}{4B_0} - 1 \,. \tag{4.8}$$

The leading coefficients B_0, C_0 and α specify the asymptotic values of metric and field. As we discuss in Appendix A.2 the values of the subleading coefficients (A_3, B_3 and β) are fixed by imposing regularity conditions (either on a NUT or a Bolt) in the bulk of the full solution of the nonlinear equations of motion.

In practice we use the IR expansions (cf. (A.8) and (A.11)) as initial conditions to integrate the equations of motion numerically to the UV. This yields a three-parameter family of solutions that are controlled by two coefficients specifying the IR behavior of the scale factors $l_a(r)$ and by the initial value Φ_0 of the scalar field. There are two distinct classes of solutions. The first class consists of regular solutions for which the metric functions $l_a(r)$ grow exponentially, the scalar field gradually decays and the boundary metric is a sphere with two non-trivial squashing parameters as in (1.63). A representative example of a NUT solution of this kind is shown in Fig. 4.2. We also find a class of singular solutions for which one or more of the metric functions $l_a(r)$ vanish at some finite value of r, leading to a curvature singularity. We will ignore the second class of solutions since they do not contribute to the wave function in the large three-volume regime.

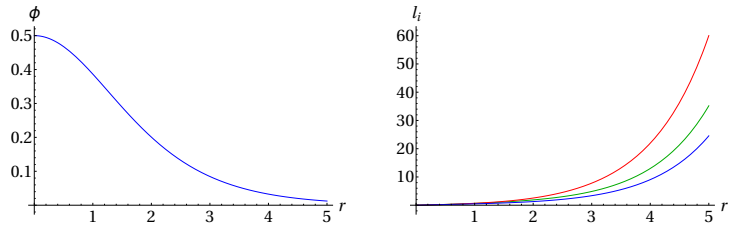

Figure 4.2: A typical solution with a NUT in the IR and with a non-trivial scalar profile in the radial direction, which asymptotes to a double squashed sphere boundary geometry.

The Bolt solutions only exist for sufficiently large, positive squashings. In this regime there is often more than one combination of IR parameters that yields the same values of the leading asymptotic parameters A, B and α.

The regularity condition on the scalar field in the interior yields a relation $\beta(\alpha)$ between the coefficients of its UV profile which depends on the squashings and

encodes information about the scalar potential. The potential (4.3) is special in the sense that, at least for sufficiently small squashings, β tends to a constant when α (or equivalently Φ_0) is taken larger. This property depends delicately on the large field regime of the potential. From a dual viewpoint this means there is a critical deformation β at which the expectation value α of the operator dual to Φ diverges. This is also a feature of the vector model we have considered in Section 3.9, and studied in [128], which serves to justify the bulk boundary comparison we explore there.

Fig. 4.3 shows the relation $\beta(\alpha)$ for $B = 0$ and for three different values of the squashing parameter A. The third panel indicates that the behavior of $\beta(\alpha)$ is qualitatively different for sufficiently negative squashings. Specifically, we find there is a phase transition at $A = -3/4$, precisely where the Ricci scalar on the boundary changes sign, such that for $A \leq -3/4$ the parameter β no longer converges. A second solution with $\alpha \neq 0$ comes into play in this regime even at $\beta = 0$. The new solution is thermodynamically subdominant, as we will see below, but may nevertheless contribute to certain observables [129, 128]. A similar behavior of $\beta(\alpha)$ is found in the entire region of configuration space (A, B) where the Ricci scalar of the boundary geometry is negative (cf. Fig. 4.1). We note also that the relation $\beta(\alpha)$ associated with the generalized Bolt solutions, shown in the first panel in Fig. 4.3, is reminiscent of the constant temperature relation found for black holes with scalar hair in this theory, as expected [130, 102].

The thermodynamic behavior of our set of solutions can be studied by evaluating their regularized, Euclidean on-shell action. Since we do not have analytic solutions we evaluate the regularized on-shell action numerically following the accurate procedure developed in [98] and summarized in Appendix A.2. In Section 3.9 we will compare this with the free $O(N)$-model. To make an accurate comparison we have to match the conformal dimensions of the deformations on both sides. Because on the CFT side the conformal dimension of the source is two, we have to use the alternative quantization of AdS, which means that we fix β on the boundary in stead of α by applying a Legendre transform [131]. Details of how to obtain this can be found in Appendix A.2. Fig. 4.4 shows the resulting free energy for a number of representative slices of constant β through the three-dimensional phase space of solutions. These indicate that the on-shell action exhibits a maximum at zero squashing and scalar field when the scalar curvature is positive.

Without a scalar field it was found in [98] that the well known Hawking-Page type phase transition from the NUT to the Bolt solutions that occurs as one increases the value of the squashing, qualitatively generalizes to the case of two squashings. We find this remains true in the presence of a scalar field, except for the fact that the range of squashings for which the NUT solutions exist

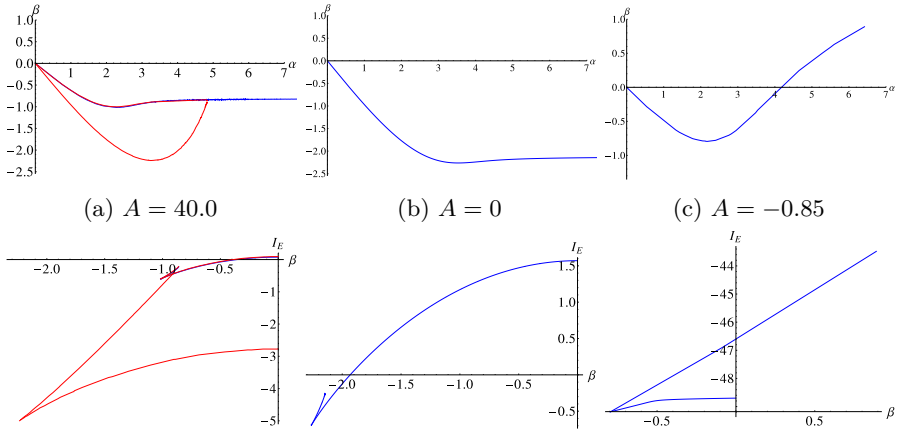

(a) $A = 40.0$ (b) $A = 0$ (c) $A = -0.85$

(d) $A = 40.0$ (e) $A = 0$ (f) $A = -0.85$

Figure 4.3: On the first line the relation $\beta(\alpha)$ that characterizes the asymptotic scalar profile is shown for $B = 0$ and three different values of the squashing parameter A. On the second line, the free energy as a function of β for the same values of the squashing A. The blue curves correspond to NUT solutions, which exist for all three values of squashings, while the red curves in panel (a) represent the two branches of Bolt solutions.

gradually shrinks and becomes centered around zero squashing for large values of Φ_0. At the same time the minimum squashing required for Bolt solutions to exist increases for increasing Φ_0, leading to a critical value above which there is a regime of squashings in which no regular solutions exist.

4.3 A CFT comparison

The study of the holographic dual field theory description of the gravitational solutions described in the previous two sections is a non-trivial problem. One approach would be to embed these solutions as backgrounds in M-theory and to identify a dual CFT. One can for instance think of the NUT/Bolt solutions as deformations of the $AdS_4 \times S^7$ solution of eleven-dimensional supergravity. In this case the dual field theory is the ABJM SCFT and we are faced with the problem of evaluating the partition function of supersymmetry breaking deformations of this theory at strong coupling. This is a formidable problem which we will not attempt to solve here. Instead, we will focus on a simplified

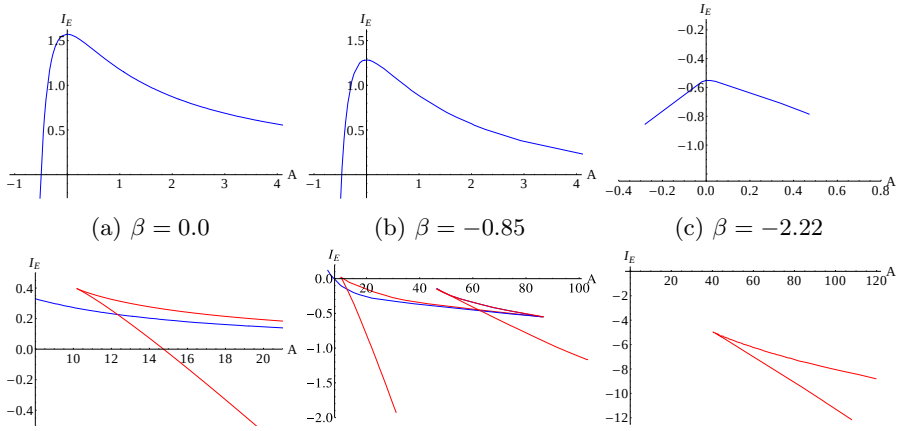

(a) $\beta = 0.0$ (b) $\beta = -0.85$ (c) $\beta = -2.22$

(d) $\beta = 0.0$ (e) $\beta = -0.85$ (f) $\beta = -2.22$

Figure 4.4: The free energy as a function of the squashing for different values of the UV deformation parameter β. The blue (red) curves represent the NUT (Bolt) solutions. In the top row the behavior around zero squashing is shown, while in the bottom row the transition from NUT to Bolt is highlighted.

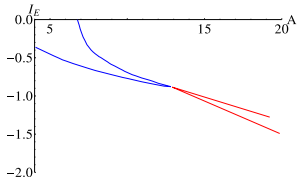

(a) $\beta = -1.4$

Figure 4.5: The free energy as a function of the squashing for $\beta = -1.4$. The blue line is given by the solutions with NUT boundary conditions. The red lines are given by the Bolt solutions. The bolt and the nut solutions overlap at a single point at this critical value of the scalar field.

model of this setup where we consider a vector-like theory on the double-squashed sphere in (1.63) in the presence of a homogeneous mass deformation.

The $O(N)$ vector models with complex deformations in three dimensions are conjectured to be described holographically by a higher-spin Vasiliev theory in AdS_4 with certain specific boundary conditions [124, 95, 125]. Through (1.53) they are also dual at the semiclassical level to Vasiliev theory in dS_4 [110, 83]. These higher-spin theories are very different from pure Einstein gravity with a cosmological constant. Despite this difference it has been found that there are

many qualitative similarities between the behaviour of the free energy of the $O(N)$ vector models and the action of Einstein gravity solutions as a function of squashings and mass deformations [96, 94, 98, 85]. We calculate the partition function of the free mass deformed $O(N)$ vector model on a double squashed sphere, the mass deformed free model partition function as

$$Z_{\text{free}}[m^2] = \int \mathcal{D}\phi e^{-I_{\text{free}} + \int d^3x \sqrt{g} m^2 \mathcal{O}(x)} \ , \tag{4.9}$$

where I_{free} is the action of the conformal, free $O(N)$ model,

$$I_{\text{free}} = \frac{1}{2} \int d^3x \sqrt{g} \left(\partial_\mu \phi_a \partial^\mu \phi^a + \frac{\mathcal{R} \phi_a \phi^a}{8} \right) . \tag{4.10}$$

Here ϕ_a are components of an N-component field transforming as a vector under $O(N)$ rotations and $\mathcal{R}$ is the Ricci scalar of the boundary geometry on which the dual is defined.

Evaluating the Gaussian integral in (4.9) amounts to computing the following determinant

$$-\log Z_{\text{free}} = F = \frac{N}{2} \log \left(\det \left[\frac{-\nabla^2 + m^2 + \frac{\mathcal{R}}{8}}{\Lambda^2} \right] \right) \ , \tag{4.11}$$

where Λ is a cutoff that we will use to regularise the UV divergences in this theory. For a single squashing the eigenvalues of the operator in (4.11) can be found in closed analytic form and read [132]

$$\begin{aligned} &\lambda_{n,q} = n^2 + A(n-1-2q)^2 - \frac{1}{4(1+A)} + m^2 \ , \\ &q = 0, 1, \ldots, \qquad n-1, \ n = 1, 2, \ldots \ . \end{aligned} \tag{4.12}$$

To find the eigenvalues on double squashed spheres we apply the numerical techniques developed in [132, 98] which enable us to determine the spectrum numerically to (in principle) any desired accuracy.

To regularise the infinite sum in (4.11) one may be tempted to use an analytic approach like ζ-function regularisation. However this method is not well-adapted to situations where the spectrum of the Laplacian is known only numerically. Therefore we use a heat-kernel type regularisation which can be implemented numerically and was discussed in detail in [85, 98].

Using a heat-kernel the sum over eigenvalues divides in a UV and an IR part. The latter converges and can readily be done numerically whereas the former contains all the divergences and should be treated with care. We regularize

this numerically by verifying how the sum over high energy modes changes if we vary the energy cutoff. From a numerical fit we then deduce the non-divergent part which we add to the sum over the low energy modes to give the total renormalized free energy. The resulting determinant after heat-kernel regularisation captures all modes with energies lower than the cutoff Λ. The contribution of modes with eigenvalues above the cutoff is exponentially small. For more details on this procedure we refer to our earlier work [98, 99].

In Figure 4.6 we show a two-dimensional slice of the resulting free energy as a function of the squashing A and a real mass deformation m^2. This intermediate result can be compared with the action of the real asymptotically locally AdS solutions shown in Figure 4.4.

An important features of this model is that the free energy diverges when $\mathcal{R}/8 + m^2$ becomes zero. This is a generalization to mass deformed theories of the divergences found in [98]. To understand this we have to inspect the IR behaviour of the free energy, which is given by a sum over upper incomplete gamma functions $\Gamma(0, \lambda_{L,k}\delta)$ where $\lambda_{L,k}$ are the eigenvalues and δ. From the definition of these, one can see that if λ approaches 0 then $\Gamma(0, \lambda_{L,k}\delta)$ diverges. Since the lowest eigenvalue of the Laplacian ∇^2 always vanishes, the first eigenvalue λ_1 of the operator in (4.11) becomes zero when the Ricci scalar vanishes. This explains the sharp features in the function $F(A, B)$ in Figure 4.6.[1] There is no corresponding divergence in the gravitational on-shell action. We believe that this discrepancy is entirely due to the fact that so far we are considering a free CFT. Indeed we will see in Chapter 5 the large N analysis of the free energy of the interacting three-dimensional $O(N)$ vector model that this divergence in the free energy is removed (see also [96]).

Differentiating the partition function with respect to the source m^2 yields the one-point function of the dual operator $\mathcal{O}$ as a function of the deformation m^2. This is shown in the right panel of Figure 4.6 for three different values of a single squashing A. The gravitational counterpart of this, plotted in Figure 4.3, is remarkably similar. Given the latter depends delicately on the details of the scalar potential, this provides a strong motivation to choose this particular potential in our comparison with the boundary theory.

[1] We should note that there are also "higher order" divergences which are less pronounced. These happen when any of the higher eigenvalues of the Laplacian cancels $\mathcal{R}/8 + m^2 \neq 0$ to give another zero eigenvalue of the operator in (4.11). These divergences always appear in the regions of the (A, B) plane where the Ricci scalar $\mathcal{R}$ in (4.1) is negative.

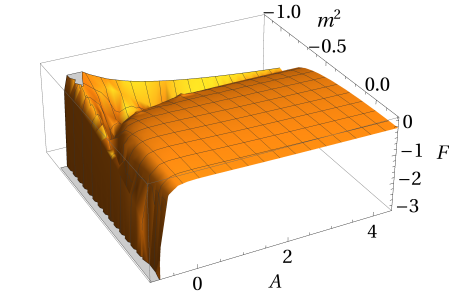

(a) In function of A and m^2

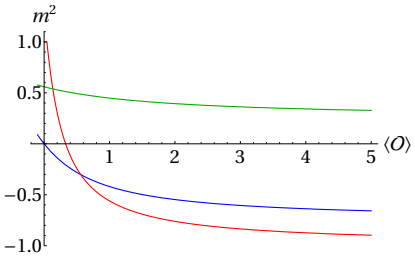

(b) m^2 in function of $\langle\mathcal{O}\rangle$ for $A = 0$ (in blue), $A = -0.85$ (in green) and for $A = 40$ (in red)

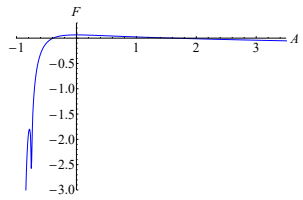

(c) $m^2 = 0.0$

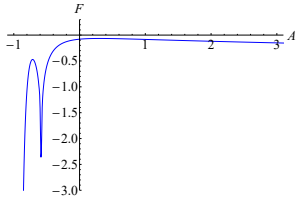

(d) $m^2 = -0.4$

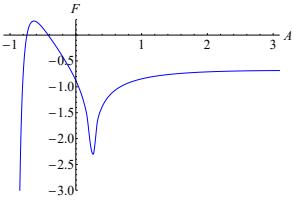

(e) $m^2 = -0.8$

Figure 4.6: In all these figures the free energy as a function of the squashing is given for different mass deformations.

4.4 Discussion

We have evaluated real Euclidean saddle point in Einstein gravity coupled to a negative cosmological constant, on a (double) squashed sphere, in the presence of a scalar field profile in a non trivial potential. Our results include a large class of geometries such as the round sphere, the Taub-NUT/Bolt, and the generalization with two squashing. This type of geometries is interesting for the presence of a phase transition at large squashing and the presence of a negative curvature boundary geometry at small squashing[2]. The type of potential we have considered is interesting in the context of AdS cosmologies, [128]. It has the peculiarity that below a minimum value β_{min} there are no regular solutions. Further, it tends to a constant β_c when α diverges. Between β_{min} and β_c the $\beta(\alpha)$ curve is double valued. The solution with lower α is thermodynamically dominant.

We found that the Taub-NUT/Bolt phase transition occurs at larger values

[2]In the double squashed case there is also a negative curvature region at large squashing.

of the squashing when we apply a scalar deformation. Above a critical value of β, there is no longer a phase transition, but regular solutions can be found in some regions of superspace. The free energy is globally peaked around the sphere and the no-scalar case. The negative curvature region is an unstable regime, and it highly affect the $\beta(\alpha)$ curve. In this regime the scalar field profile diverges in both α and β and the latter changes sign. The divergence occurs in a thermodynamically sub-dominant branch.

In the $O(N)$ vector model there are some similarities and differences. The free energy is globally peaked around the round sphere case, but the relative peak shifts as we apply a mass deformation. The vev as a function of the mass deformation show a similar behaviour seen in Einstein gravity, with the important difference that the mass deformation is never double valued. The negative curvature regime manifests itself leading to a positive, but constant, mass deformation.

Chapter 5

A Holographic Measure on Eternal Inflation

5.1 Introduction

Slow roll eternal inflation [20, 22] occurs when the effective potential V is extremely flat. The condition for eternal inflation is that $\epsilon \leq V$, where $\epsilon \equiv V_{,\phi}^2/V^2$. Since the variance of the wave function of fluctuation modes is of order $\sim V/\epsilon$, evaluated at horizon crossing, this means that quantum fluctuations in the energy density of the inflaton are large in eternal inflation. Stochastic models of the evolution of these fluctuations indicate that their backreaction leads to large amplitudes for universes with exceedingly large and infinite constant density surfaces [133, 134].

This means the usual theory of inflation based on semiclassical gravity breaks down in eternal inflation. It is therefore natural to describe eternal inflation using gauge-gravity duality. In this chapter we study a holographic toy model of eternal inflation in the no-boundary quantum state [58].

The partition functions $Z_{\rm QFT}$ in (1.53) are complex deformations of Euclidean AdS/CFT duals. This form of dS/CFT reduces in minisuperspace to formulations based on analytic continuation [106, 135, 136] and agrees to leading order with the higher-spin realization [83] where the $Sp(N)$ and $O(N)$ partition functions are inversely related. It is tempting indeed to view Euclidean AdS/CFT and dS/CFT as two real domains of a single complexified theory [137, 108, 109, 79, 138, 139]. In this view any wave function that satisfies the

Wheeler-DeWitt equation has an AdS and a dS domain. The former involves at the semiclassical level everywhere real saddle points, whereas the latter is specified by asymptotically real dS saddle points with a complex Euclidean AdS interior. We adopt this viewpoint in the remainder of this chapter.

The dual field theory partition function in (1.53) automatically treats bulk backgrounds and fluctuations in a unified manner. It is therefore ideally suited to describe eternal inflation where the separation between both breaks down. A dual description of eternal inflation plausibly involves a weakly coupled Euclidean field theory defined e.g. on the surface at the threshold of eternal inflation [103]. In realistic cosmologies this would involve an IR CFT [115]. Here we consider a simplified cosmology in which the early phase of (eternal) inflation transitions directly to an asymptotic Λ-dominated regime. This permits us to study eternal inflation directly in the UV of the dual. In fact many of the known AdS/CFT duals naturally describe a regime of eternal inflation in the dS domain of the theory because the Breitenlohner-Freedman stability bound on scalars in AdS corresponds precisely to the condition $\epsilon \leq V$ in dS.

Equation (1.53) shows that dS/CFT relates the argument of the wave function of the universe to external sources in the dual partition functions that turn on deformations of the CFT. The dependence of the partition function on the values of the sources, which include the background geometry, yields a holographic measure on the space of asymptotically locally de Sitter universes. General field theory results imply that the holographic amplitude of the undeformed CFT on the round S^3 is a local maximum with respect to scalar deformations [140, 93] and deformations of the geometry [99, 141]. Furthermore one expects the holographic measure strongly suppresses conformal backgrounds far from the round conformal structure and in particular conformal classes with a metric of negative scalar curvature. This is because the lowest eigenvalue of the conformal Laplacian on this background is negative. Hence the partition function of a weakly coupled CFT likely diverges [71], which would lead to zero amplitude for such configurations [103].

General holographic considerations therefore immediately lead to a very different perspective on the global structure of the universe in eternal inflation than the picture emerging from semiclassical gravity. Indeed Hawking and Hertog recently argued that the holographic description of eternal inflation provides evidence against the idea that eternal inflation typically leads to a highly irregular universe with a mosaic structure of bubble like patches separated by inflationary domains.

It is the purpose of this chapter to support this intuition with explicit calculations in a toy model in which the partition function can be evaluated. Specifically, we compute the partition function of the interacting $O(N)$ vector model on

a two-parameter family of squashed three spheres in the presence of a mass deformation. The latter turns on a bulk scalar satisfying the conditions for eternal inflation, and the asymptotic squashings mean we consider the Hartle-Hawking wave function in a minisuperspace model consisting of anisotropic cosmologies.

The $O(N)$ vector theory conjectured to be dual to higher-spin Vasiliev gravity in four dimensions [124, 95, 125, 83]. Higher-spin theories are very different from pure Einstein gravity. However, ample evidence [96, 85, 98] suggests that their partition functions sourced by scalar, vector and spin-2 deformations qualitatively capture the behavior of duals to Einstein gravity with AdS or dS boundary conditions. Motivated by this we view these vector theories as dual toy models for eternal inflation in Einstein gravity and aim for a qualitative understanding only.

The extended minisuperspace model we consider includes histories with constant density surfaces with negative curvature. These can be viewed as toy models of bubble like patches thought to be produced in eternal inflation. We compute the probability distribution over histories in this model, which turns out to be normalizable and globally peaked at the round three sphere. Moreover the total probability of negative Ricci scalar boundary surfaces turns out to be exponentially small. This behavior confirms the general properties discussed earlier and therefore lends support to the conjecture put forward in [103].

We also compare the holographic measure with the saddle point no-boundary measure in minisuperspace in an Einstein gravity model of eternal inflation based on a consistent truncation of M-theory compactified on $AdS_4 \times S^7$. In the dS domain these saddle points admit a regime of scalar field driven eternal inflation in the neighbourhood of the potential minimum and therefore accessible in the UV. We find the anisotropic cosmologies in this model and numerically regularize their action in order to evaluate the semiclassical wave function.

5.2 Anisotropic inflationary minisuperspace

In Chapter 4 we considered real, asymptotically locally AdS solutions, with real radial scalar field profiles. These solutions specify the AdS domain of the semiclassical Hartle-Hawking wave function. The wave function is real and exponentially decaying in this domain, and hence does not predict classical, Lorentzian cosmological evolution.

We now turn to the de Sitter domain of the wave function. At the semiclassical level this is specified by complex solutions of the same theory, given by the

action (4.2), that asymptotically tend to real, Lorentzian, locally de Sitter space. The asymptotically Lorentzian behavior of this set of solutions provides a large imaginary contribution to their Euclidean action. This means the wave function in the de Sitter domain describes an ensemble of asymptotically classical, cosmological histories [64]. In this section we evaluate the wave function in an anisotropic minisuperspace model with a scalar field using semiclassical bulk methods. In the next Section we compare our results in this approximation with a dual field theory computation of the wave function.

Complex saddle points

We consider the same minisuperspace model as before, consisting of squashed sphere boundary surfaces (1.63) with spatially homogeneous scalar field configurations. The metric of the interior saddle point solutions can thus again be written in the form (4.4), but now with complex scale factors l_a and a complex scalar field profile Φ.

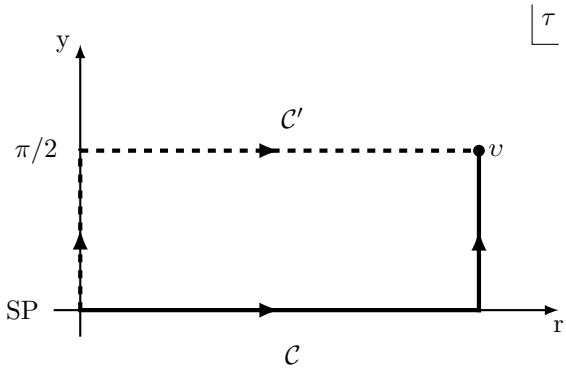

Figure 5.1: Two representations in the complex τ-plane of the same no-boundary saddle point associated with an inflationary universe. Along the horizontal part of the AdS contour $\mathcal{C}$ the geometry is an asymptotically AdS, spherically symmetric domain wall with a complex scalar field profile. Along the horizontal branch of the dS contour $\mathcal{C}'$ the saddle point behaves as a Lorentzian, inflationary universe.

To represent the solutions it is useful to introduce a complex time coordinate $\tau(r)$ defined by

$$\tau(r) \equiv \int_0^r dr' l_0(r') \ . \tag{5.1}$$

In terms of the variable τ the asymptotically dS domain of the wave function is to be found along the asymptotically horizontal line $\tau = t + i\pi/2$ in the complex τ-plane. Along this line the leading order Fefferman - Graham - Starobinsky expansion of the metric (4.5) becomes

$$ds^2 = dt^2 - e^{2t}\left(A_0\sigma_1^2 + B_0\sigma_2^2 + C_0\sigma_3^2\right) \ . \tag{5.2}$$

Here A_0, B_0, C_0 are real constants specifying the degree of asymptotic anisotropy. The Lorentzian signature of the asymptotic metric means the original scale factors l_i defined in (4.4) are to leading order purely imaginary in the dS domain. Their subleading behavior can be deduced from an asymptotic analysis of the equations of motion and is given in Appendix A. We illustrate the representation of the saddle point solutions in the complex τ-plane in Fig. 5.1. The semiclassical AdS domain of the wave function is specified by solutions that are regular in the IR and real along the real $\tau = r$ axis. The semiclassical dS domain, by contrast, involves everywhere regular complex geometries that tend to asymptotically real, Lorentzian solutions along the $\tau = t + i\pi/2$ line. The AdS contour shown in Fig. 5.1 provides a geometric representation of these complex solutions in which their interior geometry consists of a Euclidean AdS domain wall that makes a smooth (but complex) transition to a Lorentzian asymptotically dS universe. The signature of the asymptotic metric (5.2) means that the potential (4.3) in the original Euclidean action (4.2) acts in the dS regime as a positive effective potential

$$V_{\rm eff}^{dS}(\Phi) = -V = 2 + \cosh(\sqrt{2}\Phi) \tag{5.3}$$

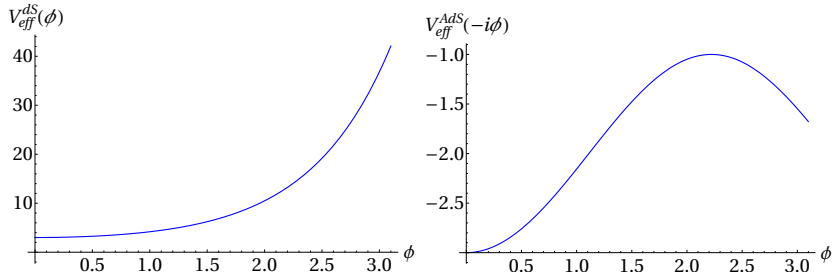

Figure 5.2: *Left panel*:The effective potential in the dS domain that gives cosmological relevant solutions. *Right panel*: The effective potential that gives relevant cosmological solutions in the AdS domain.

The argument of the wave function is real. This means that in order for the above complex solutions to be valid saddle points specifying the semiclassical wave function, the scalar field must also become real along the same line in the

τ-plane. The UV expansion (4.7) shows this requires its leading coefficient α to be imaginary, which in turn means that the scalar profile is imaginary all along the AdS part of the contour $\mathcal{C}$ shown in Fig. 5.1. The interior region of the saddle points specifying the Lorentzian dS domain of the wave function thus involves complex generalizations of Euclidean AdS domain walls. The effective potential in this AdS domain wall regime is therefore

$$V_{\text{eff}}^{AdS}(\tilde{\Phi}) = -2 - \cos(\sqrt{2}\tilde{\Phi}), \tag{5.4}$$

where $\tilde{\Phi} \equiv \mathrm{i}\Phi$, and is illustrated in the right panel of Fig. 5.2. This shows that the asymptotic dS domain of the wave function corresponds to a finite domain of IR values Φ_0 of the scalar field bounded by $|\Phi_0| < \sqrt{2}\pi/2 \equiv \Phi_c$. From an AdS perspective this is simply a consequence of the shape of the effective potential governing the inner AdS region of the saddle point solutions. From a dS perspective this bound signals the boundary of the inflationary regime of the effective potential (5.3) in the dS domain. The potential (5.3) clearly admits inflationary solutions near its minimum. For large values of the scalar field however it is too steep. The IR regularity condition of the Hartle-Hawking saddle points selects those patches of scalar potentials where the conditions for inflation hold [64]. The semiclassical wave function has no support outside these inflationary patches.

To determine for which real boundary conditions in the asymptotic dS domain regular complex solutions exist we must numerically solve the complex equations of motion derived from the action (4.2). The regularity conditions on geometry and field in the IR, either at a NUT or a Bolt, leave three free parameters; two associated with the IR behavior of the scale factors and one for the complex value Φ_0 of the scalar field. Varying these and numerically integrating the Einstein equation in the complex τ-plane to the asymptotic dS regime in the UV yields a three-parameter family of complex solutions whose action specifies the semiclassical no-boundary wave function in the dS domain. Details of this procedure are given in Appendix A.2.[1] Fig. 5.3 shows a representative example of a solution with two squashings and the scalar field turned on, along a contour $\mathcal{C}$ along which the solution exhibits an inner Euclidean AdS domain wall region.

The regularity condition on the scalar field in the interior yields a relation $\beta(\alpha)$ between the coefficients of its asymptotic profile. We show this for three different combinations of squashings in the left panel of Fig. 5.4. A characteristic feature of this model is that β is imaginary over the entire range of parameter space. The dual interpretation of this suggests that the corresponding cosmological histories behave only approximately classically in the large volume regime [81]. This may seem surprising but is perhaps related to the fact that the potential

[1] The same method was already employed in [142] to find anisotropic saddle points of the no-boundary wave function for a different potential.

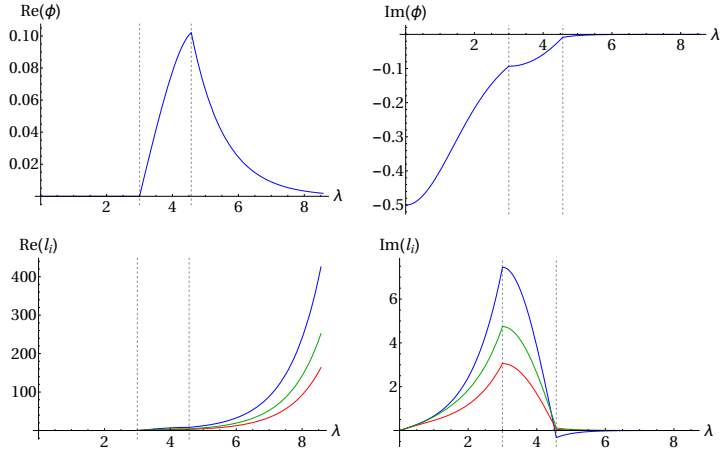

Figure 5.3: A representative example of a complex solution with a NUT in the interior and a scalar field profile, that is asymptotically locally dS with a double squashed sphere future spatial boundary. The solution is shown here along a contour $\mathcal{C}$ like the one depicted in Fig. 5.1 consisting of three segments. The top panels show the evolution of the real and imaginary components of the scalar field along this contour. The bottom panels show the real and imaginary components of the three scale factors. The values of the IR parameters are $\phi_0 = 1/2$, $\beta_4 = -1/6$ and $\gamma_4 = -11/60$.

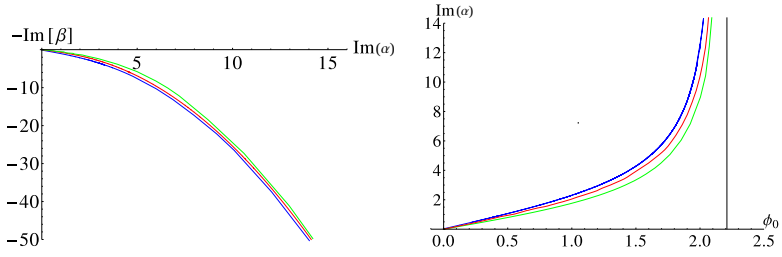

Figure 5.4: The behaviour of β as a function of α (left) and behaviour of α as a function of ϕ_0 (right). All the curves are for $B = 0$. The blue curve is for $A = 0$, the red for $A = -0.85$ and the green for $A = 40$. When ϕ_0 approaches ϕ_c, α starts to diverge.

$V_{\text{eff}}^{dS}(\Phi)$ describes a regime of eternal inflation and not slow roll inflation. One might have thought that the boundedness of the range of values Φ_0 in the IR would mean the semiclassical wave function has support over a limited range of values α in the UV. This is not the case. The right panel of Fig. 5.4 plots α

as a function of Φ_0 for three different combinations of squashings. One sees α diverges as $\Phi_0 \to \Phi_c$.

5.2.1 Anisotropic inflationary histories

The Euclidean action (4.2) of the above solutions specifies the semiclassical no-boundary wave function in the asymptotic dS domain. The complex nature of the solutions means that in the large three-volume region of superspace the wave function takes the form

$$\Psi[a, A, B, \chi] \approx \exp\{(-I_{\rm R}[a, A, B, \chi] + iS[a, A, B, \chi])/\hbar\}. \tag{5.5}$$

where $a \equiv e^t$ is the overall volume scale factor. Here $I_{\rm R}[a, A, B, \chi]$ and $-S[a, A, B, \chi]$ are the real and imaginary parts of the Euclidean action $I_{\rm E}$ of the regular complex saddle point solution that matches the real boundary data (a, A, B, χ), with (A, B) the squashing parameters and $\chi \approx -i\alpha/2a(A_0B_0C_0)^{1/3}$. In the large volume regime the phase factor S varies rapidly compared to $I_{\rm R}$,

$$|\vec{\nabla} I_{\rm R}| \ll |\vec{\nabla} S| \ . \tag{5.6}$$

Hence the wave function predicts the boundary configuration evolves classically [64]. This is analogous to the prediction of the classical behavior of a particle in a WKB state in non-relativistic quantum mechanics. Thus the NBWF in the dS domain predicts an ensemble of classical, asymptotically locally de Sitter histories that are the integral curves of S in superspace, with relative probabilities that are proportional to $\exp[-2I_{\rm R}(A, B, \chi)]$. The latter are conserved under scale factor evolution as a consequence of the Wheeler-DeWitt equation [64].

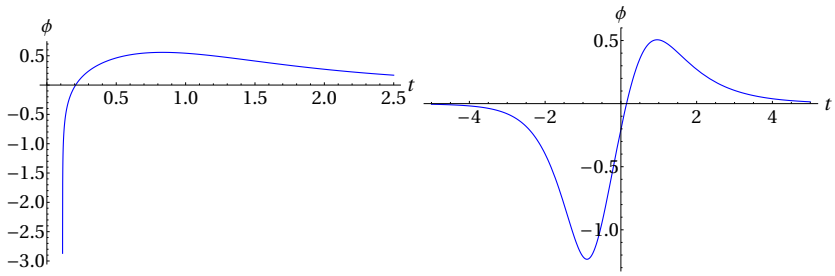

Figure 5.5: *Left panel:* An asymptotically classical history that is initially classically singular, for $\Phi_0 = 0.5$, $A = 2.3$ and $B = 0$. *Right panel:* An asymptotically classical history with a bounce in the semiclassical domain, for $\Phi_0 = 0.5$, $A = 0.16$ and $B = 0$.

The classical ensemble consists of a three-parameter family of inflationary histories that are asymptotically dS and have a certain degree of anisotropy, parameterized by (A, B) on the future boundary. The histories in this model do not exhibit a phase of reheating and slowing expansion. Instead they transition from a phase of scalar field driven inflation to a phase of accelerated expansion driven by the cosmological constant. The potential is such that the scalar field inflation is of the type of slow roll eternal inflation. Hence if one were to include inhomogeneous fluctuations, one would find that the wave function became broadly distributed, predicting an ensemble of histories with exceedingly large or even infinite constant scalar density surfaces [133, 134].

Within the minisuperspace model the classical extrapolation of the histories backwards in time is justified as long as the classicality conditions (5.6) hold. We find two distinct classes of past evolutions. For reasonably small values (A, B, χ) the classical extrapolation backwards exhibits a de Sitter like bounce to approximately the same (time reversed) history on the other side. By contrast, for large values (A, B, χ) the histories are classically past singular. Fig. 5.5 shows a representative example in each class. The classical extrapolations of all Bolt saddle points, which only exist for large squashings, are past singular. The range of squashings (A, B) for which the classical histories bounce in the past decreases for increasing χ. This is in line with our expectations for this particular scalar potential, which becomes too steep at large Φ to sustain inflation. We illustrate this in the left panel of Fig. 5.6 where we show the region in the (A, B) phase space for three different values of χ within which the classically extrapolated histories bounce.

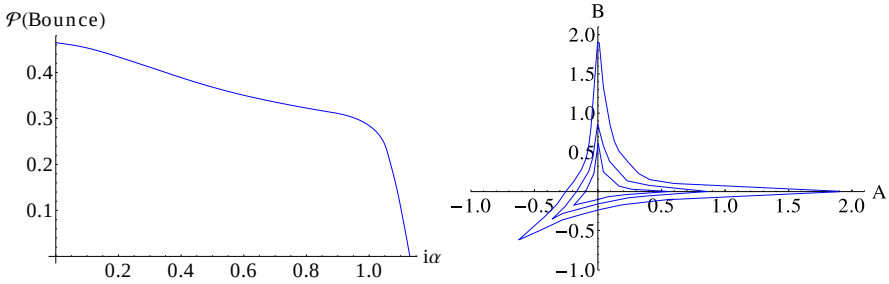

Figure 5.6: *Left panel:* The total probability for a semiclassical bounce as a function of α. *Right panel:* The three contours bound the region in the (A, B) plane for which an approximately classical bounce occurs for (from small to large) resp. $\alpha = 3/4i$, $\alpha = i/2$ and $\alpha = 0$.

The relative probabilities of the individual histories in the classical ensemble are fully specified by the regularized action of the interior AdS domain wall regime

of the saddle points. Specifically in the large three-volume region we have [110]

$$I_{\rm R}[a, A, B, \chi] = -I^{\rm reg}_{AdS}[A, B, \alpha_f] \tag{5.7}$$

where $\alpha_f \equiv \alpha(\chi)$ is defined in the AdS regime of the saddle points (cf. (4.7)) and purely imaginary for real boundary values χ in the dS domain [110]. To compute the regularized action one can perform the regularization procedure numerically as detailed in the Appendix for the real AdS solutions. However it is more convenient to consider the complex saddle points along a different contour, indicated with $\mathcal{C}'$ in Fig. 5.1. This yields a geometric representation of the solutions in which a Euclidean deformed four sphere gradually transitions to a Lorentzian asymptotically locally de Sitter space. The Lorentzian behavior of the solution along the second leg of $\mathcal{C}'$ means the real part of the Euclidean action stabilizes automatically along $\mathcal{C}'$ [64].

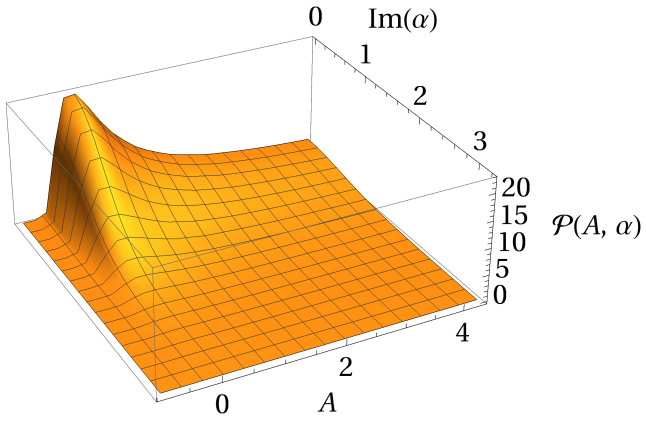

Figure 5.7: The probability distribution over anisotropic minisuperspace as a function of the squashing A and the amount of scalar field inflation parameterized by $i\alpha$.

We show a two-dimensional slice $P(A, \alpha)$ of the probability distribution in Fig. 5.7. As expected the distribution is normalizable and peaks at the pure de Sitter history with a round sphere boundary and zero scalar field. In Fig. 5.8 we show slices of constant α of this distribution $P(A)$ for three different values of the coefficient α specifying the asymptotic scalar profile. The Bolt solutions provide the dominant contribution to the probabilities at large squashings A. This is the dS counterpart of the Hawking-Page like phase transition in the AdS domain of the wave function. The total probability of histories associated with Bolt saddle points is small however and decreases for increasing scalar field.

The probability distribution over the classical ensemble can also be used to compute the total probability in this model that an asymptotically classical universe emerges form a regular bounce in the past and therefore lies in the quasiclassical realm throughout its entire history. This is obtained by integrating the probability distribution over the domain in the (A, B)-plane shown in the left of Fig. 5.6. This corresponds, for a given scalar value χ on a constant a surface, to bouncing histories when classically extrapolated backwards. We plot the probability P_{bounce} as a function of α in the right panel of Fig. 5.6, where we restriced to a single squashing. This shows that the total probability of a non-singular origin is significant in this model when the scalar field is everywhere relatively small. However, it sharply decreases outside this regime and vanishes for histories in the large field regime near the edge of the inflationary regime of the potential.

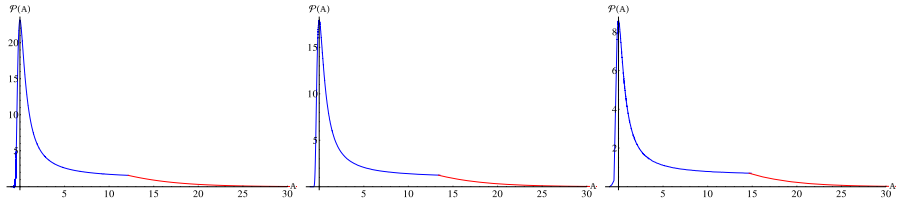

(a) $\mathcal{P}(A)$ for $\alpha = 0$ (b) $\mathcal{P}(A)$ for $\alpha = i$ (c) $\mathcal{P}(A)$ for $\alpha = 2i$

Figure 5.8: Slices of the probability distributions for $B = 0$ for three different values of α. The blue curves show the NUT contributions whereas the dominant Bolt contribution is given in red.

5.2.2 Classical Lorentzian evolution.

It is interesting to understand the influence of the negative curvature regime on the classsical Lorentzian evolution. To achieve this we introduce the Lorentzian boundary variables $\beta_\pm$ such that, [143, 144, 145],

$$\begin{aligned} \log l_1(\hat{t}) &= \beta_+(\hat{t}) + \sqrt{3}\beta_-(\hat{t}), \\ \log l_2(\hat{t}) &= \beta_+(\hat{t}) - \sqrt{3}\beta_-(\hat{t}), \\ \log l_3(\hat{t}) &= -2\beta_+(\hat{t}), \end{aligned} \tag{5.8}$$

where $\hat{t}$ is the time defined on a particular history. The Lorentzian action in this new boundary squashing parameters shows a "gravitational" potential

$$V(\beta_+, \beta_-) = 4e^{-2\beta_+}\cosh 2\sqrt{3}\beta_- - 2e^{-8\beta_+} + e^{4\beta_+}\left(1 - \cosh 4\sqrt{3}\beta_-\right). \tag{5.9}$$

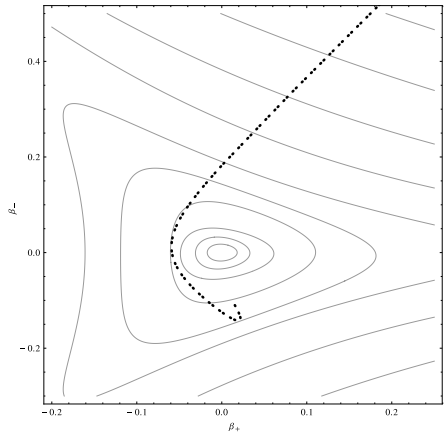

Figure 5.9: An example of the Lorentzial evolution of the anisotropy parameters β_+ and $\beta-$. As time increase they both decrease to a more isotropic configuration.

If we look at the Lorentzian evolution of the anisotropy parameters $\beta_\pm$, we see that the evolution of the squashing bounce against the equipotential lines, as a ball in a billiard. This is the typical behaviour of the mixmaster universe. Whether they approach a more isotropic or a more squashed configuration crucially depends on the sign of the potential (5.9). An example of a history whose evolution is towards a more isotropic configuration is shown in figure 5.9.

In terms of this parametrization the boundary scalar Ricci curvature is ${}^3R \propto -\frac{1}{2}V(\beta_+, \beta_-)$, [143]. The sign of the boundary Ricci scalar crucially influences the anisotropic evolution of the Lorentzian histories. When ${}^3R$ is positive the potential $V(\beta_+, \beta_-) < 0$ and the Lorentzian classical universe evolves to a more isotropic configuration in the future. On the contrary, when ${}^3R$ is negative the potential $V(\beta_+, \beta_-) > 0$ and the Lorentzian classical universe evolve to an even more anisotropic configuration. In this regime, the squashing parameters A and B reach the critical value -1 in a finite time.

5.3 A Holographic Measure

In the holographic form (1.53) the NBWF amplitude of configurations on Σ_f is specified by the partition function of deformations of Euclidean AdS/CFT duals. The arguments of the wave function enter as sources in the dual. For the geometry this means we must evaluate the dual partition function on the

double-squashed sphere (1.63). The bulk scalar sources a scalar deformation by an operator $\mathcal{O}$ of dimension one with coupling α. This is a relevant operator which in our dual $O(N)$ vector toy model induces a flow from the free to the critical $O(N)$ model. The coefficient α is imaginary in the dS domain of the wave function as discussed above. Hence we are led to evaluate the partition function, or free energy, of the critical $O(N)$ model as a function of the two squashing parameters A and B and an imaginary mass deformation $\alpha \equiv \tilde{m}^2$.

The deformed, critical $O(N)$ model is obtained from a double trace deformation $f(\phi\cdot\phi)^2/(2N)$ of the free model with in addition a source $\rho f\tilde{m}^2$ turned on for the single trace operator $\mathcal{O}\equiv(\phi\cdot\phi)$. By taking $f\to\infty$ the theory flows from its unstable UV fixed point where the source has dimension one to its critical fixed point with a source of dimension two [95]. To see this, we consider (4.9) and we introduce an auxiliary variable $\tilde{m}^2 = \frac{m^2}{\rho f} + \frac{\mathcal{O}}{\rho}$. This yields to

$$Z_{\rm free}[m^2] = \int \mathcal{D}\phi\mathcal{D}\tilde{m}^2 e^{-I_{\rm free}+N\int d^3x\sqrt{g}\left[\rho f\tilde{m}^2\mathcal{O}-\frac{f}{2}\mathcal{O}^2-\frac{1}{2f}(m^2-\rho f\tilde{m}^2)^2\right]} \ . \quad (5.10)$$

which can be written as

$$Z_{\rm free}[m^2] = \int \mathcal{D}\tilde{m}^2 e^{-\frac{N}{2f}\int d^3x\sqrt{g}(m^2-\rho f\tilde{m}^2)^2} Z_{\rm crit}[\tilde{m}^2] \ , \quad (5.11)$$

with

$$Z_{\rm crit}[\tilde{m}^2] = \int \mathcal{D}\phi e^{-I_{\rm free}+N\int d^3x\sqrt{g}\left[\rho f\tilde{m}^2\mathcal{O}-\frac{f}{2}\mathcal{O}^2\right]} \ . \quad (5.12)$$

Inverting (5.11) yields $Z_{\rm crit}$ as a function of $Z_{\rm free}$:

$$Z_{\rm crit}[\tilde{m}^2] = e^{\frac{Nf\rho^2}{2}\int d^3x\sqrt{g}\tilde{m}^4}\int \mathcal{D}m^2 e^{N\int d^3x\sqrt{g}\left(\frac{m^4}{2f}-\rho\tilde{m}^2m^2\right)} Z_{\rm free}[m^2] \ . \quad (5.13)$$

The value of ρ can be determined by comparing two point functions in the bulk with those in the boundary theory [85]. For the $O(N)$ model this implies $\rho=1$, which agrees with the transformation from critical to free in [97].[2]

To compute $Z_{\rm crit}(A,B,\alpha)$ we use the partition function, (4.9), of the free mass deformed $O(N)$ vector model on a double squashed sphere and then evaluate (5.13) in a large N saddle point approximation. We substitute our result for $Z_{\rm free}$ in (5.13) and evaluate the integral in a large N saddle point approximation to compute the partition function of the critical model.

The first factor outside the path integral in (5.13) diverges in the large f limit, which we cancel by adding the appropriate counterterms. The saddle point

[2]The above calculation can be repeated for the $Sp(N)$ model by putting $\rho=-i$[85].

equation then becomes, for homogeneous deformations

$$\int d^3x\sqrt{g}\left(\frac{m^2}{f}-\tilde{m}^2\right)=-\frac{\partial \log Z_{\text{free}}[m^2]}{\partial m^2}\ , \tag{5.14}$$

where the first term on the left hand side vanishes for large f. Solving this for m^2 and inserting the result in (5.13) yields $Z_{crit}[\tilde{m}^2]$.

Because α is imaginary we also have to plug in an imaginary value for $\tilde{m}^2$. The saddle point equation has infinitely many solutions for a fixed imaginary value $\tilde{m}_0^2$. There is always one greater than $-\mathcal{R}/8$ and the rest is smaller than this value. To make sure we include all the relevant solutions, we need to do a careful study of the m^2-plane to determine where the steepest descent contour for m^2 lies. For the single squashed sphere this was already discussed in detail in [85], in which it was found[3] that the relevant steepest-descent contour could always be deformed to pass through the saddle point that lies to the right of the point where $m^2=-\mathcal{R}/8$.

To apply this procedure to our model with one squashing, we first calculate Z_{Free} as a function of (complex) m^2 using the numerical techniques described above and we then numerically invert (5.14) to find the behaviour of the complex deformation m^2 as a function of imaginary $\tilde{m}^2$. The relation between these two deformations is shown in Figure 5.10, where the real and imaginary parts of m^2 are plotted as a function of $i\tilde{m}^2$ for three different values of A. Notice that m^2 is restricted to be larger than $-\mathcal{R}/8$, as can be seen from the plot of the real part of m^2 where it is clear that for large $i\tilde{m}^2$, $m^2\to-\mathcal{R}/8$. From the left plot we also see that the imaginary part of m^2 tends to zero whenever $i\tilde{m}^2$ becomes large.

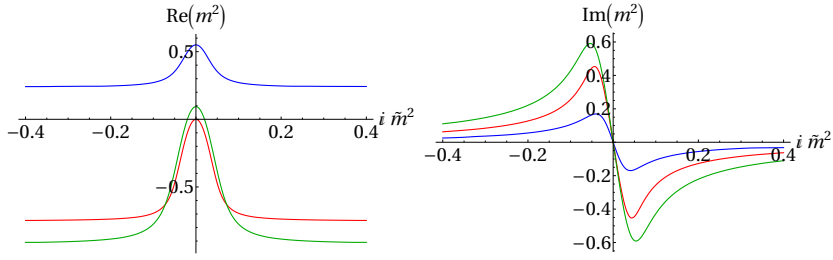

Figure 5.10: The real and imaginary solutions of the saddle point equation (5.14) are shown for three different values of a single squashing, i.e. $A=-0.8$ (blue), $A=0$ (red) and $A=2.06$ (green). For large $i\tilde{m}^2$ we have $\text{Re}(m^2)\to-\mathcal{R}/8$.

[3]It was also found that for the $Sp(N)$ model the saddle point contour is ill-defined such that the non-perturbative (in N), critical $Sp(N)$ model does not exist.

Inserting the saddle point relation $m^2(\tilde{m}^2)$ in (5.13) yields the partition function $Z_{\rm crit}[A, B, \tilde{m}^2]$ which we illustrate in Figure 5.11, where we plot a two-dimensional slice of the holographic probability distribution in anisotropic minisuperspace as a function of the mass deformation corresponding to the asymptotic scalar profile and of one squashing parameter. The distribution has a global maximum at zero squashing and zero deformation corresponding to the pure de Sitter history, in agreement with the result based on a bulk calculation. When the scalar is turned on however, the local maximum shifts towards positive values of A - a feature which is absent in the bulk result - which we illustrate in Figure 5.12 where we plot three one-dimensional slices of the distribution for three different values of $\tilde{m}^2$.

As anticipated the sharp features associated with the divergences of the free energy in the free $O(N)$ model discussed above have disappeared, resulting in a smooth and normalizable distribution over the entire configuration space. We should emphasize however that in our calculation of $Z_{\rm crit}$ starting from $Z_{\rm free}$ we have taken in account only the regions of configuration space for which the free theory is not manifestly unstable. This restriction appears to be born out by the natural measure on configuration space and selects the region of parameter space where $\mathcal{R}/8 \geq m^2$. By contrast, the distribution defined by $Z_{\rm crit}$ extends over boundary configurations where this inequality does not hold and includes, in particular, boundary geometries with negative curvature. Remarkably, the distribution is well defined in this regime of superspace also. In fact it is evident from Figure 5.11 that the total probability of $\mathcal{R} < 0$ histories is exponentially small.

5.4 Discussion

Holographic cosmology provides a radically new perspective on eternal inflation. We have initiated an exploration of its implications in the toy model context given by the interacting $O(N)$ vector model defined on a two-parameter family of squashed three spheres and deformed by a mass term. We have evaluated its partition function as a function of the three asymptotic parameters. Through dS/CFT this specifies a holographic measure on a minisuperspace of anisotropic deformations of dS with scalar field matter in the regime of eternal inflation, in higher-spin gravity. We find that the amplitude is low for conformal boundary surfaces far from the round conformal structure. This is in line with general field theory expectations and lends support to the conjecture that the exit from eternal inflation is reasonably smooth, producing universes that are relatively regular on the largest scales with globally finite surfaces of constant density.

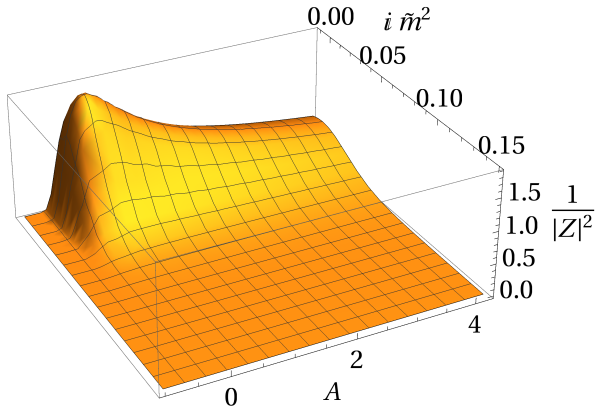

Figure 5.11: A two-dimensional slice of the holographic probability distribution in anisotropic minisuperspace as a function of the mass deformation $\tilde{m}^2$ corresponding to the asymptotic scalar profile and one squashing A that parameterizes the amount of asymptotic anisotropy.

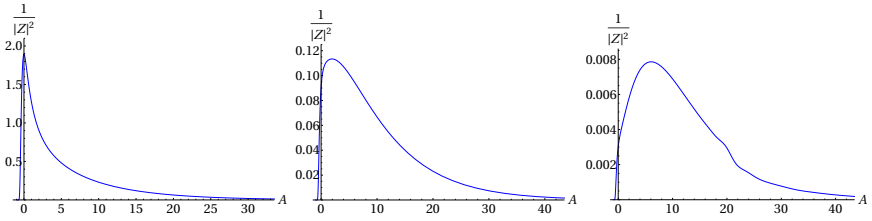

(a) $\tilde{m}^2 = 0.0$ (b) $\tilde{m}^2 = 0.05i$ (c) $\tilde{m}^2 = 0.1i$

Figure 5.12: Three one-dimensional slices of the probability distribution in anisotropic minisuperspace for three different values of $\tilde{m}^2$. The local maximum shifts towards larger values of the asymptotic anisotropy in histories with more scalar field inflation.

A reliable theory of eternal inflation is important to sharpen the predictions of slow roll inflation. This is because the dynamics of eternal inflation specifies the prior over the zero modes, or bulk slow roll backgrounds, which in turn determines the predictions of the precise spectral properties of CMB fluctuations on observable scales [111]. The generic features of the pattern of fluctuations in holographic models of inflation were extensively studied [135, 146, 147, 148, 149]. A well-defined measure on eternal inflation will sharpen these predictions by selecting a specific subset of RG flows or slow roll backgrounds.

Chapter 6

Discussion

6.1 Summary and conclusion

A quantum gravity description of de Sitter space appears to be needed if we want to understand the intimate nature of our own universe. Holography appears to be a property of quantum gravity theories and, therefore, it is crucial to understand how this principle can be incorporated in cosmology. This would lead to the so called dS/CFT correspondence, which relates the wave function of the universe to the partition function of a dual field theory defined on the boundary.

A quantum gravity theory of dS space is affected by several issues, and our understanding is limited. The theory accommodates multiple definition of the wave function of the universe and, therefore, different measures. Further, the existence of two different asymptotic boundaries and the presence of a cosmological horizon pose conceptual problems that need to be understood.

In addition, there is the problem that we do not know the partition function of ABJM theory, which is dual to AdS_4 solution of Einstein gravity, and can be used to compute the full cosmological measure. To explore the quantum version of dS space we proceeded only qualitatively. In this thesis work we have compared our bulk results with the partition function of the model dual to Vasiliev higher spin theory of gravity. That is the $O(N)$ vector model in the presence of different type of complex deformations. Under certain type of deformations the theory is known to be affected by divergences. We explored these divergences in the context of Einstein gravity, and we resolved them in the sense that we have found they correspond to a non-classical behaviour of

the wave function.

In this research work we have explored all these issues. In Chapter 2 we have found the holographic form of the Tunneling wave function, and we have compared it with certain relevant small perturbations of the $O(N)$ vector model. In this chapter we have found that the growing behaviour of the partition function in AdS familiar from Euclidean AdS/CFT is equivalent to the amplitude of the Tunneling wave function in cosmology. The way the Tunneling wave function is defined, naturally selects boundary observables only at future infinity. In contrast the no-boundary wave function have access to both boundaries (past and future infinity). This can already be seen in the semiclassical form of the two wave functions, (1.22) and (1.42). The modes, and thus the expanding or contracting phases of the universe are encoded in the phases of the wave functions, and thus do not have any influence on their holographic probabilities.

In Chapter 3 we have analyzed the behaviour of the divergence found in the U(N) vector model. We have shown that, in Einstein gravity, a similar divergence appears in the presence of saddle points predicting Lorentzian histories that are Schwarzschild de Sitter black hole with negative mass. The diverging behaviour corresponds to a vanishing probability measure of the Hartle-Hawking state, and to an un-physical diverging probability measure for the Tunneling state. This divergence occurs in a configuration where the classicality condition is not satisfied, so that the solutions do not predict any classical Lorentzian history. Configurations like negative mass black holes should be excluded from the physical configuration space, and we should discard their contribution to the full measure.

The $Sp(N)$ vector model is known to diverge at negative mass deformations. Further, if we deform the round S^3 sphere along two independent directions, we can explore a regime with negative boundary curvature. We have explored these types of deformations in chapter 4 in the context of standard AdS/CFT correspondence, and in chapter 5 in the context of cosmology. We showed that in Einstein gravity a divergence similar to the one observed in the $Sp(N)$ vector model, appears in saddle point solutions predicting tachyonic scalar field profile on the future boundary. These saddle points do not predict any classical behaviour of the wave function. Our results of chapter 4, are a generalization of the AdS-Taub NUT/Bolt deformed by a second squashing and in the presence of non-trivial scalar field profile. We showed that the NUT/Bolt phase transition do not occur for sufficiently large scalar deformations. This phase transition cannot be seen in Vasiliev theory, nevertheless this provides an important tool to explore a quantum description of dS space, at least qualitatively. The results of chapter 5 are relevant in cosmology. We have analyzed the Lorentzian histories that are of a mixmaster universe. Depending on the boundary values of the

squashing and of the scalar field the histories might bounce or be singular in the past. We have evaluated the probability measure for these histories and we have compared it with the partition function of the $O(N)$ vector model in the presence of a critical complex deformation. In this way we got an holographic measure of eternal inflation.

In this thesis work we pushed our understanding of the dS/CFT correspondence a step further. We have analyzed how holography selects either the tunneling or the no-boundary state. We have explored similarities and the differences between Einstein and Vasiliev theories. It is tempting to conjecture that a divergence in the latter can be traced to a wave function, defined in Einstein gravity, in a non-classical regime. With this comparison in our hands, we have analyzed the full probability measure for different kinds of inflationary universes.

6.2 Outlook

We have already discussed some possible future work in this direction, in the discussion of every single chapter. Here we present a more general overview. A first step can be done once we will a feasible form of the partition function of ABJM. In this way we will have a concrete way to compute the full cosmological measure.

One day astrophysicist will be able to refine their observations and provide more restrictions on cosmological observables. This might exclude one of the two wave functions proposal. Now that we have a way to compute the full cosmological measure (at least qualitatively), and that we know how holography selects either one or the other wave function, we might test the theory against observations.

The Hartle-Hertog proposal has been shown in the semiclassical approximation only. A further direction is to explore this correspondence also beyond the semiclassical level, i.e. by including loop corrections, or by employing different techniques to evaluate it, [150, 151, 152, 153, 154, 155]. This would push the Hartle-Hertog proposal a step further.

Another insight is to explore the nature of the two boundaries of dS space. In recent years, the so called ER=EPR conjecture [156, 157], lead to a better understanding of the entanglement in field theory, and to a better understanding of quantum gravity itself. In this new description entanglement in field theory can be described by a wormhole that connects two observers on different (or same) boundaries. A future direction is to understand if the ER=EPR conjecture

can be translated to dS space, to analyze the role of the two boundaries and of the cosmological horizon in a holographic scenario.

Finally there are still many open questions that might be answered through holography. We still do not have a microcanonical description of the entropy of the cosmological horizon. We have not answered yet to the question on what is the meaning of boundary data that are casually disconnected to a physical observer covered by an horizon. We do not have a good understanding on how to incorporate this holographic set-up in a deeper theory, i.e. string theory. We know that string theory has an infinite spectrum of higher spin massive fields. If a suitable limit where their masses disappear is explored, one might hope to recover the same spectrum observed in Vasiliev theory. This is the so called tensionless limit, and might provide a suitable path to connect our results with a deeper theory such as string theory. In that case we might have a stringy description of the dS/CFT correspondence. String theory predicts a vast number of dS vacua, and the holographic wave function of the universe might provide a measure to select them.

Appendix A

Appendix

A.1 Basis change.

The wave function can be written in terms of the new asymptotic variables. The details of this basis change can be found in [81], and here we summarize the results.

α basis.

$$\Psi_{HH}[\gamma_{ij},\alpha,\eta] = \int d\chi e^{\int d^3x G(\gamma_{ij},\alpha,h_{ij},\chi,\eta)} \Psi_{HH}[h_{ij},\chi]\,, \tag{A.1}$$

where the generating function is

$$\begin{aligned} G(\gamma_{ij},\alpha,h_{ij},\chi,\eta) = \frac{\sqrt{\gamma}}{\kappa\eta^3}\left(1+\eta^2\left(\gamma^{ij}h_{ij}+\frac{R_{(\gamma)}}{2}\right)\right) \\ -\frac{\sigma}{2}\eta^{-\sigma}\alpha^2\gamma^{3/2\sigma}+\sigma\eta^{-\lambda_+}\alpha\gamma^{\lambda_+/2\sigma}-\frac{\lambda_+\sqrt{\gamma}}{2\eta^3}\chi^2\,. \end{aligned} \tag{A.2}$$

β basis.

$$\Psi_{HH}[\gamma_{ij},\beta,\eta] = \int d\chi e^{\int d^3x G(\gamma_{ij},\beta,h_{ij},\chi,\eta)} \Psi_{HH}[h_{ij},\chi]\,, \tag{A.3}$$

where the generating function is

$$G(\gamma_{ij},\beta,h_{ij},\chi,\eta)=\frac{\sqrt{\gamma}}{\kappa\eta^3}\left(1+\eta^2\left(\gamma^{ij}h_{ij}+\frac{R_{(\gamma)}}{2}\right)\right)$$
$$+\frac{\sigma}{2}\eta^{\sigma}\beta^2\gamma^{3/2\sigma}-\sigma\eta^{-\lambda_-}\beta\gamma^{\lambda_-/2\sigma}-\frac{\lambda_-\sqrt{\gamma}}{2\eta^3}\chi^2\,. \tag{A.4}$$

A.2 Anisotropic Euclidean AdS solutions.

The goal of these appendices is to give the technical details associated with the physics of gravitational theories that have a squashed sphere boundary. First we start with the equations of motion and afterwards the UV and IR expansions of the fields are given. Afterwards we give our method to numerically calculate this action.

A.2.1 Equations of motion

The equations of motion can be obtained by substituting the metric (4.4) into the action (4.2) and by varying this respectively with respect to l_0, l_1, l_2, l_3 and Φ,

$$
\begin{aligned}
&\frac{{l_0}^2{l_3}^2}{{l_1}^2{l_2}^2}+\frac{{l_0}^2{l_2}^2}{{l_1}^2{l_3}^2}+\frac{{l_0}^2{l_1}^2}{{l_2}^2{l_3}^2}-\frac{2{l_0}^2}{{l_1}^2}-\frac{2{l_0}^2}{{l_2}^2}-\frac{2{l_0}^2}{{l_3}^2}+4l_0^2V(\phi)+\frac{4{l_1}'{l_2}'}{l_1l_2}+\frac{4{l_1}'{l_3}'}{l_1l_3}\\
&+\frac{4{l_2}'{l_3}'}{l_2l_3}-2{\phi'}^2=0\ ,\\
&-\frac{4{l_0}'{l_1}'}{l_0l_1}-\frac{4{l_0}'{l_3}'}{l_0l_3}-\frac{{l_0}^2{l_3}^2}{{l_1}^2{l_2}^2}+\frac{3{l_0}^2{l_2}^2}{{l_1}^2{l_3}^2}-\frac{{l_0}^2{l_1}^2}{{l_2}^2{l_3}^2}-\frac{2{l_0}^2}{{l_1}^2}+\frac{2{l_0}^2}{{l_2}^2}-\frac{2{l_0}^2}{{l_3}^2}\\
&+4{l_0}^2V(\phi)+\frac{4{l_1}''}{l_1}+\frac{4{l_1}'{l_3}'}{l_1l_3}+\frac{4{l_3}''}{l_3}+2{\phi'}^2=0\ ,\\
&-\frac{4{l_0}'{l_2}'}{l_0l_2}-\frac{4{l_0}'{l_3}'}{l_0l_3}-\frac{{l_0}^2{l_3}^2}{{l_1}^2{l_2}^2}-\frac{{l_0}^2{l_2}^2}{{l_1}^2{l_3}^2}+\frac{3{l_0}^2{l_1}^2}{{l_2}^2{l_3}^2}+\frac{2{l_0}^2}{{l_1}^2}-\frac{2{l_0}^2}{{l_2}^2}-\frac{2{l_0}^2}{{l_3}^2}\\
&+4{l_0}^2V(\phi)+\frac{4{l_2}''}{l_2}+\frac{4{l_2}'{l_3}'}{l_2l_3}+\frac{4{l_3}''}{l_3}+2{\phi'}^2=0\ ,\\
&-\frac{4{l_0}'{l_1}'}{l_0l_1}-\frac{4{l_0}'{l_2}'}{l_0l_2}+\frac{3{l_0}^2{l_3}^2}{{l_1}^2{l_2}^2}-\frac{{l_0}^2{l_2}^2}{{l_1}^2{l_3}^2}-\frac{{l_0}^2{l_1}^2}{{l_2}^2{l_3}^2}-\frac{2{l_0}^2}{{l_1}^2}-\frac{2{l_0}^2}{{l_2}^2}+\frac{2{l_0}^2}{{l_3}^2}\\
&+4{l_0}^2V(\phi)+\frac{4{l_1}''}{l_1}+\frac{4{l_1}'{l_2}'}{l_1l_2}+\frac{4{l_2}''}{l_2}+2{\phi'}^2=0\ ,\\
&{l_0}^2\frac{\partial V(\phi)}{\partial\phi}+\frac{{l_0}'\phi'}{l_0}-\frac{{l_1}'\phi'}{l_1}-\frac{{l_2}'\phi'}{l_2}-\frac{{l_3}'\phi'}{l_3}-\phi''=0
\end{aligned}
\tag{A.5}
$$

These equations of motion are valid for both the AdS and dS domain of the wave function, for this reason the variables are understood to be a function of τ, defined in (5.1) and $'$ means a derivative with respect to τ. The AdS equations of motion (discussed in Chapter 3) get retrieved by setting $\tau = r$, and the Lorentzian dS solutions (discussed in Chapter 4) lie along the line $\tau = t + i\pi/2$.

A.2.2 Solutions

IR NUT

For the NUT solutions we know that around the NUT, denoted here by τ_*, the metric should look like $\mathbb{R}^4$

$$ds^2 = d\tau^2 + \frac{(\tau-\tau^*)^2}{4}(\sigma_1^2+\sigma_2^2+\sigma_3^2)\ . \tag{A.6}$$

Therefore we can expand the fields around $\tau = \tau^*$ with the following Ansatz

$$\begin{aligned}
\Phi(\tau) &= \Phi_0 + \Phi_k(\tau-\tau^*)^k, \\
l_1(\tau) &= \frac{1}{2}(\tau-\tau^*) + \beta_{k+1}(\tau-\tau^*)^{k+1}\ , \\
l_2(\tau) &= \frac{1}{2}(\tau-\tau^*) + \gamma_{k+1}(\tau-\tau^*)^{k+1}\ , \\
l_3(\tau) &= \frac{1}{2}(\tau-\tau^*) + \delta_{k+1}(\tau-\tau^*)^{k+1}\ ,
\end{aligned} \tag{A.7}$$

where k runs from 1 to ∞. By plugging in this Ansatz into the equations of motion (A.5) we get the following leading order terms

$$\begin{aligned}
l_1(\tau) &= \frac{1}{2}(\tau-\tau^*) + \beta_3(\tau-\tau^*)^3 + \frac{1}{1920}\Bigg(-4V(\Phi_0)^2 - 576V(\Phi_0)\gamma_3 \\
&\quad - 6912{\gamma_3}^2 + 144V(\Phi_0)\beta_3 - 6912\gamma_3\beta_3 + 4608{\beta_3}^2 \\
&\quad - 3\left(\frac{\partial V(\Phi_0)}{\partial\Phi_0}\right)^2\Bigg)(\tau-\tau^*)^5 + \mathcal{O}\left((\tau-\tau^*)^7\right)\ , \\
l_2(\tau) &= \frac{1}{2}(\tau-\tau^*) + \gamma_3(\tau-\tau^*)^3 + \frac{1}{1920}\Bigg(-4V(\Phi_0)^2 + 144V(\Phi_0)\gamma_3 \\
&\quad + 4608{\gamma_3}^2 - 576V(\Phi_0)\beta_3 - 6912\gamma_3\beta_3 + 6912{\beta_3}^2 \\
&\quad - 3\left(\frac{\partial V(\Phi_0)}{\partial\Phi_0}\right)^2\Bigg)(\tau-\tau^*)^5 + \mathcal{O}\left((\tau-\tau^*)^7\right)\ , \\
l_3(\tau) &= \frac{1}{2}(\tau-\tau^*) - \left(\frac{1}{12}V(\Phi_0) + \beta_3 + \gamma_3\right)(\tau-\tau^*)^3 + \frac{1}{1920}\Bigg(16V(\Phi_0)^2 \\
&\quad + 624V(\Phi_0)\gamma_3 + 4608{\gamma_3}^2 + 624V(\Phi_0)\beta_3 + 16128\gamma_3\beta_3 + 4608{\beta_3}^2 \\
&\quad - 3\left(\frac{\partial V(\Phi_0)}{\partial\Phi_0}\right)^2\Bigg)(\tau-\tau^*)^5 + \mathcal{O}\left((\tau-\tau^*)^7\right)\ , \\
\Phi(\tau) &= \Phi_0 + \frac{1}{8}\frac{\partial V(\Phi_0)}{\partial\Phi_0}(\tau-\tau^*)^2 + \Bigg(\frac{1}{288}V(\Phi_0)\frac{\partial V(\Phi_0)}{\partial\Phi_0} \\
&\quad + \frac{1}{192}\frac{\partial V(\Phi_0)}{\partial\Phi_0}\frac{\partial^2 V(\Phi_0)}{\partial\Phi_0^2}\Bigg)(\tau-\tau^*)^4 + \mathcal{O}\left((\tau-\tau^*)^6\right)\ .
\end{aligned} \tag{A.8}$$

This expansion is controlled by the three real parameters β_3, γ_3 and Φ_0 which are ultimately related to the two squashing parameters A and B together with the coefficients A_3 and B_3 of the subleading terms and the two free parameters in the UV expansion of the scalar field α and β, at the asymptotic boundary.

IR Bolt

We can do the same thing for the Bolt solutions. In this case we know that the metric should look like $\mathbb{R}^2 \times S^2$ around the Bolt position τ_*, that is

$$ds^2 = d\tau^2 + \frac{(\tau-\tau^*)^2}{4}\sigma_1^2 + \beta_0^2\sigma_2^2 + \gamma_0^2\sigma_3^2 \ . \tag{A.9}$$

Therefore we take the following Ansatz for the expansion of the fields around $\tau = \tau^*$,

$$\begin{aligned} &\Phi(\tau) = \Phi_0 + \Phi_k(\tau-\tau^*)^k, && l_1(\tau) = \beta_0 + \beta_k(\tau-\tau^*)^k \ , \\ &l_2(\tau) = \gamma_0 + \gamma_k(\tau-\tau^*)^k \ , && l_3(\tau) = \frac{1}{2}(\tau-\tau^*) + \delta_{k+1}(\tau-\tau^*)^{k+1} \ , \end{aligned} \tag{A.10}$$

with k going from 1 to ∞. If we solve the equations of motion (A.5) with this Ansatz, we get

$$\begin{aligned}
l_1(\tau) &= \gamma_0 + \left(\frac{1}{4\gamma_0} - \frac{V(\Phi_0)\gamma_0}{4}\right)(\tau-\tau^*)^2 \\
&\quad - \left(\frac{11}{192{\gamma_0}^3} - \frac{V(\Phi_0)}{24\gamma_0} + \gamma_4 + \frac{\gamma_0}{32}\left(\frac{\partial V(\Phi_0)}{\partial\Phi_0}\right)^2\right)(\tau-\tau^*)^4 \\
&\quad + \mathcal{O}\left((\tau-\tau^*)^6\right) \ , \\
l_2(\tau) &= \gamma_0 + \left(\frac{1}{4\gamma_0} - \frac{V(\Phi_0)\gamma_0}{4}\right)(\tau-\tau^*)^2 + \gamma_4(\tau-\tau^*)^4 + \mathcal{O}\left((\tau-\tau^*)^6\right) \ , \\
l_3(\tau) &= \frac{1}{2}(\tau-\tau^*) - \frac{(\tau-\tau^*)^3}{12{\gamma_0}^2} \\
&\quad + \left(\frac{V(\Phi_0)^2}{160} + \frac{53}{1920{\gamma_0}^4} - \frac{V(\Phi_0)}{40{\gamma_0}^2} - \frac{1}{320}\left(\frac{\partial V(\Phi_0)}{\partial\Phi_0}\right)^2\right)(\tau-\tau^*)^5 \\
&\quad + \mathcal{O}\left((\tau-\tau^*)^7\right) \ , \\
\Phi(\tau) &= \Phi_0 + \frac{1}{4}\frac{\partial V(\Phi_0)}{\partial\Phi_0}(\tau-\tau^*)^2 \\
&\quad + \frac{1}{192\gamma_0^2}\frac{\partial V(\Phi_0)}{\partial\Phi_0}\left(-4 + 3{\gamma_0}^2(2V(\Phi_0) + \frac{\partial^2 V(\Phi_0)}{\partial\Phi_0^2})\right)(\tau-\tau^*)^4 \\
&\quad + \mathcal{O}\left((\tau-\tau^*)^6\right) \ .
\end{aligned} \tag{A.11}$$

We chose to parametrize this expansion by the three independent real parameters γ_0, γ_4 and Φ_0 which are again mapped to the squashing parameters A, B and α, β in the UV. Notice that to get the NUT or Bolt double squashing results without scalar field we have to put $\Phi_0 = 0$ and $V(\Phi) = \Lambda$ in the initial conditions above, effectively reducing the above expansions and equations of motion to the ones discussed in [98].

UV

The asymptotic solutions are the same for both the NUT and the bolt. To find them, we look at the asymptotic form of the metric

$$ds^2 = d\tau^2 + e^{2\tau}(A_0\sigma_1^2 + B_0\sigma_2^2 + C_0\sigma_3^2) \ . \tag{A.12}$$

If we use that the scalar field potential around $\Phi = 0$ behaves as $V(\Phi) \sim \Lambda - \Phi^2$, we can make the Ansatz of a Fefferman-Graham expansion

$$\begin{aligned} &\Phi(\tau) = \alpha e^{-\tau} + \beta e^{-2\tau} + \dots \ , \qquad l_1(\tau) = A_0 e^{\tau} + A_k e^{(1-k)\tau} \ , \\ &l_2(\tau) = B_0 e^{\tau} + B_k e^{(1-k)\tau} \ , \qquad l_3(\tau) = C_0 e^{\tau} + C_k e^{(1-k)\tau} \ , \end{aligned} \tag{A.13}$$

where the sum over k goes over all positive integers. The constants are determined by solving the equations of motion (A.5), order by order, giving the following consistent series expansion

$$\begin{aligned} l_1(\tau) &= A_0 e^{\tau} + \frac{1}{16 {A_0}{B_0}^2{C_0}^2}\Big(-5{A_0}^4 + 2{A_0}^2{B_0}^2 + 3{B_0}^4 + 2{A_0}^2{C_0}^2 \\ &\quad - 6{B_0}^2{C_0}^2 \qquad + 3{C_0}^4 - 2{A_0}^2{B_0}^2{C_0}^2\alpha^2\Big)e^{-\tau} + A_3 e^{-2\tau} + \mathcal{O}(e^{-3\tau}) \ , \\ l_2(\tau) &= B_0 e^{\tau} + \frac{1}{16 {A_0}{B_0}^2{C_0}^2}\Big(3{A_0}^4 + 2{A_0}^2{B_0}^2 - 5{B_0}^4 - 6{A_0}^2{C_0}^2 \\ &\quad + 2{B_0}^2{C_0}^2 \qquad + 3{C_0}^4 - 2{A_0}^2{B_0}^2{C_0}^2\alpha^2\Big)e^{-\tau} + B_3 e^{-2\tau} \\ &\quad + \mathcal{O}(e^{-3\tau}) \ , \\ l_3(\tau) &= C_0 e^{\tau} + \frac{1}{16 {A_0}{B_0}^2{C_0}^2}\Big(3{A_0}^4 - 6{A_0}^2{B_0}^2 + 3{B_0}^4 + 2{A_0}^2{C_0}^2 + 2{B_0}^2{C_0}^2 \\ &\qquad - 5{C_0}^4 - 2{A_0}^2{B_0}^2{C_0}^2\alpha^2\Big)e^{-\tau} - \left(\frac{A_3 C_0}{A_0} - \frac{B_3 C_0}{B_0} - \frac{2}{3}C_0\alpha\beta\right)e^{-2\tau} \\ &\qquad + \mathcal{O}(e^{-3\tau}) \ , \\ \Phi(\tau) &= \frac{\alpha}{2(A_0 B_0 C_0)^{1/3}}e^{-\tau} + \frac{\beta}{4(A_0 B_0 C_0)^{2/3}}e^{-2\tau} + \mathcal{O}(e^{-3\tau}) \ . \end{aligned} \tag{A.14}$$

We have performed this expansion up to eight order and have verified that it is controlled by the seven parameters $\{A_0, B_0, C_0, A_3, B_3, \alpha, \beta\}$. The coefficients

α and β appearing in the expansion of Φ are undetermined by the equations of motion, here we rescaled them to the most convenient convention making sure it is conform with the literature. Notice that when we are deep into the dS domain $\tau = t + i\pi/2$, which makes the scale factors imaginary, giving the Lorentzian metric from (5.2).

Since the equations of motion (A.5) are invariant under constant shifts of the radial coordinate, one can set $A_0 = \frac{1}{4}$ by an appropriate shift of τ. One can now identify B_0 and C_0 with the squashing parameters in (1.63) as follows

$$A = \frac{1}{4C_0^2} - 1 \,, \qquad B = \frac{1}{4B_0^2} - 1 \,. \tag{A.15}$$

The parameters A_3, B_3 and β are independent from the point of view of the UV expansion but are ultimately fixed in terms of A, B and α by the regularity conditions that we imposed for the numerical solutions of the full nonlinear equations of motion.

From IR to UV

It is worth discussing how we constructed the numerical solutions of the full nonlinear equations of motion in (A.5). Let us start with the AdS-Taub-NUT solutions. For these we picked real values for the parameters a_3, b_3 and ϕ_0 in the IR expansion (A.8). For each such value we then numerically integrated the equations of motion from $r = r_*$ to some large value of r_c. If the resulting numerical solution does not exhibit a singularity at an intermediate value of the radial coordinate r we declared the solution to be regular and read of the asymptotic parameters B_0, C_0 and α and β in (A.14) which we then relate to the squashing parameters A and B using (A.15). As expected we find that there are no restrictions on the parameters A and B, i.e. as we vary a_3 and b_3 for a fixed ϕ_0 we can explore the whole (A, B) plane. If we take a non-zero value for ϕ_0 we will reach the same conclusion with the only difference that the region in the (a_3, b_3) plane that gives valid UV solutions shifts to higher values of a_3 and b_3 when ϕ_0 increases as can be seen in Figure A.1.

The procedure we used to construct the AdS-Taub-Bolt solutions is again very similar. We start with the IR expansion in (A.11), vary the parameters γ_0 and γ_4 and integrate numerically the equations of motion. Finally, we read off the asymptotic parameters B_0 and C_0 from the behaviour of the numerical solutions at large r and deduce the corresponding values of A and B using the relation in (A.15). However, there is an important difference between these solutions and the AdS-Taub-NUT solutions. For a fixed value of B there are critical values of A below/above which there are no AdS-Taub-Bolt solutions. This leads

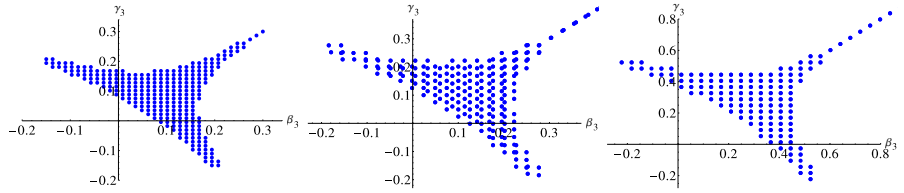

Figure A.1: Initial conditions for a_3 and b_3 that give rise to non-singular solutions. From left to the right we took $\phi_0 = 0, 1, 2$.

to curves in the (A, B) plane and the AdS-Taub-Bolt solutions exist only for values of the squashing parameters that are below or above these critical curves. Furthermore for every value of (A, B) for which Bolt solutions exist there are two possible solutions of the equations of motion which we dub "positive" and "negative" branch. All of these features are extensions of the familiar behaviour of the analytically known AdS-Taub-Bolt solutions with $B = 0$ discussed in [158, 66] and for which more details can be found in [98].

A.2.3 Evaluating the numerical action

A.2.4 Euclidean Action

To evaluate the action, it is easiest to use the on-shell version of (4.2):

$$I_{\rm E} = -2\pi \int d\tau\, l_1(\tau) l_2(\tau) l_3(\tau) V(\Phi(\tau)) \\ - 2\pi \Big(l_2(\tau) l_3(\tau) l_1'(\tau) + l_1(\tau) l_3(\tau) l_2'(\tau) + l_1(\tau) l_2(\tau) l_3'(\tau) \Big)_{\tau=\tau_{\rm c}} \qquad \text{(A.16)}$$

where $\tau_{\rm c}$ is the cut-off radius at which we take the boundary $\partial\mathcal{M}$.

It is interesting to focus on the evaluation of the action for our AdS solutions (thus assuming that $\tau = r$, the radial AdS coordinate). Namely, these lead to the thermodynamical properties that were discussed in Section 4. As usual for asymptotically locally AdS space, the value of the on-shell action diverges, and one needs to implement a regularization procedure. We apply the usual tools of holographic renormalization which were used for the single squashed AdS-NUT/Bolt solutions in [66]. This procedure amounts to adding infinite counterterms to the action in (A.16) that make it finite on-shell. These counterterms are universal for a given gravitational theory and thus we can

simply apply the results of [66] to our setup. The counterterms are given by

$$S_{\rm ct} = \frac{1}{8\pi}\int_{\partial\mathcal{M}} d^3x\sqrt{h}\left(2+\frac{\mathcal{R}}{2}+\frac{\Phi^2}{2}\right)\,, \tag{A.17}$$

where $\mathcal{R}$ is the scalar curvature of the boundary metric h_{ij}. Evaluating this counterterm action yields

$$S_{\rm ct} = \pi\frac{2({l_1}^2{l_2}^2+{l_2}^2{l_3}^2+{l_1}^2{l_3}^2)+2{l_1}^2{l_2}^2{l_3}^2(4+\Phi^2)-{l_1}^4-{l_2}^4-{l_3}^4}{2l_1l_2l_3}\,. \tag{A.18}$$

Substituting our asymptotic expansions of the functions $l_i(\tau)$ and the scalar field (A.14) gives[1]

$$S_{\rm ct} = \pi\Big(4A_0B_0C_0\epsilon^{3\tau}-\frac{1}{4A_0B_0C_0}\Big(A_0^4+B_0^4+C_0^4-2B_0^2C_0^2-2A_0^2B_0^2 \\ -2A_0^2C_0^2+2(A_0B_0C_0)^{4/3}\alpha^2\Big)\epsilon^{\tau}-\frac{2}{3}\alpha\beta+\mathcal{O}(\epsilon^{-\tau})\Big)_{\tau=\tau_{\rm c}}\,. \tag{A.19}$$

The asymptotic form of the original on-shell gravitational action in (A.16) reads

$$I_{\rm E} = -\pi\Big(4A_0B_0C_0\epsilon^{3\tau}-\frac{1}{4A_0B_0C_0}\Big(A_0^4+B_0^4+C_0^4-2B_0^2C_0^2-2A_0^2B_0^2 \\ -2A_0^2C_0^2+2(A_0B_0C_0)^{4/3}\alpha^2\Big)\epsilon^{\tau}+\mathcal{O}(1)\Big)_{\tau=\tau_{\rm c}}\,. \tag{A.20}$$

As expected the sum

$$I_{\rm E}^{\rm ren} = I_{\rm E}+S_{\rm ct}\,, \tag{A.21}$$

remains finite in the $\tau=\tau_{\rm c}\to\infty$ limit and thus this sum can serve as a good regularized on-shell action.

Since our gravitational solutions are constructed numerically, evaluating the regularized on-shell action $S_{\rm ren}$ is tricky. The difficulty comes from the fact that one has to add a large positive and a large negative number and this could lead to numerical instabilities. To remedy this, we found it useful to employ the following strategy. From (A.20) we know how the on-shell action diverges at large values of τ. We can thus evaluate numerically this on-shell action at large but finite values of r and fit the resulting values to the function

$$f = De^{3\tau_c}+Ee^{2\tau_c}+Fe^{\tau_c}+G+He^{-\tau_c}+Ie^{-2\tau_c}\,. \tag{A.22}$$

[1] Notice that to expand the scalar field, we have to assume that it rolled down its potential such that the potential is approximated by $V(\Phi)\approx\Lambda-\Phi^2+\ldots$.

We can then read of the coefficients D, E, and F and use the first three terms in (A.22) as our numerical counterterm action that should be added to S to produce a finite result. If there is no scalar field, the value of G is the final value for the renormalized action.

In the case of the AdS theories we considered we have to do some more work if there is a non-zero scalar field. Because in the free $O(N)$ model we want to analyse the deformation by an operator of dimension $\Delta = 1$, the scheme of alternate quantization comes into play and we have to evaluate the action in terms of β. To achieve this we have to perform a Legendre transform by adding the following term [131, 159]

$$S_- = -\int_{\partial\mathcal{M}} d^3x\sqrt{h}\Phi\pi_\Phi \ , \tag{A.23}$$

where π_Φ is the canonical momentum of Φ at the boundary

$$\pi_\Phi = \frac{1}{\sqrt{h}}\frac{\delta(I_{\rm E} + S_{\rm ct})}{\delta\Phi} = \partial_\tau\Phi + \Phi \ . \tag{A.24}$$

After plugging in the asymptotic expansions in this term, we get

$$S_- = 2\pi\alpha\beta + \mathcal{O}(e^{2\tau}) \ . \tag{A.25}$$

Thus to get the complete action, we have to add to G the constant parts from (A.19) and (A.25). The procedure is equivalent to the one discussed in A.1.

As a consistency check of our numerical results we should find that the coefficient E in (A.22) is approximately 0. We found that this value usual was of the order of $\mathcal{O}(10^{-10})$, but became bigger, up to order $\mathcal{O}(10^{-4})$, for squashings close to -1.

To evaluate the dS actions it is sufficient to evaluate the action along the path $\mathcal{C}'$ in the complex τ plane, see Fig. 5.1. Due to the properties of the dS solutions the real part of the action will tend to a constant along the Lorentzian part of the contour, while all the divergent terms are encapsulated by the imaginary part of the action.

A.3 Anisotropic dS solutions.

The method to find the dS-Taub-NUT solutions is very similar to the AdS case, except that we now have to evaluate the equations of motion along a contour in the complex τ-plane. Due to the special nature of the potential chosen here [64, 81], the classical solutions all lie along a horizontal line at $\tau = i\pi/2 + t$.

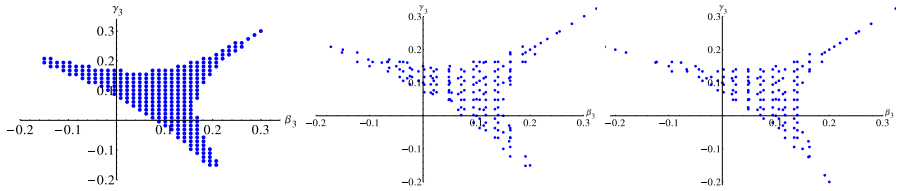

Figure A.2: Initial conditions for a_3 and b_3 that give rise to non-singular solutions. From the left to the right $\phi_0 = 0, 1/2i, 3/4i$.

Evaluating the equations of motion along this line for large τ will learn us if the initial conditions give valid solutions that do not evolve into a singularity. The initial conditions (β_3, γ_3) that give valid solutions are just minus the ones from the AdS solutions without a scalar field. However, when ϕ_0 gets increased, the initial conditions do not change significantly in this case.

The dS counterpart of the Bolt solutions can be found by making the AdS initial conditions imaginary. The other properties of the AdS-Bolt solutions carry over in a straightforward way, e.g. there is only a limited region in parameter space were these solutions exist, and there is always a positive and negative branch.

From IR to UV

In the double squashed case the initial conditions giving regular asymptotic solutions, resemble a triangular shape also in this case. The only difference is that increasing ϕ_0 does not significantly alter the behaviour of the dS initial conditions. This can be seen in figure A.2, for a choice of $\phi_0 = 0, 1/2i, 3/4i$.

The dS counterpart of these Bolt solutions and the numerical calculation of the action is a straightforward generalization of the discussion of Appendix A.2.

Bibliography

[1] Edwin Hubble. A relation between distance and radial velocity among extra-galactic nebulae. *Proc. Nat. Acad. Sci.*, 15:168–173, 1929.

[2] Arno A. Penzias and Robert Woodrow Wilson. A Measurement of excess antenna temperature at 4080-Mc/s. *Astrophys. J.*, 142:419–421, 1965.

[3] Alexei A. Starobinsky. Spectrum of relict gravitational radiation and the early state of the universe. *JETP Lett.*, 30:682–685, 1979. [Pisma Zh. Eksp. Teor. Fiz.30,719(1979)].

[4] Viatcheslav F. Mukhanov and G. V. Chibisov. Quantum Fluctuations and a Nonsingular Universe. *JETP Lett.*, 33:532–535, 1981. [Pisma Zh. Eksp. Teor. Fiz.33,549(1981)].

[5] Viatcheslav F. Mukhanov and G. V. Chibisov. The Vacuum energy and large scale structure of the universe. *Sov. Phys. JETP*, 56:258–265, 1982. [Zh. Eksp. Teor. Fiz.83,475(1982)].

[6] C. L. Bennett, A. Banday, K. M. Gorski, G. Hinshaw, P. Jackson, P. Keegstra, A. Kogut, George F. Smoot, D. T. Wilkinson, and E. L. Wright. Four year COBE DMR cosmic microwave background observations: Maps and basic results. *Astrophys. J.*, 464:L1–L4, 1996.

[7] Eiichiro Komatsu et al. Results from the Wilkinson Microwave Anisotropy Probe. *PTEP*, 2014:06B102, 2014.

[8] G. Hinshaw et al. Nine-Year Wilkinson Microwave Anisotropy Probe (WMAP) Observations: Cosmological Parameter Results. *Astrophys. J. Suppl.*, 208:19, 2013.

[9] C. L. Bennett et al. Nine-Year Wilkinson Microwave Anisotropy Probe (WMAP) Observations: Final Maps and Results. *Astrophys. J. Suppl.*, 208:20, 2013.

[10] J. Dunkley et al. The Atacama Cosmology Telescope: Cosmological Parameters from the 2008 Power Spectra. *Astrophys. J.*, 739:52, 2011.

[11] Jonathan L. Sievers et al. The Atacama Cosmology Telescope: Cosmological parameters from three seasons of data. *JCAP*, 1310:060, 2013.

[12] P. A. R. Ade et al. Planck 2013 results. XXII. Constraints on inflation. *Astron. Astrophys.*, 571:A22, 2014.

[13] P. A. R. Ade et al. Planck 2013 results. XVI. Cosmological parameters. *Astron. Astrophys.*, 571:A16, 2014.

[14] P. A. R. Ade et al. Planck 2013 results. XV. CMB power spectra and likelihood. *Astron. Astrophys.*, 571:A15, 2014.

[15] P. A. R. Ade et al. Planck 2013 results. I. Overview of products and scientific results. *Astron. Astrophys.*, 571:A1, 2014.

[16] D. J. Fixsen. The Temperature of the Cosmic Microwave Background. *Astrophys. J.*, 707:916–920, 2009.

[17] M. J. Reid, J. A. Braatz, J. J. Condon, K. Y. Lo, C. Y. Kuo, C. M. V. Impellizzeri, and C. Henkel. The Megamaser Cosmology Project: IV. A Direct Measurement of the Hubble Constant from UGC 3789. *Astrophys. J.*, 767:154, 2013.

[18] Alan H. Guth. The Inflationary Universe: A Possible Solution to the Horizon and Flatness Problems. *Phys. Rev.*, D23:347–356, 1981.

[19] Andrei D. Linde. A New Inflationary Universe Scenario: A Possible Solution of the Horizon, Flatness, Homogeneity, Isotropy and Primordial Monopole Problems. *Phys. Lett.*, B108:389–393, 1982.

[20] Alexander Vilenkin. The Birth of Inflationary Universes. *Phys. Rev.*, D27:2848, 1983.

[21] Andrei D. Linde. Chaotic Inflation. *Phys. Lett.*, B129:177–181, 1983.

[22] Andrei D. Linde. Eternally Existing Selfreproducing Chaotic Inflationary Universe. *Phys. Lett.*, B175:395–400, 1986.

[23] Andrei D. Linde. Fast roll inflation. *JHEP*, 11:052, 2001.

[24] Renata Kallosh, Andrei Linde, and Alexander Westphal. Chaotic Inflation in Supergravity after Planck and BICEP2. *Phys. Rev.*, D90(2):023534, 2014.

[25] Fedor L. Bezrukov and Mikhail Shaposhnikov. The Standard Model Higgs boson as the inflaton. *Phys. Lett.*, B659:703–706, 2008.

[26] A. O. Barvinsky, A. Yu. Kamenshchik, and A. A. Starobinsky. Inflation scenario via the Standard Model Higgs boson and LHC. *JCAP*, 0811:021, 2008.

[27] J. L. F. Barbon and J. R. Espinosa. On the Naturalness of Higgs Inflation. *Phys. Rev.*, D79:081302, 2009.

[28] Katherine Freese, Joshua A. Frieman, and Angela V. Olinto. Natural inflation with pseudo - Nambu-Goldstone bosons. *Phys. Rev. Lett.*, 65:3233–3236, 1990.

[29] David H. Lyth and Andrew R. Liddle. *The primordial density perturbation: Cosmology, inflation and the origin of structure.* 2009.

[30] Leonardo Senatore. TASI 2012 Lectures on Inflation. In *Proceedings, Theoretical Advanced Study Institute in Elementary Particle Physics: Searching for New Physics at Small and Large Scales (TASI 2012): Boulder, Colorado, June 4-29, 2012*, pages 221–302, 2013.

[31] Daniel Baumann. Inflation. In *Physics of the large and the small, TASI 09, proceedings of the Theoretical Advanced Study Institute in Elementary Particle Physics, Boulder, Colorado, USA, 1-26 June 2009*, pages 523–686, 2011.

[32] William H. Kinney. TASI Lectures on Inflation. 2009.

[33] B. P. et al Abbott. Observation of gravitational waves from a binary black hole merger. *Phys. Rev. Lett.*, 116:061102, Feb 2016.

[34] S. Perlmutter et al. Measurements of the cosmological parameters Omega and Lambda from the first 7 supernovae at z>=0.35. *Astrophys. J.*, 483:565, 1997.

[35] S. Perlmutter et al. Discovery of a supernova explosion at half the age of the Universe and its cosmological implications. *Nature*, 391:51–54, 1998.

[36] S. Perlmutter et al. Measurements of Omega and Lambda from 42 high redshift supernovae. *Astrophys. J.*, 517:565–586, 1999.

[37] Adam G. Riess et al. Observational evidence from supernovae for an accelerating universe and a cosmological constant. *Astron. J.*, 116:1009–1038, 1998.

[38] Adam G. Riess et al. A Redetermination of the Hubble Constant with the Hubble Space Telescope from a Differential Distance Ladder. *Astrophys. J.*, 699:539–563, 2009.

[39] Dionysios Anninos. De Sitter Musings. *Int. J. Mod. Phys.*, A27:1230013, 2012.

[40] Steven Weinberg. The cosmological constant problem. *Rev. Mod. Phys.*, 61:1–23, Jan 1989.

[41] Lee Smolin. Quantum gravity with a positive cosmological constant. 2002.

[42] S. W. Hawking. Black holes and thermodynamics. *Phys. Rev. D*, 13:191–197, Jan 1976.

[43] G. W. Gibbons and S. W. Hawking. Cosmological Event Horizons, Thermodynamics, and Particle Creation. *Phys. Rev.*, D15:2738–2751, 1977.

[44] Marcus Spradlin, Andrew Strominger, and Anastasia Volovich. Les Houches lectures on de Sitter space. In *Unity from duality: Gravity, gauge theory and strings. Proceedings, NATO Advanced Study Institute, Euro Summer School, 76th session, Les Houches, France, July 30-August 31, 2001*, pages 423–453, 2001.

[45] Raphael Bousso. TASI Lectures on the Cosmological Constant. *Gen. Rel. Grav.*, 40:607–637, 2008.

[46] James B. Hartle, S.W. Hawking, and Thomas Hertog. Vector Fields in Holographic Cosmology. *JHEP*, 1311:201, 2013.

[47] Don N. Page. Lectures on quantum cosmology. pages 135–170, 1990.

[48] S. W. Hawking. Lectures on Quantum Cosmology. In *Quantum Gravity and Cosmology, Proceedings, 8th Summer Institute, Kyoto, Japan, May 7-11,1985*, pages 170–206, 1986.

[49] David L. Wiltshire. An Introduction to quantum cosmology. In *Cosmology: The Physics of the Universe. Proceedings, 8th Physics Summer School, Canberra, Australia, Jan 16-Feb 3, 1995*, pages 473–531, 1995.

[50] Jonathan J. Halliwell. Introductory Lectures on Quantum Cosmology. In *7th Jerusalem Winter School for Theoretical Physics: Quantum Cosmology and Baby Universes Jerusalem, Israel, 27 December 1989 - 4 January 1990*, pages 159–243, 1990.

[51] Gianluca Calcagni. *Classical and Quantum Cosmology*. Graduate Texts in Physics. Springer, 2017.

[52] B. S. DeWitt. Quantum theory of gravity. in the canonical theory. *Phys. Rev.*, 160:1113–1148, Aug 1967.

[53] Carlo Rovelli. Notes for a brief history of quantum gravity. In *Recent developments in theoretical and experimental general relativity, gravitation and relativistic field theories. Proceedings, 9th Marcel Grossmann Meeting, MG'9, Rome, Italy, July 2-8, 2000. Pts. A-C*, pages 742–768, 2000.

[54] J.J. Sakurai and J. Napolitano. *Modern Quantum Mechanics*. Addison-Wesley, 2011.

[55] Steven Weinberg. *Lectures on Quantum Mechanics*. Cambridge University Press, 2 edition, 2015.

[56] A. Vilenkin. Boundary conditions in quantum cosmology. *Phys. Rev. D*, 33:3560–3569, Jun 1986.

[57] A. Vilenkin. Quantum cosmology and the initial state of the universe. *Phys.Rev.*, D37:888, 1988.

[58] J.B. Hartle and S.W. Hawking. Wave Function of the Universe. *Phys.Rev.*, D28:2960–2975, 1983.

[59] Peter Breitenlohner and Daniel Z. Freedman. Stability in Gauged Extended Supergravity. *Annals Phys.*, 144:249, 1982.

[60] Peter Breitenlohner and Daniel Z. Freedman. Positive Energy in anti-De Sitter Backgrounds and Gauged Extended Supergravity. *Phys. Lett.*, B115:197–201, 1982.

[61] Alexei A. Starobinsky. Isotropization of arbitrary cosmological expansion given an effective cosmological constant. *JETP Lett.*, 37:66–69, 1983.

[62] Charles Fefferman and C. Robin Graham. Conformal invariants. *Astérique Numéro hors série 'The mathematical heritage of Élie Cartan (Lyon, 1984)' (1985) 95–116*, 1985.

[63] Charles Fefferman and C. Robin Graham. The ambient metric. 2007.

[64] J. Hartle, S.W. Hawking, and T. Hertog. The Classical Universes of the No-Boundary Quantum State. *Phys.Rev.*, D77:123537, 2008.

[65] Gabriele Conti and Thomas Hertog. Two Wave Functions and dS/CFT on $S^1 \times S^2$. 2014.

[66] Roberto Emparan, Clifford V. Johnson, and Robert C. Myers. Surface terms as counterterms in the ads-cft correspondence. *Phys. Rev. D*, 60:104001, Oct 1999.

[67] J. B. Hartle, S.W. Hawking, and T. Hertog. No-Boundary Measure of the Universe. *Phys.Rev.Lett.*, 100:201301, 2008.

[68] Gerard 't Hooft. Dimensional reduction in quantum gravity. In *Salamfest 1993:0284-296*, pages 0284–296, 1993.

[69] Leonard Susskind. The World as a hologram. *J. Math. Phys.*, 36:6377–6396, 1995.

[70] Juan Martin Maldacena. The Large N limit of superconformal field theories and supergravity. *Int. J. Theor. Phys.*, 38:1113–1133, 1999. [Adv. Theor. Math. Phys.2,231(1998)].

[71] Edward Witten. Anti-de Sitter space and holography. *Adv. Theor. Math. Phys.*, 2:253–291, 1998.

[72] Eva Silverstein. (A)dS backgrounds from asymmetric orientifolds. In *Strings 2001: International Conference Mumbai, India, January 5-10, 2001*, 2001.

[73] Raphael Bousso and Joseph Polchinski. Quantization of four form fluxes and dynamical neutralization of the cosmological constant. *JHEP*, 06:006, 2000.

[74] Shamit Kachru, Renata Kallosh, Andrei D. Linde, and Sandip P. Trivedi. De Sitter vacua in string theory. *Phys. Rev.*, D68:046005, 2003.

[75] Alexander Maloney, Eva Silverstein, and Andrew Strominger. De Sitter space in noncritical string theory. In *Workshop on Conference on the Future of Theoretical Physics and Cosmology in Honor of Steven Hawking's 60th Birthday Cambridge, England, January 7-10, 2002*, pages 570–591, 2002.

[76] Ulf H. Danielsson, Sheikh S. Haque, Paul Koerber, Gary Shiu, Thomas Van Riet, and Timm Wrase. De Sitter hunting in a classical landscape. *Fortsch. Phys.*, 59:897–933, 2011.

[77] Raphael Bousso. Bekenstein bounds in de Sitter and flat space. *JHEP*, 04:035, 2001.

[78] T. Banks, W. Fischler, and S. Paban. Recurrent nightmares? Measurement theory in de Sitter space. *JHEP*, 12:062, 2002.

[79] C. M. Hull. Timelike T duality, de Sitter space, large N gauge theories and topological field theory. *JHEP*, 07:021, 1998.

[80] Michael Gutperle and Andrew Strominger. Space - like branes. *JHEP*, 04:018, 2002.

[81] Thomas Hertog, Ruben Monten, and Yannick Vreys. Lorentzian Condition in Holographic Cosmology. 2016.

[82] Ofer Aharony, Oren Bergman, Daniel Louis Jafferis, and Juan Maldacena. N=6 superconformal Chern-Simons-matter theories, M2-branes and their gravity duals. *JHEP*, 0810:091, 2008.

[83] Dionysios Anninos, Thomas Hartman, and Andrew Strominger. Higher Spin Realization of the dS/CFT Correspondence. 2011.

[84] Simone Giombi. Higher Spin — CFT Duality. In *Proceedings, Theoretical Advanced Study Institute in Elementary Particle Physics: New Frontiers in Fields and Strings (TASI 2015): Boulder, CO, USA, June 1-26, 2015*, pages 137–214, 2017.

[85] Dionysios Anninos, Frederik Denef, and Daniel Harlow. Wave function of Vasiliev's universe: A few slices thereof. *Phys.Rev.*, D88(8):084049, 2013.

[86] Shamik Banerjee, Alexandre Belin, Simeon Hellerman, Arnaud Lepage-Jutier, Alexander Maloney, Djordje Radicevic, and Stephen Shenker. Topology of Future Infinity in dS/CFT. *JHEP*, 11:026, 2013.

[87] J. J. Halliwell and S. W. Hawking. Origin of structure in the universe. *Phys. Rev. D*, 31:1777–1791, Apr 1985.

[88] J. J. Halliwell. Correlations in the wave function of the universe. *Phys. Rev. D*, 36:3626–3640, Dec 1987.

[89] Peter W. Higgs. Integration of Secondary Constraints in Quantized General Relativity. *Phys. Rev. Lett.*, 1:373–374, 1958. [Erratum: Phys. Rev. Lett.3,66(1959)].

[90] C. J. Isham and K. V. Kuchar. Representations of Space-time Diffeomorphisms. 1. Canonical Parametrized Field Theories. *Annals Phys.*, 164:288, 1985.

[91] C. J. Isham and K. V. Kuchar. Representations of Space-time Diffeomorphisms. 2. Canonical Geometrodynamics. *Annals Phys.*, 164:316, 1985.

[92] Karel V. Kuchař. Canonical geometrodynamics and general covariance. *Foundations of Physics*, 16(3):193–208, 1986.

[93] Igor R. Klebanov, Silviu S. Pufu, and Benjamin R. Safdi. F-Theorem without Supersymmetry. *JHEP*, 1110:038, 2011.

[94] Gabriele Conti, Thomas Hertog, and Ellen van der Woerd. Holographic Tunneling Wave Function. *JHEP*, 12:025, 2015.

[95] I.R. Klebanov and A.M. Polyakov. AdS dual of the critical O(N) vector model. *Phys.Lett.*, B550:213–219, 2002.

[96] Sean A. Hartnoll and S. Prem Kumar. The O(N) model on a squashed S^3 and the Klebanov-Polyakov correspondence. *JHEP*, 0506:012, 2005.

[97] Dionysios Anninos, Frederik Denef, George Konstantinidis, and Edgar Shaghoulian. Higher Spin de Sitter Holography from Functional Determinants. *JHEP*, 1402:007, 2014.

[98] Nikolay Bobev, Thomas Hertog, and Yannick Vreys. The NUTs and Bolts of Squashed Holography. *JHEP*, 11:140, 2016.

[99] Nikolay Bobev, Pablo Bueno, and Yannick Vreys. Comments on Squashed-sphere Partition Functions. 2017.

[100] Gabriele Conti, Thomas Hertog, and Yannick Vreys. Holographic Measure on Eternal Inflation. pages –, 2017.

[101] Stephen H. Shenker and Xi Yin. Vector Models in the Singlet Sector at Finite Temperature. 2011.

[102] Thomas Hertog and Gary T. Horowitz. Designer gravity and field theory effective potentials. *Phys. Rev. Lett.*, 94:221301, 2005.

[103] S. W. Hawking and Thomas Hertog. A Smooth Exit from Eternal Inflation. 2017.

[104] Vijay Balasubramanian, Jan de Boer, and Djordje Minic. Mass, entropy and holography in asymptotically de Sitter spaces. *Phys.Rev.*, D65:123508, 2002.

[105] Andrew Strominger. The dS / CFT correspondence. *JHEP*, 10:034, 2001.

[106] Juan Martin Maldacena. Non-Gaussian features of primordial fluctuations in single field inflationary models. *JHEP*, 0305:013, 2003.

[107] Edward Witten. Quantum gravity in de Sitter space. 2001.

[108] James B. Hartle, S.W. Hawking, and Thomas Hertog. Accelerated Expansion from Negative Λ. 2012.

[109] James B. Hartle, S.W. Hawking, and Thomas Hertog. Quantum Probabilities for Inflation from Holography. *JCAP*, 1401(01):015, 2014.

[110] T. Hertog and J. Hartle. Holographic No-Boundary Measure. *JHEP*, 1205:095, 2012.

[111] Thomas Hertog. Predicting a Prior for Planck. *JCAP*, 1402:043, 2014.

[112] Tanmay Vachaspati and Alexander Vilenkin. On the Uniqueness of the Tunneling Wave Function of the Universe. *Phys.Rev.*, D37:898, 1988.

[113] J. Garriga and A. Vilenkin. In defense of the "tunneling" wave function of the universe. *Phys. Rev. D*, 56:2464–2468, Aug 1997.

[114] Alexander Vilenkin. Approaches to quantum cosmology. *Phys.Rev.*, D50:2581–2594, 1994.

[115] Andrew Strominger. Inflation and the dS / CFT correspondence. *JHEP*, 0111:049, 2001.

[116] Alejandra Castro and Alexander Maloney. The Wave Function of Quantum de Sitter. *JHEP*, 11:096, 2012.

[117] R. Bousso and S.W. Hawking. Lorentzian condition in quantum gravity. *Phys.Rev.*, D59:103501, 1999.

[118] Gary T. Horowitz and Robert C. Myers. The value of singularities. *Gen.Rel.Grav.*, 27:915–919, 1995.

[119] James Hartle and Thomas Hertog. Quantum transitions between classical histories. *Phys. Rev.*, D92(6):063509, 2015.

[120] S.W. Hawking and Don N. Page. Thermodynamics of Black Holes in anti-De Sitter Space. *Commun.Math.Phys.*, 87:577, 1983.

[121] Kostas Skenderis. Lecture notes on holographic renormalization. *Class.Quant.Grav.*, 19:5849–5876, 2002.

[122] Vijay Balasubramanian, Per Kraus, and Albion E. Lawrence. Bulk versus boundary dynamics in anti-de Sitter space-time. *Phys. Rev.*, D59:046003, 1999.

[123] Vijay Balasubramanian, Per Kraus, Albion E. Lawrence, and Sandip P. Trivedi. Holographic probes of anti-de Sitter space-times. *Phys. Rev.*, D59:104021, 1999.

[124] E. Sezgin and P. Sundell. Massless higher spins and holography. *Nucl. Phys.*, B644:303–370, 2002. [Erratum: Nucl. Phys.B660,403(2003)].

[125] Simone Giombi and Xi Yin. Higher Spin Gauge Theory and Holography: The Three-Point Functions. *JHEP*, 09:115, 2010.

[126] A. H. Taub. Empty space-times admitting a three parameter group of motions. *Annals of Mathematics*, 53(3):472–490, 1951.

[127] E. Newman, L. Tamubrino, and T. Unti. Empty space generalization of the Schwarzschild metric. *J. Math. Phys.*, 4:915, 1963.

[128] Adam Bzowski, Thomas Hertog, and Marjorie Schillo. Cosmological singularities encoded in IR boundary correlations. *JHEP*, 05:168, 2016.

[129] Juan Martin Maldacena. Eternal black holes in anti-de Sitter. *JHEP*, 04:021, 2003.

[130] Thomas Hertog and Gary T. Horowitz. Holographic description of AdS cosmologies. *JHEP*, 04:005, 2005.

[131] Igor R. Klebanov and Edward Witten. AdS / CFT correspondence and symmetry breaking. *Nucl. Phys.*, B556:89–114, 1999.

[132] B. L. Hu. Scalar Waves in the Mixmaster Universe. I. The Helmholtz Equation in a Fixed Background. *Phys. Rev. D*, 8:1048–1060, Aug 1973.

[133] Andrei D. Linde, Dmitri A. Linde, and Arthur Mezhlumian. Nonperturbative amplifications of inhomogeneities in a selfreproducing universe. *Phys. Rev.*, D54:2504–2518, 1996.

[134] James Hartle, S. W. Hawking, and Thomas Hertog. The No-Boundary Measure in the Regime of Eternal Inflation. *Phys. Rev.*, D82:063510, 2010.

[135] Paul McFadden and Kostas Skenderis. Holography for Cosmology. *Phys.Rev.*, D81:021301, 2010.

[136] Juan Maldacena. Einstein Gravity from Conformal Gravity. 2011.

[137] Kostas Skenderis, Paul K. Townsend, and Antoine Van Proeyen. Domain-wall/cosmology correspondence in adS/dS supergravity. *JHEP*, 08:036, 2007.

[138] Robbert Dijkgraaf, Ben Heidenreich, Patrick Jefferson, and Cumrun Vafa. Negative Branes, Supergroups and the Signature of Spacetime. 2016.

[139] E. A. Bergshoeff, J. Hartong, A. Ploegh, J. Rosseel, and Dieter Van den Bleeken. Pseudo-supersymmetry and a tale of alternate realities. *JHEP*, 07:067, 2007.

[140] Daniel L. Jafferis, Igor R. Klebanov, Silviu S. Pufu, and Benjamin R. Safdi. Towards the F-Theorem: N=2 Field Theories on the Three-Sphere. *JHEP*, 06:102, 2011.

[141] Sebastian Fischetti and Toby Wiseman. On Universality of Holographic Results for (2+1)-Dimensional CFTs on Curved Spacetimes. 2017.

[142] Sebastian F. Bramberger, Shane Farnsworth, and Jean-Luc Lehners. Wavefunction of anisotropic inflationary universes with no-boundary conditions. *Phys. Rev.*, D95(8):083513, 2017.

[143] Kazuya Fujio and Toshifumi Futamase. Appearance of classical Mixmaster Universe from the No-Boundary Quantum State. *Phys. Rev.*, D80:023504, 2009.

[144] Stephen W. Hawking and Julian C. Luttrell. The Isotropy of the Universe. *Phys. Lett.*, B143:83, 1984.

[145] W. A. Wright and I. G. Moss. The Anisotropy of the Universe. *Phys. Lett.*, B154:115–119, 1985.

[146] P. Binetruy, E. Kiritsis, J. Mabillard, M. Pieroni, and C. Rosset. Universality classes for models of inflation. *JCAP*, 1504(04):033, 2015.

[147] Jaume Garriga, Kostas Skenderis, and Yuko Urakawa. Multi-field inflation from holography. *JCAP*, 1501(01):028, 2015.

[148] Adam Bzowski, Paul McFadden, and Kostas Skenderis. Holography for inflation using conformal perturbation theory. *JHEP*, 04:047, 2013.

[149] Niayesh Afshordi, Claudio Coriano, Luigi Delle Rose, Elizabeth Gould, and Kostas Skenderis. From Planck data to Planck era: Observational tests of Holographic Cosmology. *Phys. Rev. Lett.*, 118(4):041301, 2017.

[150] Hideo Kodama. Holomorphic wave function of the universe. *Phys. Rev. D*, 42:2548–2565, Oct 1990.

[151] T. Thiemann. Quantum spin dynamics (QSD). *Class. Quant. Grav.*, 15:839–873, 1998.

[152] T. Thiemann. Quantum spin dynamics (qsd). 2. *Class. Quant. Grav.*, 15:875–905, 1998.

[153] H. Garcia-Compean, O. Obregon, and C. Ramirez. Noncommutative quantum cosmology. *Phys. Rev. Lett.*, 88:161301, 2002.

[154] J. Ambjorn, J. Jurkiewicz, and R. Loll. Reconstructing the universe. *Phys. Rev.*, D72:064014, 2005.

[155] Jan Ambjorn, Jerzy Jurkiewicz, and Renate Loll. The self-organizing quantum universe. *Sci. Am.*, 299N1:42–49, 2008.

[156] M. van Raamsdonk. Building up Space-Time with Quantum Entanglement. *International Journal of Modern Physics D*, 19:2429–2435, 2010.

[157] J. Maldacena and L. Susskind. Cool horizons for entangled black holes. *Fortschritte der Physik*, 61:781–811, September 2013.

[158] Andrew Chamblin, Roberto Emparan, Clifford V. Johnson, and Robert C. Myers. Large N phases, gravitational instantons and the nuts and bolts of AdS holography. *Phys. Rev.*, D59:064010, 1999.

[159] Ioannis Papadimitriou. Multi-Trace Deformations in AdS/CFT: Exploring the Vacuum Structure of the Deformed CFT. *JHEP*, 05:075, 2007.

List of publications

1. G. Conti, T. Hertog. *Two wave functions and dS/CFT on $S^1 \times S^2$*. JHEP 10.1007/JHEP06(2015)101. `hep-th/1412.3728`.

2. G. Conti, T. Hertog, E. van der Woerd. *Holographic Tunneling Wave Function*. JHEP 10.1007/JHEP12(2015)025. `hep-th/1506.07374`.

3. G. Conti, T. Hertog, Y. Vreys. *Holographic Measure on Eternal Inflation*. `hep-th/1708.xxxx`.

FACULTY OF SCIENCE
DEPARTMENT OF PHYSICS AND ASTRONOMY
INSTITUTE FOR THEORETICAL PHYSICS
Celestijnenlaan 200D
B-3001 Leuven
http://www.fys.kuleuven.be/itf